Molecular Recognition and Metallo-supramolecular Complex Forming Ability of some Tridentate Ligands and Oligomers

A Dissertation

Submitted to the Indian Institute of Technology Guwahati
As Partial Fulfillment for the Degree of

Doctor of Philosophy in Chemistry

Submitted by

Bolin Chetia

Department of Chemistry

Indian Institute of Technology Guwahati

Guwahati, Assam-781039, India.

April 2010

Molecular Recognition and Metallo-supramolecular Complex Forming Ability of some Tridentate Ligands and Oligomers

Submitted by

Bolin Chetia

Roll No. 04612211

Department of Chemistry

Indian Institute of Technology Guwahati

Guwahati, Assam-781039, India.

April 2010

Dedicated to

My Family Members

INDIAN INSTITUTE OF TECHNOLOGY GUWAHATI

Department of Chemistry

STATEMENT

I do hereby declare that the matter embodied in this thesis is the result of investigations carried out by me in the Department of Chemistry, Indian Institute of Technology Guwahati, Guwahati, Assam, India under the supervision of Dr. Parameswar Krishnan Iyer, Department of Chemistry, Indian Institute of Technology Guwahati, Guwahati, Assam, India.

In keeping with the general practice of reporting scientific observations, due acknowledgements have been made wherever the work described is based on the findings of other investigators.

April, 2010. **(Bolin Chetia)**

IIT Guwahati

INDIAN INSTITUTE OF TECHNOLOGY GUWAHATI

Department of Chemistry

CERTIFICATE

This is to certify that the work contained in the thesis entitled **"Molecular recognition and metallo-supramolecular complex forming ability of some tridentate ligands and oligomers"** by Bolin Chetia, a Ph. D. student of the Department of Chemistry, Indian Institute of Technology Guwahati, for the award of degree of Doctor of Philosophy has been carried out under my supervision and this work has not been submitted elsewhere for a degree.

April, 2010.
IIT Guwahati

Dr. Parameswar Krishnan Iyer
Supervisor
Department of Chemistry
IIT Guwahati

INDIAN INSTITUTE OF TECHNOLOGY GUWAHATI

Department of Chemistry

CERTIFICATE OF COURSE WORK

This is to certify that Bolin Chetia has satisfactorily completed all the courses required for the Ph. D degree program. These courses include

1) CH 601 : Physical Methods in Chemistry
2) CH 605 : Applied Crystallography
3) CH 621 : New Reagents for Organic Synthesis
4) CH 632 Advanced Group Theory and Applications

Prof. A. Chattopadhyay
Head,
Department of Chemistry
IIT Guwahati

Prof. T. Punniyamurthy
Secretary,
Departmental Post Graduate Program Committee
Department of Chemistry
IIT Guwahati

ACKNOWLEDGEMENT

At the very out set, I would like to express my deep sense of gratitude to my supervisor, Dr. Parameswar Krishnan Iyer, for his excellent guidance, helping to learn chemistry and always believing in me. He provided me the opportunity and resources to be creative, inspired me to do my best, making sure I am progressing along a forward path. It is these things that have given me the most confidence in my scientific abilities.

I would like to acknowledge my sincere gratitude to all my Doctoral Committee members, Dr. Gopal Das, Dr. Debasis Manna and Dr. A. Perumal for their insightful advices and valuable suggestions.

I would like to take the opportunity to thank all the faculty members who had helped me in one way or another to finish this PhD work for and all the initial help with learning chemistry.

I am thankful to Amarjyoti Borthakur Sir who showed me the way of chemistry.

I am thankful to the Head of Department, Chemistry, IITG for allowing me to use the Instruments Facilities like FT-IR, UV/Visible and Flourescence spectrophotometer and the Head, Central Instruments Facility (CIF) for providing me Instruments facilities like NMR and Mass spectrometer.

I am thankful to Mr. Babulal Das for Single Crystal XRD analysis, Mr. Chandan Borgohain, Mr. Kulakamal Senapati, Mr. Madhurjya Borah and Mr Kh.Kesho Singh of Central Instruments Facility for their help in spectroscopic measurements and all the non-teaching staff of Department of Chemistry for their help during my Ph.D. tenure.

I would like to thank my past and present labmates Pranjalda, Ballav, Gunin, Prasanta, Atul, Muthuraj, Sukanti for lending their hands of support whenever needed and valuable suggestions during my Ph.D. life.

I am also thankful to all Research Scholars, friends, M.Sc. and B.Tech. students who made my stay here and there more enjoyable.

I would like to thank my teachers of Dibrugarh University who always gave me inspiration and encouragement to fulfill my research work and my colleagues and Jituda who always gave me the helping hand to continue the Ph.D. work.

I thank my wife Pari for her encouragement and helping hand in every step of my research and sisters, Sabita and Dipti, my in-laws and all my family members for their love and moral support during my research work.

I am thankful to all my well wishers who always gave me the inspiration to complete my research work.

Finally, I thank my parents who always gave me inspiration, encouragement and strength and because of whom I have reached this position and without their love and support this work would not have been completed.

April, 2010. **Bolin Chetia**

Abstract

Supramolecular chemistry is a highly interdisciplinary field of science, which may be defined as "Chemistry beyond the molecule" that results from the association of two or more chemical species by non-covalent interactions. In this thesis entitled, "*Molecular recognition and metallo-supramolecular complex forming ability of some tridentate ligands and oligomers*" we have presented the utilization of simple ligand systems for the development of synthetic receptors capable of selectively recognizing neutral and anionic guests as well as for the formation of metallo-supramolecular complexes by interaction with metal salts.

In the Chapter-1 the principles, perspectives and recent developments in the field of supramolecular chemistry is described. An extensive survey of the literature is also reported that highlights on the development and use of bis-benzimidazole type of ligands as well as the overall objective of the thesis work is defined.

In the next chapter the utilization of a simple ligand 2,6-bis(2-benzimidazolyl)pyridine, **bbp,** as a receptor for the recognition of urea and thiourea is reported. The advantage of this ligand is its ease of preparation, simplicity and high stability. It was observed that the receptor and guest molecules formed highly stable supramolecular complexes with urea and thiourea via self-assembly and which were characterized by means of UV/Visible and fluorescence spectroscopy in solution. We have also prepared the supramolecular complexes of receptor **bbp** and urea and characterized by X-ray crystallography.

In the Chapter-3 the same receptor **bbp** was utilized for the detection of toxic benzene metabolites like hydroquinone, catechol, resorcinol etc. Despite their carcinogenicity these compounds have never received enough attention. Supramolecular complex formation between **bbp** and guest molecules was studied by simple techniques like UV/Visible and fluorescence spectroscopy and by single crystal X-ray analysis.

In the chapter-4a we have extended the utility of the ligand **bbp** towards the recognition of anions. The binding of anionic guest species with **bbp** can be monitored using UV/Visible, fluorescence spectroscopy and ^{1}H NMR techniques. The analysis showed that **bbp** can be used as chemosensor for fluoride selectively.

Based on the utility of **bbp** for anion recognition we have prepared a new ligand 1,3-bis(5,6-dimethyl-1H-benzo[d]imidazol-2-yl)benzene, **bbb** and have studied its binding ability with anions. In comparison to the **bbp** ligand, **bbb** contains four methyl groups on the benzimidazol part, because of which the steric factor come into play and enhances the selectivity. Development of **bbb** towards the detection of anions has been studied using UV/Visible, fluorescence spectroscopy and ^{1}H NMR techniques.

In the Chapter-5 the synthesis of monomers **5a** and **5b** having hexyl chain as a spacer is discussed. The formation and properties of their metallo-supramolecular complexes with few metal ions is confirmed by observing the changes in UV/Vis and fluorescence spectroscopic study. Monomer **5a** displayed prominent changes in UV/Vis and fluorescence spectra indicating the formation of stronger complexes with different metal ions in comparison to **5b** which showed minor changes since it forms weaker organometallic C-H bond. TGA analysis of the complexes showed high thermal stability. Viscosity studies confirm the formation of self-assembling aggregates.

In the Chapter-6 the synthesis of monomers **6a**, **6b**, **6c** and **6d** having pentaethylene glycol as a spacer with benzthiazol and benzoxazol based ligands is reported. Further their metallo-supramolecular complex formation with different transition metal ions was studied by UV/Vis and fluorescence spectroscopy. The optical and thermal properties of these complexes were also studied. Additionally, the pentaethylene glycol part was used to study their interaction with potassium metal resulting in folding of the ligand along with the formation of supramolecular complexes.

CONTENTS

1.1. General overview

This chapter describes the principles, perspectives, and recent developments in the field of supramolecular chemistry, which has grown exponentially in the past few decades as indicated by the large number of articles, reviews, and books.[1] Supramolecular chemistry is a highly interdisciplinary field of science, which may be defined as "Chemistry beyond the molecule" that results from the association of two or more chemical species by non-covalent interactions.[2] The functional self-assembled systems formed by non-covalent interactions show numerous applications including sensors, electronic and photonic materials or ion transport channels.[3]

Supramolecular chemistry can be classified broadly into host-guest chemistry and self-assembly. The former involves the combination of small molecules, comprising a host that specifically accommodates a guest, thus leading to molecular recognition. The latter describes the building up of non-covalent arrays of defined geometry from specifically engineered molecular components. The forces involved in supramolecular chemistry are hydrogen bonding, electrostatic interactions, van der Waals, π-π stacking, charge transfer interactions etc.[4] Unlike covalent forces, these forces are weaker and can be easily disrupted. Self assembly shows the spatial confinement through spontaneous connection of a few or many components, which result in discrete or extended entities at molecular or supramolecular level.

1.2. Host-Guest Chemistry

The field of host-guest chemistry began with the development of crown ethers by Pedersen in the 1960s (Figure 1.1). His major breakthrough was first presented in a paper in 1967.[5] The other great contributor to this field was Cram.[6] He distinguished between hosts and guests by identifying hosts as organic molecules with convergent binding sites, and, guests as either molecules or ions with divergent binding sites.

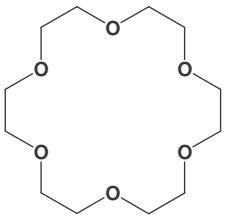

1.1

Figure 1.1: *18-Crown-6*

Cram's definition is the concept that one molecule, a guest, goes into a larger molecule, a host. Once inside the host, the guest remains as a result of forces that depend on the interaction between the specific molecules. This host-guest relationship is not necessarily a permanent state, but it should last sufficiently long enough to be measurable by such means as UV/Vis, IR-spectroscopy or NMR.

1.3. Molecular Recognition

Molecular recognition, *i.e.* the ability of molecules and functional groups to recognize and interact with each other, is fundamentally important for understanding many chemical phenomena, e.g., drug–receptors, enzyme–substrate recognition, adhesion of molecules to surfaces, self-assembly of molecules, etc. The recognition is binding with a purpose and the process occurs through a set of structurally well-defined intermolecular interactions. Thus, molecular recognition implies the storage and read out of molecular information. Although, the term recognition was initially used in connection with biological systems, but in the beginning of the 1970's it is used in the selective complexation of metal ions.[7] Since then it is used and has become a major area of chemical research.

Molecular recognition is largely driven by non-covalent interactions between molecules and their associated functional groups. The strengths of these non-covalent interactions are dependent on both distance and orientation. A list of non-covalent interactions and how the energy of attraction (or repulsion) varies with distance is shown in Figure. 1.2.[8] As the

non-covalent interactions are largely electrostatic in nature, these interactions have been studied computationally. Accurate and precise experimental measures of non-covalent interactions as functions of distance, however, remain a considerable challenge even today.[9]

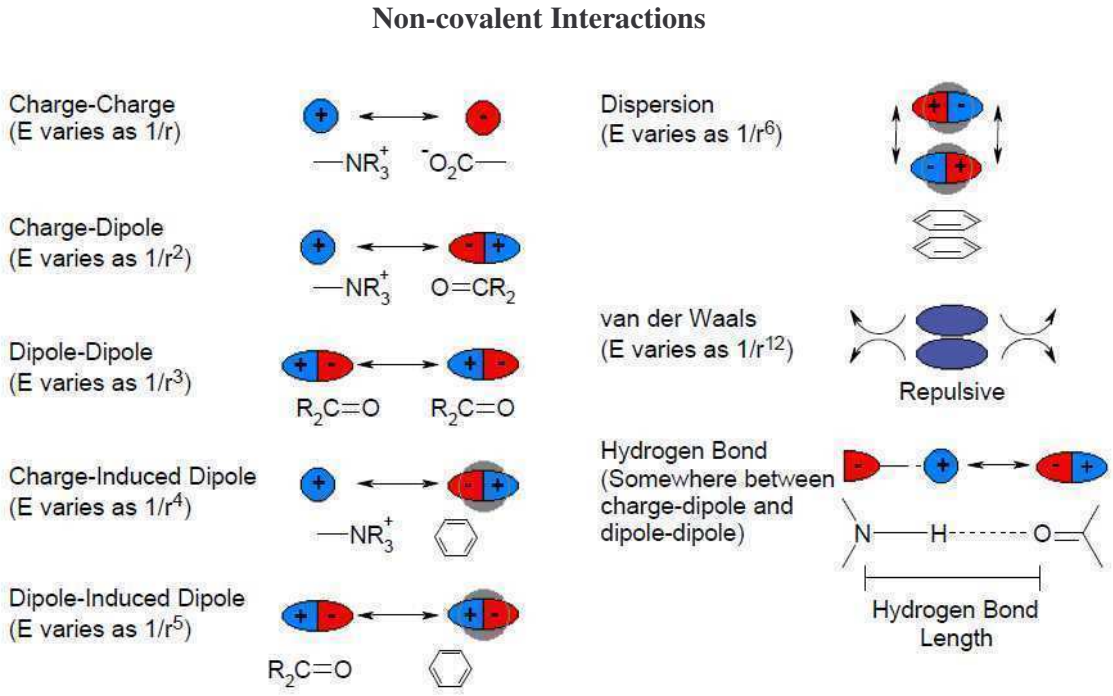

Figure 1.2: *Types of non-covalent interactions and their distance dependence (reproduced in part from Mathews and Van Holde). E is the electronic interaction and r is distance.*

1.4. Molecular Receptors

Molecular receptors can be defined as organic structures which can bind selectively ionic or molecular substrates (or both) by means of various intermolecular interactions to form a supermolecule. Paul Ehrlich first introduced the concept of receptors and Emil Fischer in 1894 enunciated the idea of selective nature and "lock and key" image of steric fit, which formed the basis of molecular recognition. In the last few decades, this field is attracting more importance because of their significance in intermolecular chemistry and in chemical selectivity. This receptor chemistry is not confined to only transition metal ions but

extending to all types of substrates: cationic, anionic, or neutral molecules of organic, inorganic, or biological nature.[10]

Achievements of molecular recognition depend on the design of molecular receptors so that it can create numerous non-covalent binding interactions with the guest molecule and sense its molecular size, shape, and architecture. Receptor should contain some intramolecular cavities, clefts or pockets to which guest molecule can fit, which is known as concave receptors. Another significant point is the flexibility of supramolecular systems which is of great importance in biological receptor-substrate interactions.

1.5. Recognition of Neutral Molecules

The recognition and binding of neutral molecules make use of donor-acceptor, electrostatic and mainly hydrogen bonding interactions. The acyclic or macrocyclic receptors must contain clefts or cavities into which binding of substrates take place.[11] To recognize organic substrates the receptor requires some suitable binding subunits which make the receptor more or less rigidly connected as architectures of macrocyclic or cage-like nature.[12]

Designing of receptors for neutral molecules is still relatively more challenging and less explored domain. Naturally occurring cyclodextrins were the first receptor molecules whose binding properties towards organic molecules were recognized and extensively studied.[13] Different types of synthetic macrocyclic receptors have been reported which can bind both charged and uncharged organic substrates. One of the receptor *Carcerands*[14] can bind highly reactive species such cyclobutadiene[15] or orthoquinones[16] inside the cavity.

Hamilton[17] reported a macrocyclic receptor which form complex with barbituric acid through hydrogen bonding (Figure 1.3). Another cleft was reported which formed complex with adenine through hydrogen bonding and act as a receptor.[18] Some other examples of

container molecules that can bind different guest molecules inside the cavity are cyclophane, cubic azacyclophane, [4]- and [6]-calixarenes, cavitand, cryptophane etc.

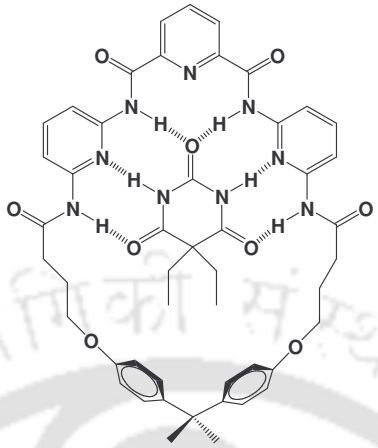

Figure 1.3: *Hydrogen bonding of barbituric acid in a macrocylic receptor.*

Bell[19] and co-workers designed a series of heterocyclic receptor for urea (Figure 1.4). They used hydrogen bonding sites of the complexes for the recognition of urea.

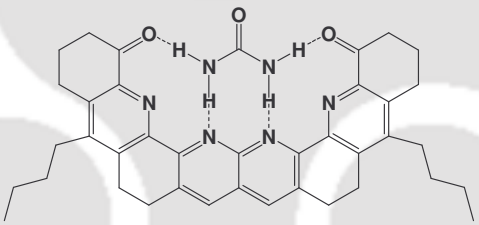

Figure 1.4: *Hydrogen bonding of urea and heterocyclic receptor.*

Ray[20] and co-workers synthesized a new class of receptors having Dibenz[*c*,*h*]acridine as spacers and showed that the four nitrogen atoms present in the internal cavity bind with urea (Fig. 1.5).

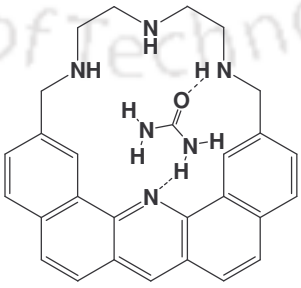

Figure 1.5: *Hydrogen bonding of urea and a receptor having Dibenz[c,h]acridine as spacer.*

Goswami[21] and co-workers designed and synthesised a neutral fluorescent macrocyclic receptor for the recognition of urea in chloroform (Figure 1.6). Receptor showed a significant fluorescence quenching on complexation with urea and thiourea.

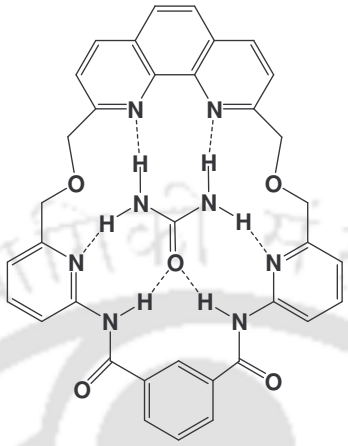

Figure 1.6: *Complexation of macrocylic receptor and urea.*

Very large, rigid cavities required to bind big molecules are very difficult to construct. This perception led to formation of non-macrocyclic hosts having open space that can bind to organic molecules easily with high affinity.

1.6. Recognition of Anions

Molecular receptors designed to bind anionic guests or ion pairs have attracted much interest recently[22] due to their significance in a plethora of biological, chemical and environmental processes.[23] Anions are ubiquitous throughout the natural systems playing many essential roles. For example, they carry genetic information (DNA is a polyanion). It is also essential in the formation of enzyme-substrate and enzyme-cofactor complexes and also in the interaction of proteins and RNA or DNA. Anion channels and carriers are involved in the transport of small anions such as chloride, phosphate, and sulphate and thus taking part in maintaining osmotic balance.[24] On the other hand, anions can have deleterious effects on the environment. For example, nitrate and sulphate are present in the

acid rain, pertechnetate are generated from the re-processing of nuclear fuel, phosphate and nitrates from agriculture, constitute major pollution hazarders. There is therefore a demand for the production of selective anion receptor and sensor species that can allow in the field detection of particular species.

Despite their popularity, the design of 'substrate specific' synthetic receptors still remains a great challenge for supramolecular scientists in comparison to the design of receptors for cations. There are a number of reasons for this. Anions are larger than isoelectronic cations[25] and therefore have a lower charge to radius ratio. This shows that electrostatic binding interactions are less effective than they would be for the corresponding isoelectronic cation.

Table 1.1 *A comparison of the radii r of isoelectronic cations and anions in octahedral environments*

Cation	r [A°]	Anion	r [A°]
Na^+	1.16	F^-	1.19
K^+	1.52	Cl^-	1.67
Rb^+	1.66	Br^-	1.82
Cs^+	1.81	I^-	2.06

Anions may be sensitive to pH values (becoming protonated at low pH and so losing their negative charge), so receptors must function within the pH range to the target anion**.** As anions have a wide range of geometries, therefore a higher degree of design is required to make a receptor selective for a particular anionic guest.

Solvent effects also play an important role in controlling anion binding strength and selectivity. Electrostatic interactions generally dominate over other recognition forces and hydroxylic solvents can form strong hydrogen bonds with anions. Because of that, an anion receptor must compete with the solvent environment in which the anion recognition takes place. For example, a neutral receptor that binds anions through hydrogen-bonding

interactions may less capable of competing with the polar protic salvation shell surrounding the target anion in a hydroxylic solvent and hence receptor may function as an anion receptor in aprotic organic solvents. On the other hand, a polar solvent can compete more effectively with polar solvents.

1.7. Overview of Synthetic Anion Receptor

The birth of 'anion coordination chemistry' might be considered to be the report by Park and Simmons in 1968.[26] In this work, the halide binding properties of several macrobicyclic receptors, consisting of two ammonium bridge-head centres spanned by three alkyl linkers, were reported (Figure 1.7).

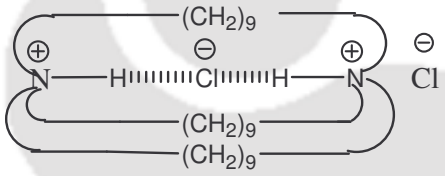

Figure 1.7: *Structure of chloridekatapinato-in.in-1, 1 l-diazabicyclo[9.9.9]nonacosanebis (ammonium) chloride.*

Following Simmons and Park's report the next step forward came in the mid-1970s. At that time Lehn and co-worker began to explore the opportunities behind anion coordination chemistry in polyammonium macrocycles.[27] They clearly demonstrated the strong binding of anion to the charged cavity and the selective nature of the cryptates towards chloride or bromide (Figure 1.8).

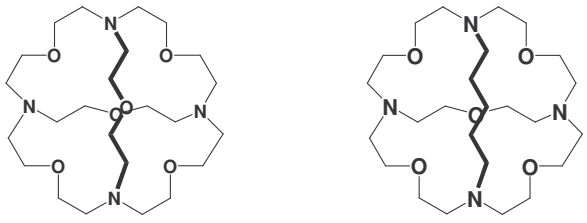

Figure 1.8: *Structures of cryptand-like receptors.*

Lehn and co-workers, also reported an ellipsoidal hexaprotonated cryptand and which was found to be selective for linear anions such as azide N_3^- ion (Figure 1.9).[28]

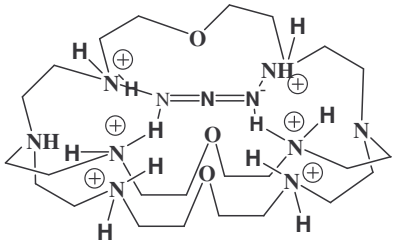

Figure 1.9: *Structure of cryptand that binds azide selectively*

.

Schmidtchen proposed a series of quaternary ammonium groups arranged in a tetrahedral manner which bind the anions solely by electrostatic interactions (Figure 1.10). He successfully "tuned" the selectivity of the receptors for particular halides.[29]

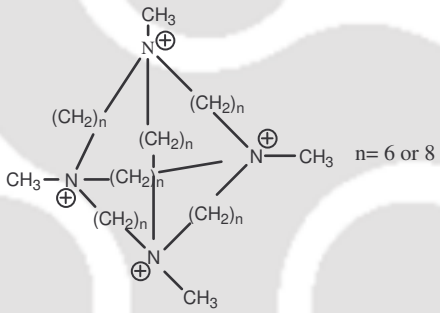

Figure 1.10: *Structure of cage cations.*

A wide variety of neutral synthetic anion receptors are known which occurs through hydrogen-bonding interactions to affect anion recognition. These include amides, ureas or pyrroles. In 1986, Pascal and co-workers reported (1,3,5)cyclophane as a neutral host for anion complexation and for the first time they utilized the amide N-H….anion interaction to recognize anions (Figure 1.11).[30] This receptor was found to bind fluoride anions in DMSO-*d6* solution by ^{1}H and ^{19}F NMR spectroscopic studies.

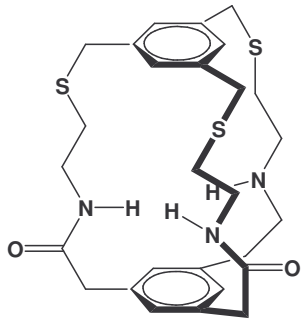

Figure 1.11: *Structure of Pascal's amide based cyclophane anion receptor.*

Reinhoudt and co-workers reported a series of acyclic tripodal receptors containing amide groups (Figure 1.12).[31] They showed that these hosts strongly bind to the dihydrogen phosphate than chloride or hydrogen phsophate and which occur exclusively by hydrogen bonds.

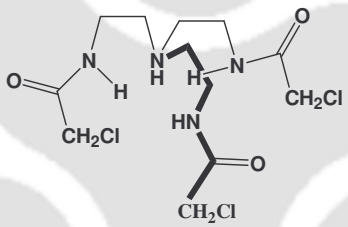

Figure 1.12: *Structure of acyclic tripodal receptor containing amide group.*

S.J. Loeb and co-workers reported a general review covering both cyclic and acyclic anion receptors containing amide groups built on solely organic framework.[32]

Urea and thio-urea groups are also used to construct a number of receptors which played an important role in the recognition of anions. In 1992, C.S. Wilcox and co-workers[33] reported urea based receptor that binds very strongly to ion pairs containing sulfonates, phosphates and carboxylates in chloroform and their data suggested that complexation is due to hydrogen bond formation between the urea and anion.

Luigi Fabbrizzi[34] in his review explained the urea and thiourea based different anion receptors (Figure 1.13). Again, A.D. Hamilton and co-workers[35] reported in their review different types of cyclic urea and thiourea based anion receptors.

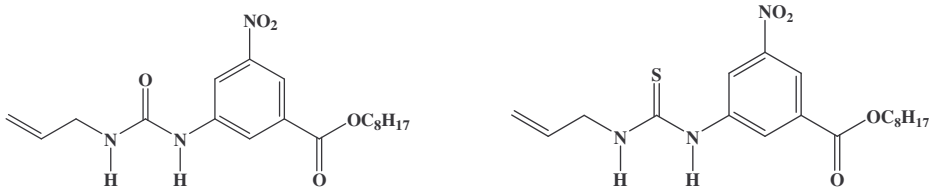

Figure 1.13: *Structures of urea and thiourea based anion receptors.*

1.8. Supramolecular Polymer

Supramolecular polymers are formed by monomeric units held together with directional and reversible secondary interactions.[36] Since these interactions are influenced by external parameters like temperature or mechanical stimuli drastic changes in polymer properties like elasticity and solution viscosity occur. Architectural and dynamic parameters that determine polymer properties, such as degree of polymerization, lifetime of the chain, and its conformation, are a function of the strength of the non-covalent interaction, which can reversibly be adjusted. A large number of supramolecular polymers could be prepared by hydrogen bonding.

R.P. Sijbesma[37] in his article discussed the development and properties of supramolecular polymers based on quadruple hydrogen bonds between self-complementary ureidotriazine(UTr) and ureidopyrimidinone (UPy) functional groups.

In Supramolecular polymers, the average degree of polymerization (DP) is determined by the strength of the end group interaction.[38] The degree of polymerization is dependent on the concentration of the solution and the association constant.

Again a high association constant between the repeating units is must to obtain polymers with high molecular weight. In analogy with covalent condensation polymers, the chain length of supramolecular polymers can be tuned by the addition of monofunctional “chain stoppers”.

Another approach of supramolecular polymers is based on the reversibility of metal-coordination bonding. This is an excellent tool for the synthesis of Supramolecular system

as the ligand structures can be varied by classical organic chemistry and the desired strength as well as reversibility can be attained due to the variety of available ligand types and metal ions. G.F. Swiegers and co-workers[39] in his review proposed different types of supramolecular systems constructed from metal-ligand bonds which include lattice, cyclic, filamentous and interlaced motifs. In his review, on organic/inorganic polymers, M. Rehahn[40] proposed a classification on the different types of coordination polymers.

A. Ciferri[41] in his article on supramolecular polymerizations mentioned the possible classifications based on assembling mechanisms. He mentioned that the equilibrium polymers are the supramolecular polymers where the linear chains are self-assembled, open, growing to a distribution of degree of polymerizations, and in a state of thermodynamic equilibrium sensitive to solvent type, concentration and external variables. Among the different techniques for the formation of supramolecular polymer, one of the easiest ways is by the coordination of metal-ligand interactions. These interactions should be strong enough to retain the polymer chain in the solution and these polymers should show properties of polymers like enhanced viscosity in comparison to monomeric units.

The self-assembly polymerization of ditopic macromolecules via metal–ligand binding is a facile route for the preparation of metallo-supramolecular polymers in which the metal–ligand interaction is dynamic in nature and thus acts as the supramolecular motif. In fact, due to their potential usefulness in a plethora of applications like catalysis, light-emitting devices, sensory materials, metallopolymers have become a most prominent research theme at the interface of metal-organic chemistry and polymer science. Utilizing a variety of non-covalent interactions, several recent studies have demonstrated that different types of building block can be assembled with supramolecular motifs, yielding polymer materials that span a broad range of structures and properties[42]

By varying metal–ligand binding motifs different types of binding characteristics[43] (e.g., thermodynamic and kinetic stabilities) can be obtained and which in turn can be utilized to tune the nature of the resulting supramolecular materials.[44]

Within this chapter, coordination polymers formed by incorporation of metal ions and organic ligand molecules will be discussed. The systems should be synthesized by a supramolecular approach.

In 1968, A. Ripamonti and co-workers[45] first reported the soluble coordination polymers which was beryllium phosphinates (Figure 1.14). They studied the solution properties which indicate that these compounds are linear polymers which undergo a reversible degradation influenced by the nature of the solvent, concentration, and temperature.

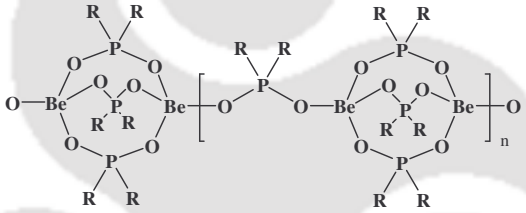

Figure 1.14: *First soluble, reversible co-ordination polymer of beryllium phosphinate system.*

L.A. Paquette and co-workers[46] synthesized tris(spirotetrahydrofuranyl) Ionophores and reported the formation of rod like supramolecular ionic polymer from homoditopic dimer. The bifacial ligand reacts with one equivalent of $LiClO_4$ or $LiBF_4$ to form rod like ionic polymers.

Wang and Reynolds[47] reported a series of polymers containing nickel bis(dithiolene) linkages along the polymer main chain which are highly soluble in both aqueous and organic solvents (Figure 1.15).

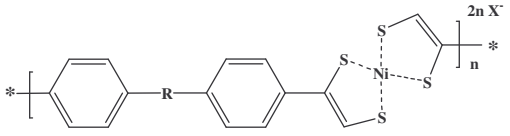

Figure 1.15: *Nickel bis(dithiolene) coordination polymer.*

Craig and co-workers[48] reported pyridine-palladium based homologous reversible coordination polymers (Figure 1.16).

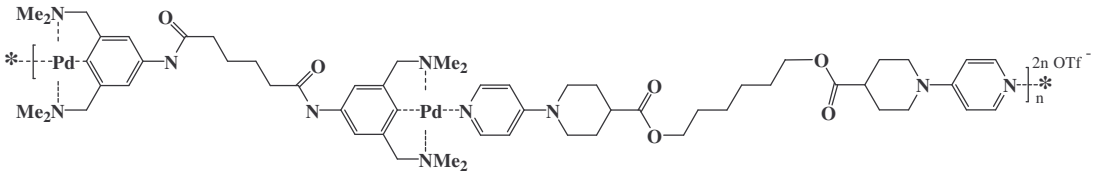

Figure 1.16: *Palladium-pyridine coordination polymers.*

Vermonden and co-workers[49] reported pyridine-2,6-dicarboxylic acid bifunctional ligands having oligoethylene glycol as a spacer to form water soluble reversible coordination polymers with zinc ions (Figure 1.17). Formation of polymer was confirmed by viscosity measurements.

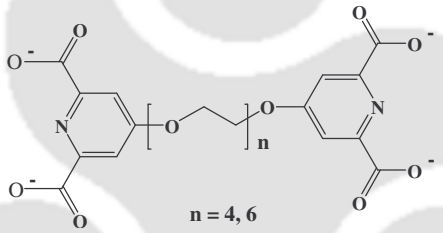

Figure 1.17: *Ditopic ligand having pyridine-2,6-dicarboxylic acid.*

Rehahn[50] for the first time, presented well-defined soluble transition-metal coordination polymers from kinetically unstable pseudotetrahedral copper(1)- and silver(1)-phenanthroline complexes (Figure 1.18). The stability of the complexes was studied by ^{1}H and ^{I3}C NMR spectroscopy.

Rehahn and coworkers[53] also reported soluble ruthenium-terpyridine polymers.

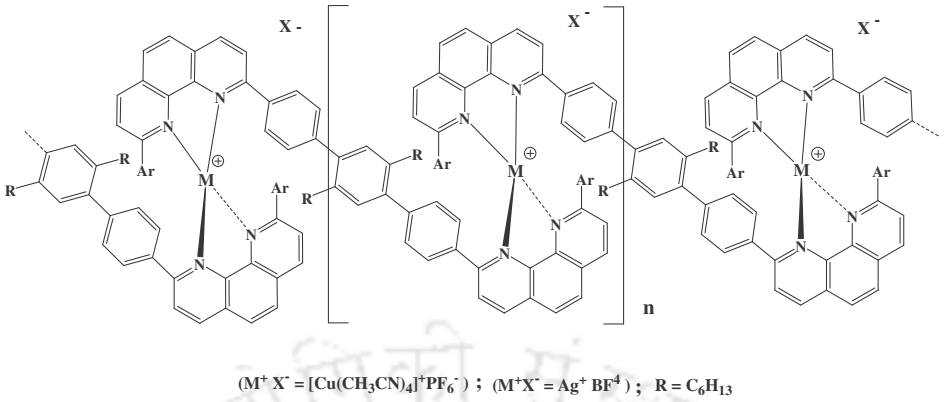

Figure 1.18: *Copper(1)- and silver(1)-phenanthroline complexes.*

In his review, Schubert[51] reported different 2,2′:6′,2″-terpyridine (tpy) based ligands which form coordination polymers. Constable and co-workers[52] reported different types of ditopic and tritopic terpyridine based ligands to form polymers (Figure 1.19).

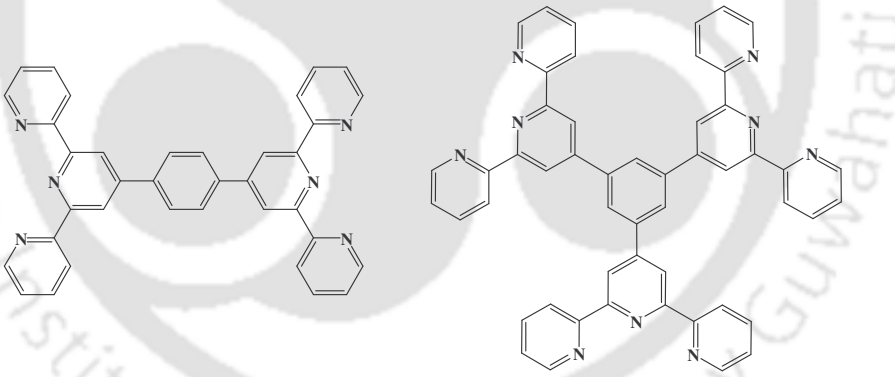

Figure 1.19: *Structure of tpy based ditopic and tritopic ligands.*

Later on, ditopic terpyridine based ligands having flexible and polymeric spacers have been reported by Schubert.[54]

Rowan and Beck[55] reported the synthesis of ditopic ligand from terpyride-related ligand 2,6-bis(1′-methylbenzimidazolyl)-4-hydroxypyridine having pentaethyleneglycol as a spacer, which form metallo-supramolecular polymers that are photoactive

mechanoresponsive gels (Figure 1.20). The ditopic ligand can form both 2:1 and 3:1 metal complexes with transition metal and lanthanide ions respectively.

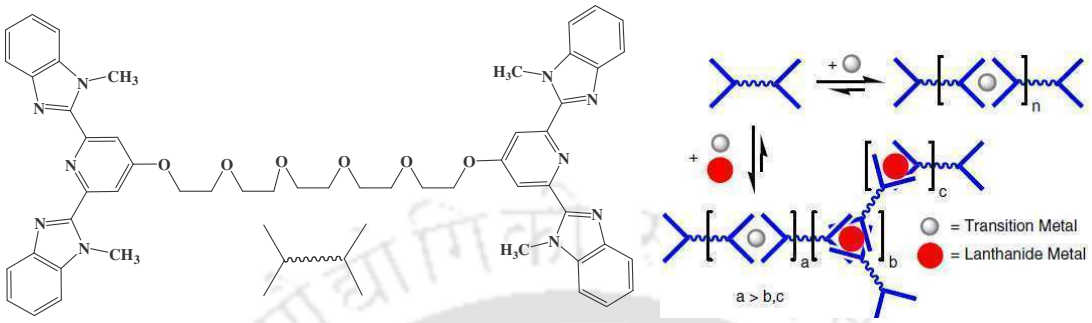

Figure 1.20: *Schematic representation of the metallo-supramolecular polymerization of ditopic ligands with transition and lanthanide metal ions.*

Utilizing the same ligand, different ditopic macromonomers have been reported by Rowan and Weder,[56] having different spacers like poly(2,5-dialkoxy-p-phenylene ethynylene), poly(2,5-dioctyloxy-p-xylylene) etc. (Figure 1.21). which form metallo-supramolecular conjugated polymers with different metal ions that can be readily solution-processed.

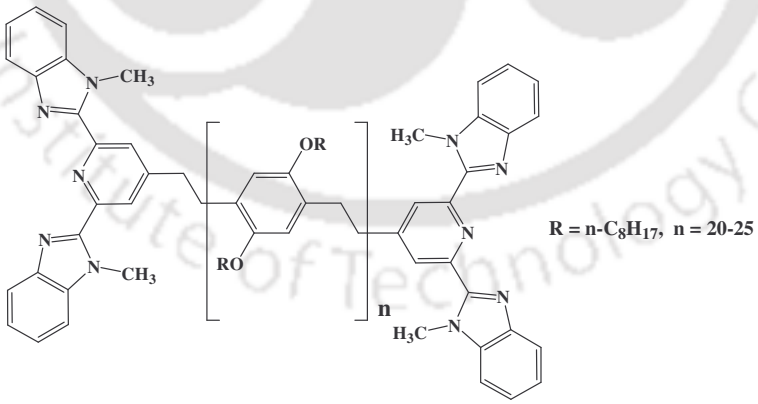

(a)

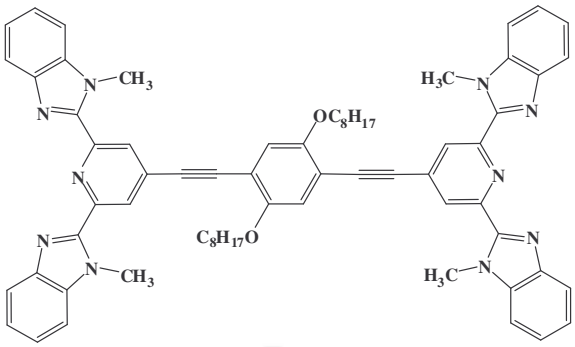

(b)

Figure 1.21: *(a) Structure of ditopic monomer having acetylene as a spacer, (b) Structure of poly(2,5-dioctyloxy-p-xylylene) (PPX)*

1.9. Objective of the present work

Recognition of neutral molecules and sensing of anions have been in constant news since last few decades. The present work focused on the design and synthesis of novel receptors capable of recognizing chemical and biological guest molecules, sensing of anions. We have utilized benzimidazolyl based ligands towards the detection of different types of neutral organic guest molecules which are toxic chemicals like urea, thiourea, phenol, hydroquinone, resorcinol, catechol, *p*-benzoquinone, etc. by the formation hydrogen-bonded complexes in the presence of competitive solvent environment which is a proof of their potential application in chemical and biological sensing. Beside this, the utilization of these types of ligands in anion sensing is also studied.

Another interesting field is the metallo-supramolecular polymers, which has plethora of applications, in several overlapping fileds. The present work also focused on the synthesis of new types of ditopic ligands having aliphatic spacers and the formation of the metallo-supramolecular complexes with few metal ions and study of their properties in solution as well as in solid state.

Although, terpyridine and 2,6-*bis*(benzimidazol-2-yl)pyridine (**bbp**) are both tridentate ligands having similar chelating property, **bbp** ligand has more potential because of the

extensive π-delocalization and its rigidity and planarity. The factors for choosing the benzimidazol based ligands for our purpose was because the synthesis was simple, yield was very high and stability towards air/moisture was very good.[57] It also has multiple binding sites, has a well-defined open cavity with a rigid overall structure that helps to predict its interaction and relative binding with guest molecules with a fair degree of accuracy. These ligands are of considerable interest due to their binding sites for metals in several biological systems, especially as mimics of histidine-imidazole systems.[58]

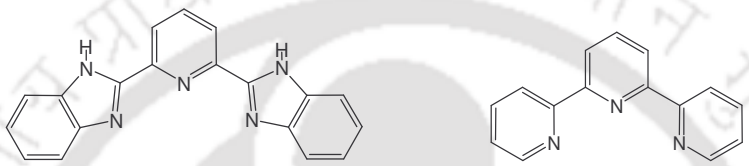

(a) bbp (b) trpy

Figure 1.22: *Structures of (a) 2,6-bis(benzimidazol-2-yl)pyridine (**bbp**) and (b) terpyridine (**trpy**).*

Although the chemistry of the **bbp** ligand with some transition metals like iron,[59] zinc,[60] cadmium[61] etc. and with lanthanides[62] have been studied well but the recognition and sensing properties of the **bbp** ligand is still unexplored.

You and co-workers synthesized the Zn, Cd and In complexes with 2,6-*bis*(benzimidazol-2-yl)pyridine and have shown their blue luminescent properties.[60, 61]

Aghatabay and co-workers synthesized complexes of Fe(II), Zn(II), Cd(II) and Hg(II) with 2,6-*bis*(benzimidazol-2-yl)pyridine ligand and shown the antimicrobial activity (Figure 1.23).[63]

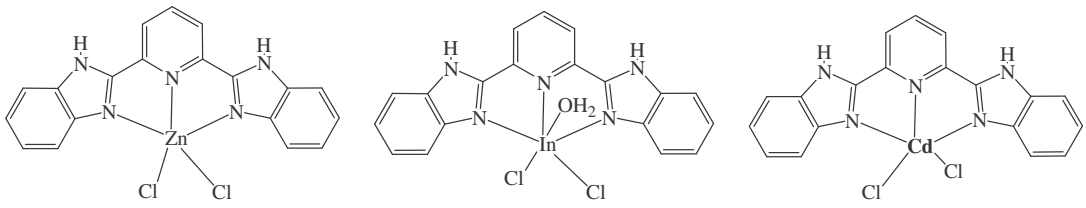

(a) (b) (c)

Figure 1.23: *Structures of **(a)** [Zn(bbp)Cl$_2$, **(b)** [In(bbp)Cl$_2$(H$_2$O)] and (c) [Cd(bbp)Cl$_2$].*

Nair et al. synthesized and characterized the ruthenium (II) complex $[Ru(bbp)_2]Cl_2$ and studied their DNA binding and cleavage properties.[64]

Haga and co-workers reported the molecular design of a proton-induced molecular switch based on rod-shaped Ru-dinuclear complexes with *bis*-tridentate 2,6-*bis*(benzimidazol-2-yl)pyridine derivatives (Figure 1.24).[65]

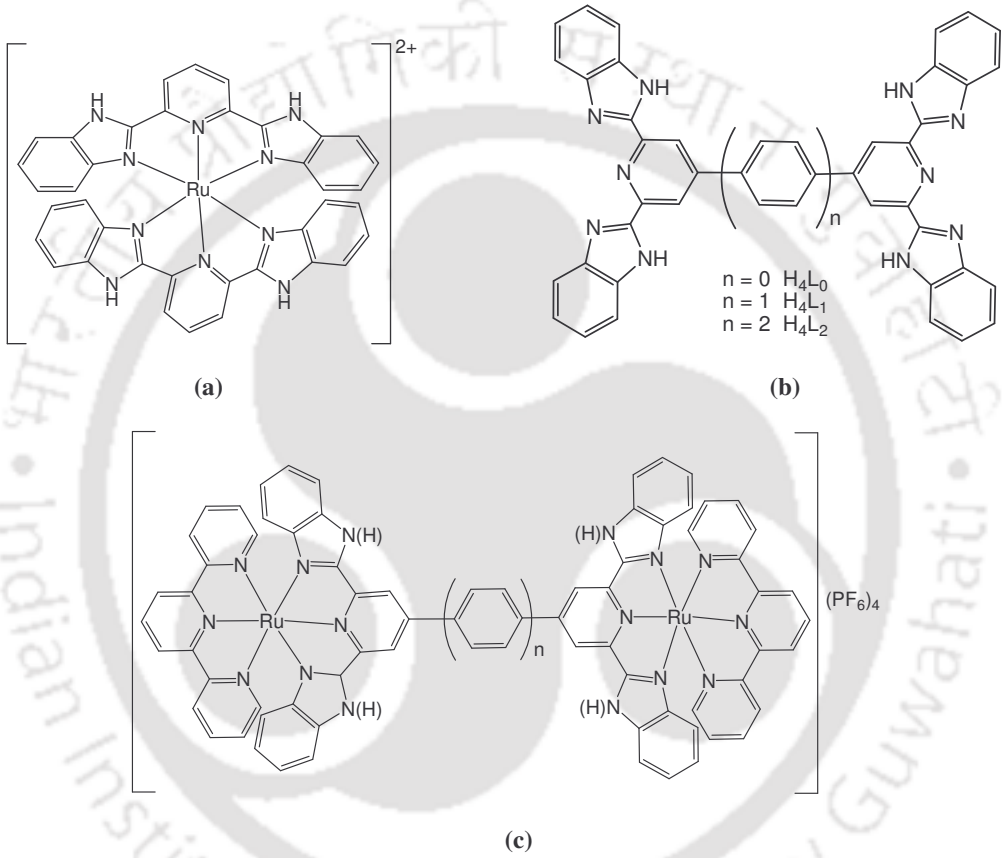

Figure 1.24: *Structure of (a)$[Ru(bbp)_2]^{2+}$, (b) bis-tridentate 2,6-bis(benzimidazol-2-yl)pyridine derivatives, (c) $[Ru_2(btbbp)(trpy)_2](PF_6)_4$.*

The present work reports on the formation of supramolecular complexes of benzimidazol based ligands with different guest molecules and metallo-supramolecular complexes of ditopic ligands with different metal ions. The work presented in the proceeding chapters of the thesis will be primarily focused on the following aspects:

a) Preparation of ligand 2,6-*bis*(benzimidazol-2-yl)pyridine (bbp), characterization and formation of supramolecular complexes with different organic neutral guest molecules having amide moiety like urea, thiourea etc.

b) Study of the complex formation in solution state by means of UV/Vis and fluorescence spectroscopy and in solid state by X-ray diffraction analysis.

c) hydrogen bonded supramolecular complex formation with different toxic organic chemicals like metabolites of benzene, e.g. phenol, hydroquinone, catechol, resorcinol, benzoquinone etc. and study of their properties in solution as well as in the solid state.

d) sensing of anions by the use of **bbp** ligand by UV/Vis and fluorescence spectroscopy and ^{1}H NMR techniques.

e) preparation of ligand (1,3-bis(5,6-dimethyl-1H-benzo[d]imidazol-2-yl)benzene), **bbb** and its characterization, study the anion sensing of this ligand by means of UV/Vis and fluorescence spectroscopy and ^{1}H NMR techniques.

f) preparation of 2,6-bis(1′-methylbenzimidazolyl)-4-hydroxypyridine and 2,6-bis(1′-methylbenzimidazolyl)-4-hydroxybenzene based ligands, synthesis of ditopic ligands by the use of the above ligands and characterization by different techniques.

g) supramolecular complex formation of these ditopic ligands with different metal ions is investigated by titration experiments applying UV/Vis and fluorescence spectroscopy and thermal stability of the complexes have been studied.

h) preparation of benzoxazole and benzothiazole based ligands, synthesis of ditopic ligands from these having pentaethylene glycol as a spacer and characterization.

i) supramolecular complex formation with different metal ions. The optical properties of the resulting complex units are investigated by UV/Vis and fluorescence spectroscopy and thermal stabilities of the complexes have been studied.

1.10. References

1. (a) Lehn, J.-M. *Angew. Chem. Int. Ed. Engl*. **1988**, *27*, 89. (b) Schneider, H.-J.; Yatsimirsky, A. *Principles and Methods in Supramolecular Chemistry, John Wiley & Sons, Ltd.*, *Chichester.* **1999**. (c) Diederich, F.; Stang, P.J.; Tykwinski, R.R. *Modern Supramolecular Chemistry, Strategies for Macrocycle Synthesis, Wiley-VCH*, **2007.**
2. (a) Lehn, J.-M. *Supramolecular Chemistry: Concepts and Perspectives VCH, Weinheim*, **1995**. (b) Steed, J. W.; Atwood, J. L. *Supramolecular Chemistry John Wiley & Sons, Ltd., Chichester.* **2000**.
3. Prodi, L.; Bolletta, F.; Montalti, M.; Zaccherowni, N. *Coor. Chem. Rev*. **2000**, *205*, 59. (b) McQuade, D. T.; Pullen, A. E.; Swager, T. M. *Chem. Rev*. **2000**, *100*, 2537. (c) Tour, J. M. *Acc. Chem. Res*. **2000**, *33*, 791. (d) Würthner, F. *Angew. Chem. Int. Ed*. **2001**, *40*, 1037. (e) Chabinye. M.; Chen, X.; Holmlin, R. E.; Jacobs, H.; Skulason, H.; Frisbie, C. D.; Mujica, V.; Ratner, M. A.; Rampi, M. A.; Whitesides, G. M. *J. Am. Chem. Soc*. **2002**, *124*, 11730. (f) Würthner, F. *Chem. Commun*, **2004**, *14*, 1564. (g) Würthner, F. *et. al*. *J. Am.Chem. Soc*. **2004**, *126*, 10611. (h) Brabee. C. J.; Saricifci, N. S.; Hummelen, J. C. *Adv. Funct. Mater*. **2001**, *11*, 15. (i) Sakai, N.; Matile, S. *Chem. Commun*, **2003**, 2514. (j) Bong, D. T.; Clark, T.D.; Granja, J. R.; Ghadiri, M. R. *Angew. Chem. Int. Ed*. **2001**, *40*, 988. (k) Beginn, U. *Adv. Mater*. **1998**, *10*, 1391.
4. (a) Rebek Jr, J. *Angew. Chem. Int. Ed. Engl.* **1990**, *29*, 245. (b) Vögtle, F. *Suparmolecular Chemistry*; John Wiley & Sons: New York, **1991.** (c) Amabilino, D. B.; Stoddart, J. F. *Chem. Rev.* **1995**, *95*, 2725. (d) Fyfe, M. C. T.; Stoddart, J. F. *Acc. Chem. Res.* **1997**, *30*, 393. (e) Harada, A.; Li, J.; Kamachi, M. *Nature* **1992**, *356*, 325-327. (f) Harada, A.; Li, K.; Kamachi, M. *Nature* **1994**, *370*, 126.
5. Pedersen, C. J. *J. Am. Chem. Soc.* **1967**, *89*, 7017.

6. Cram, D. J.; Cram, J. M. *Container Molecules and their Guests*; Monographs in supramolecular chemistry; No. 4; Royal Society of Chemistry: Cambridge, **1994**, 1-5.
7. Lehn, J.-M. *Struct. Bonding,* **1973**, *16*, 1.
8. Mathews, C. K.; Van Holde, K. E. *Biochemistry*; 2nd ed.; The Benjamin/Cummings Publishing Co., Inc.: Redwood City CA, **1996**.
9. (a) Murray, J. S.; Politzer, P. *J. Mol. Struct. (Theochem)* **1998**, *425*, 107-114. (b) Politzer, P.; Murray, J. S. *Fluid Phase Equilibria* **2001**, *185*, 129.
10. Lehn, J.-M. in *Perspecitives in Coordination Chemistry*, (Eds.: Williams, A. F.; Floriani, C. and Merbach, A. E.), VHCA, Basel, and VCH, Weinheim, **1992**, p. 447.
11. (a) Rebek, J. *Topics Curr. Chem*. **1988**, *149*, 189. (b) Rebek, J. *Angew. Chem. Int. Ed. Engl*. **1990**, *29*, 245. (c) Hamilton, A. D. in [A.26], p.1; *Bioorg. Chem. Frontiers* **1991**, *2*, 115.
12. (a) Seel, C. and Vogtle, F. *Angew. Chem. Int. Ed. Engl.* **1992**, *31*, 528. (b) Sun, Y. and Martell, A. E. *Tetrahedron*, **1990**, *46*, 2725.
13. Bender, M. L. and Komiyama, M. *Cyclodextrin Chemistry*, Springer, Berlin, **1978.**
14. (a) Cram, D. J. *Nature* **1992**, *356*, 29. (b) Tanner, M. E.; Knobler, C. B. and Cram, D. J. *J. Org. Chem.* **1992**, *57*, 40.
15. Cram, D. J.; Tanner, M. E.; Thomas, R. *Angew. Chem. Int. Ed. Engl.* **1991**, *30*, 1024.
16. Robbins, T. A. and Cram, D. J. *J. Am. Chem. Soc.* **1993**, *115*, 12199
17. Hamilton, A. D. in [A.26], p.1; *Bioorg. Chem. Frontiers* **1991**, *2*, 115.
18. (a) Rebek, J. *Topics Curr. Chem*. **1998**, *149*, 189. (b) Rebek, J., Jr. *Acc. Chem. Res*. **1990**, *23*, 399.
19. Bell, T.W.; Liu, J. *J. Am. Chem. Soc*. **1988**, *110*, 3673.

20. Ray, J.K.; Halder, M.K.; Gupta, S.; Kar, G.K. *Tetrahedron* 2000, 56, 909.

21. Goswami, S.; Mukherjee, R.; Ray, J. *Org. Lett*. **2005**, *7*, 1283.

22. (a) Gale, P.A. *Coord. Chem. Rev*. **2000**, *199*, 181. (b) Gale, P.A. *Coord. Chem. Rev*. **2001**, *213*, 79. (c) Gale, P.A. *Coord. Chem. Rev*. **2003,** *240,* 191. (d) Beer, P.D.; Gale, P.A. *Angew. Chem. Int. Ed*. **2001,** *40,* 486.

23. (a) Martinez-Máñez R.; Sancenón, F. *Chem. Rev*. **2003**, *103*, 4419. (b) Beer, P. D.; Gale, P. A. *Angew. Chem. Int. Ed.* **2001**, *40*, 486.

24. (a) Christianson, D.W.; Lipscomb, W.N. *Acc. Chem. Res.* **1989,** *22,* 62. (b) Berg, J.M. *Acc. Chem. Res*. **1995,** *28,* 14. (c) Puglisi, J.D.; Chen, L.; Frankel, A.D.; Williamson, J.R. *Proc. Natl. Acad. Sci. U.S.A*. **1993,** *90,* 3680.

25. Shannon, R. D. *Acta Cryst.***1976**, *A32*, 751.

26. Park, C.H;. Simmons, H.E. *J. Am. Chem. Soc.* **1968**, *90*, 2431.

27. Graf, E.; Lehn, J.-M. *J. Am. Chem. Soc*. **1976**, *98*, 6403.

28. Lehn, J.-M.; Sonveaux, E.; Willard, A.K. *J. Am. Chem. Soc*. **1978**, *100*, 4914.

29. (a) Schmidtchen, F.P.; *Angew. Chem. Int. Ed*. **1977**, *16*, 720. (b) Schmidtchen, F.P. and Muller, G. *J. Chem. Soc. Chem. Commun.* , **1984**, 1115.

30. PascalJr, R.A.; Spergel, J.; Engen, D.V. *Tetrahedron Lett.* **1986**, *27*, 4099.

31. Valiyaveettil, S.; Engbersen, J.F.J.; Verboom, W.; Reinhoudt, D.N. *Angew.Chem. Int. Ed.*, **1993**, *32*, 900.

32. Bondy, C.R.; Loeb, S.J. *Coord. Chem. Rev*. **2003**, *240*, 77.

33. Smith, P.J.; Reddington, M.V.; Wilcox, C.S. *Tetrahedron Lett.* **1992**, *35*, 6085.

34. Amendola, V.; Bonizzoni, M.; D.E.-Gómez, Fabbrizzi, L.; Licchelli, M.; Sancen´on, F.; Taglietti, A. *Coord. Chem. Rev.*, **2006**, *250*, 1451.

35. Choi, K.; Hamilton, A.D. *Coord. Chem. Rev.,* **2003**, *240,* 101.

36. Brunsveld, L.; Folmer, B. J. B.; Meijer, E. W.; Sijbesma. R. P.; *Chem. Rev.* **2001,** *101,* 4071.

37. ten Cate. A.T.; Sijbesma, R.P. *Macromol. Rapid. Commun*. **2002**, *23*, 1094.

38. Martin, R.B. *Chem. Rev*. **1996**, *96(8),* 3043.

39. Swiegers, G.F. and Malefetse, T.J. *Chem. Rev.* **2000,** *100,* 3483.

40. Rehahn, M. Acta Polymer. **1998,** *49*, 201.

41. Ciferri, A. *Macromol. Rapid Commun*. **2002**, *23*, 511.

42. (a) Brunsveld, L.; Folmer, B. J. B.; Meijer, E. W.; Sijbesma, R. P. *Chem. Rev.* **2001,** *101*, 4071. (b) Ciferri, A. *Macromol. Rapid Commun.* **2002**. *23*, 511. (c) Hofmeier, H. and Schubert, U.S. *Chem. Commun*. **2005,** 2423. (d) Hofmeier, H.; Hoogenboom, R.; Wouters, M. E. L.; and Schubert, U. S. *J. Am. Chem. Soc*. **2005,** *127*, 2913. (e). Meier, M. A. R.; Wouters, D.; Ott, C.; Guillet, P.; Fustin, C.-A.; Gohy, J.-F.; and Schubert, U. S. *Macromolecules* **2006,** *39*, 1569. (f) Gerhardt, W. W.; Zucchero, A.J.; Wilson, J. N.; South, C. R.; Bunz, U. H. F.; Weck, M. *Chem. Commun.* **2006,** 2141.

43. (a) Nguyen, P.; GómeZ-Elipe, P.; Manners, I. *Chem. Rev*. **1999,** *99*, 1515. (b) Wolf, M. O. *Adv. Mater.* **2001,** *13*, 545. (c) Schubert, U. S. and Eschbaumer, C. *Angew. Chem., Int. Ed*. **2002,** *41*, 2892. (d) Holder, E.; Langeveld, B. M.W.; and . Schubert, U. S. *Adv. Mater.* **2005,** *17*, 1109. (e) Holliday, B. J. and Swager, T. M. *Chem. Commun*. **2005,** 23.

44. (a) Schmatloch,S.; González, M. F.; Schubert, U. S. *Macromol. Rapid Commun.* **2002,** *23*, 957. (b) Yount, W. C.; Juwarker, H. and Craig, S. L. *J. Am. Chem. Soc.* **2003,** *125*, 15302. (c) Vermonden, T.; van der Gucht, J.; de Waard, P.; Marcelis, A. T. M.; Besseling, N. A. M.; Sudhölter, E. J. R.; Fleer, G. J. and Stuart, M. A. C. *Macromolecules*, **2003,** *36*, 7035. (d) Loveless, D. M.; Jeon, S. L. and Craig, S. L. *Macromolecules* **2005,** *38*, 10171. (e) Yount, W. C.; Loveless, D. M. and Craig, S. L. *J. Am. Chem. Soc*. **2005,** *127*, 14488. (f) Schmittel, M.; Kalsani, V.; Kishore, R. S. K.; Cölfen, H.; and Bats, J. W. *J. Am. Chem. Soc*. **2005,** *127*, 11544.

45. Gemiti, F.; Giancotti, V.; Ripamonti. A. *J. Chem. Soc. A*, **1968**, 763.

46. Paquette, Leo A.; Tae, J. *J. Am. Chem. Soc.* **2001**, *123*, 4974.

47. Wang, F.; Reynolds, J.R. *Macromolecules,* **1990**, *23*, 3219.

48. Yount, W.C.; Juwarker, H.; Craig, S.L. *J. Am. Chem. Soc***. 2003**, *125*, 15302.

49. Vermonden, T.; van der Gucht, J.; Waard, P.de.; Marcelis, A.T. M.; Besseling, N. A. M.; Sudholter, E. J. R.; Fleer, G.J.; Cohen Stuart, M. A. *Macromolecules* **2003,** *36,* 7035.

50. Velten, U.; Lahn, B.; Rehahn, M. *Macromol. Chem. Phys***. 1997,** *198***,** 2789.

51. Schubert, U.S.; Eschbaumer, C.; *Angew. Chem. Int. Ed*. **2002**, *41*, 2892.

52. Constable, E.C.; Cargill Thompson, A.M.W. *J. Chem. Soc., Dalton Trans.* **1992**, 3467.

53. Kelch, S.; Rehahn, M. *Macromolecules,* **1999**, *32*, 5818.

54. Schmatloch, S.; Gonzalez, M.; Schubert, U.S. *Macromol. Rapid. Commun.* **2002**, *23*, 957.

55. (a) Beck, J.B.; Rowan, S.J. *J. Am. Chem. Soc*. **2003**, *125*, 13922. (b) Zhao, Y.; Beck, J.B.; Rowan, S.J.; Jamieson, A.M. *Macromolecules*, **2004**, *37*, 3529. (c) Weng. W.; Beck, J.B.; Jamieson, A.M.; Rowan, S.J. *J. Am. Chem. Soc*. **2006**, *35*, 11663.

56. (a) Knapton, D.; Rowan, S.J.; Weder, C. *Macromolecules,* **2006**, *39*, 651. (b) Knapton, D.; Iyer, P.K.; Rowan, S.J.; Weder, C. *Macromolecules,* **2006**, *39*, 4069. (c) Iyer, P.K.; Beck, J.B.; Weder, C.; Rowan, S.J. *Chem. Commun*. **2005**, 319. (d) Knapton, D.; Burnworth, M.; Rowan, S.J.; Weder, C. *Angew. Chem. Int. Ed*. **2006**, *45*, 5825. (e) Burnworth, M.; Knapton. D.; Rowan. S.J.; Weder, C.. *J. Inorg. Organomet. Polym. Mater*. **2007**, *1*, 91.

57. (a) Addison, A. W.; Burke, P. J. *J. Heterocycl. Chem.* **1981**, *18*, 803. (b) Addison, A. W.; Rao, T.N.; Wahlgren, C.G. *J. Heterocycl. Chem.* **1983**, *20*, 1481.

58. Gilbert, J.G.; Addison, A.W.; Butcher, R.J. *Inorg. Chim. Acta.* **2000**, *308*, 22.

59. Boca, R.; Baran, P.; Dlhá, L.; Fuess, H.; Haase, W.; Renz, F.; Linert, W.; Svoboda, I.; Werner, R. *Inorg. Chim. Acta* **1997**, *260*, 129.

60. Liu, S.-G.; Zuo, J-L.; Wang, Y.; Li, Y-Z.; You, X.-Z. *J. Phy. Chem. Sol*. **2005**, *66,* 735.

61. Liu, S.-G.; Zuo, J-L., Li, Y.-Z.; You, X.-Z. *J. Mol. Str.* **2004**, *705*, 153.

62. (a) Wang, S.; Luo, Q.; Zhou, X.; Zeng, Z. *Polyhedron* **1993**, *12*, 1939. (b) Froidevaux, P.; Harrowfield, J.M.; Sobolev, A.N. *Inorg. Chem.* **2000,** *39,* 4678.

63. Aghatabay, Naz M.; Neshat, A.; Karabiyik, T.; Somer,; M.; Haciu, D.; Dülger, B. *Eur. J. Med. Chem.* **2007**, *42*, 205.

64. Vaidyanathan, V. G.; Nair, B. U. *J. Inorg. Biochem*. **2002**, *91*, 405.

65. Haga, M.-a.; Takasugi, T.; Tomie, A.; Ishizuya, M.; Yamada, T.; Hossain, M. D.; Inoue, M. *J. Chem. Soc., Dalton Trans.* **2003**, 2069.

Abstract

The use of 2,6-bis(2-benzimidazolyl)pyridine as a neutral receptor enables the formation of highly stable supramolecular complexes with urea and thiourea via self-assembly and which were characterized by optical spectroscopy techniques and X-ray diffraction analysis. This receptor utilizes the imine nitrogen located on its outer core in addition to the cavity to form hydrogen-bonded adducts with high binding affinity, thus providing a unique and simple design for chemical and biological recognition.

2.1 Introduction

Noteworthy progress made to design and synthesize novel receptors capable of recognizing chemical and biological guest molecules has contributed greatly in the development of supramolecular chemistry.[1] Major challenges that need attention are the development of structurally simple and stable receptors that would have better utility and much wider applicability. Urea is toxic and a well-known pollutant that causes serious biological disorders.[2, 3] Urea is an end product of nitrogen metabolism and a well-known protein denaturant that can cause damage in concentrations as low as micromolar range. Thus, the need to develop structurally simple synthetic receptors capable of detecting urea in low concentrations is utmost important for clinical chemistry.[4]

Although some research groups[5] synthesized and reported macrocyclic receptors for the recognition of urea, it was difficult to construct molecules having very large and rigid cavities required to bind bigger molecules / guests. This perception led to formation of non-macrocyclic hosts having open space that can bind to organic neutral molecules easily and with high affinity.

Thiourea is confirmed to be a human carcinogen based on adequate evidence of carcinogenicity on experimental animals.[6] Thiourea inhibited lignin degradation by phanerochaete chrysosporium.[7] When administered in drinking water, it induced thyroid adenomas and carcinomas in rats. Thiourea also increases the solubility of membrane proteins. Most of the amino acids contain O, N and S as binding sites, thus, it becomes important to study the binding nature of thiourea with synthetic receptors so that they may be targeted as drugs.

This chapter deals with the use of 2,6-bis(2-benzimidazolyl)pyridine ligand, **bbp** (Figure 2.1) for the recognition of neutral organic guests such as urea, thiourea etc. by the use of UV/Vis and fluorescence spectroscopy and single crystal X-ray analysis.

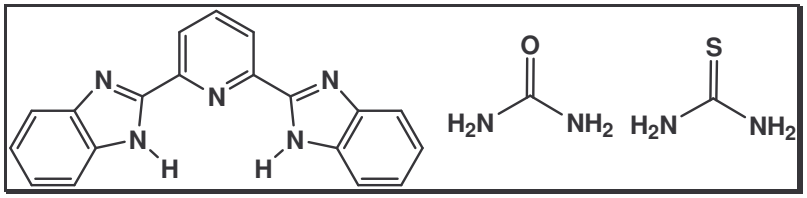

Figure 2.1: *2,6-Bis(2-benzimidazolyl)pyridine, **bbp**, urea and thiourea.*

2.2 Results and discussion

2,6-bis(2-benzimidazolyl)pyridine, **bbp** the tridentate ligand has been used for the recognition and sensing of urea, thiourea etc. using UV/Vis and fluorescence spectroscopy and the formation of stable supramolecular complexes by X-ray diffraction analysis. Compound **bbp** was chosen as a receptor candidate as its preparation was simple and high yielding, it possesses multiple binding sites and its stability towards air/moisture is very good.[8] Moreover, **bbp** also has a well-defined open cavity with a rigid overall structure that helps to predict its interaction and relative binding with guest molecules with a fair degree of accuracy.[9]

2.2.1 UV/Visible Spectroscopy

Supramolecular complex formation was studied by simple technique of UV/Visible titration which was performed in dry acetonitrile.

To evaluate the solution state properties of receptor **bbp**, a titration was performed by careful addition of 0.1 equivalents of urea aliquots at regular intervals to **bbp**. The spectroscopic changes were recorded by means of UV/Vis spectroscopy in acetonitrile. The choice of solvents is restricted by the insolubility of **bbp** in nonpolar solvents. On increasing the concentration of urea, the initial absorption band (Figure 2.2) having λ_{max} at 327 nm showed a marginal but progressive decrease in intensity with broadening and formation of a clear isosbestic point at 277 nm, indicating the presence of at least one stable species at equilibrium.

Due to the low basicity of urea, the decrease in λ_{max} intensity of **bbp** and the development of newer bands do not occur significantly, but the presence of a distinct isosbestic point is due to the formation of a stable donor–acceptor complex between **bbp** and urea. The inset of Figure 2.2 shows that a limiting value is reached on forming a 1:1 adduct between **bbp** and urea. The effect of solvents on hydrogen bonding was studied by performing titrations in DMSO, DMF, methanol, and ethanol. Different sets of isosbestic points were obtained in the DMSO and DMF titrations with low binding constants. However, titration in alcohols showed very minor spectral changes and the binding constants were difficult to estimate.

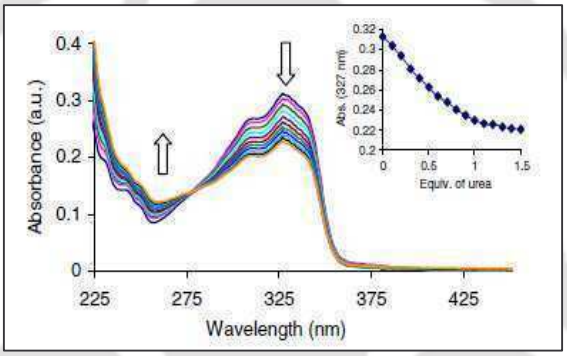

Figure 2.2: *UV/visible spectrum of receptor **bbp** (6.35 x 10^{-6}M in dry CH_3CN) during titration with urea from 0 to 1 equiv (v/v). Inset— titration profile of the band at 327 nm corresponding to the **bbp: urea** H-bonded complex.*

The binding ability of receptor **bbp** towards the detection of thiourea has also been studied. The binding was evaluated by titrating 0.1 equivalents of thiourea aliquots into a solution of **bbp** in acetonitrile at regular intervals and recording the changes in UV/Vis and fluorescence spectra.

It was observed that on increasing the concentration of thiourea, progressive decrease of intensity in the initial absorption band (Figure 2.3) having λ_{max} at 327 nm and a new peak at 249 nm with higher intensity develops which is due to the formation of stable complex between **bbp** and thiourea. This family of spectra shows formation of an isosbestic point at 263 nm indicating the presence of at least one species at equilibrium. Thus the gradual

decrease in the band intensity at 327 nm and formation of a new higher intensity blue-shifted band at 249 nm with a clear isosbestic point is proof for the formation of hydrogen-bonded complex between **bbp** and thiourea. The low concentrations at which these spectroscopic changes were observed clearly reveal that this receptor **bbp** can be used for the recognition of urea and thiourea.

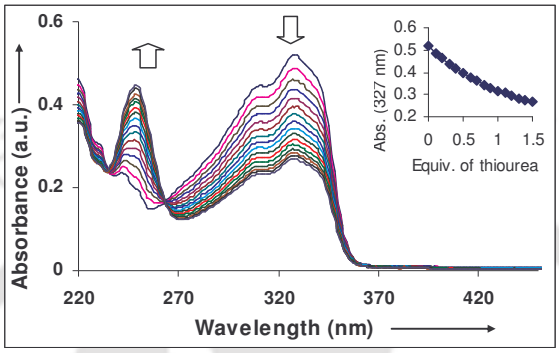

Figure 2.3: *UV/visible spectrum of receptor **bbp** (9.50 x 10^{-6}M in dry CH_3CN) during titration with thiourea from 0 to 1.5 equiv (v/v). Inset— titration profile of the band at 327 nm corresponding to the bbp: thiourea H-bonded complex.*

2.2.2 Fluorescence Spectroscopy

Complexation studies of **bbp** receptor were also carried out by fluorescence spectroscopy which showed that the spectrum of **bbp** is clearly modified on the formation of a complex with urea. Titration experiments carried out by the addition of 0.1 equiv of urea to **bbp** showed that the 375 nm band in the fluorescence spectrum was diminished by over 70% of the initial intensity. A large quenching in intensity was observed up to the addition of 0.5 equiv of urea after which the changes were minor. Excess urea did not alter the spectrum signifying that the emission occurs always from the low energy electronic states. This indicates that on formation of the donor–acceptor complex between urea and **bbp**, the excited state is modified leading to the quenching of fluorescence. Thus, self-association has a large effect on the optical properties of **bbp** in solution and could be used for the sensing of neutral guests.

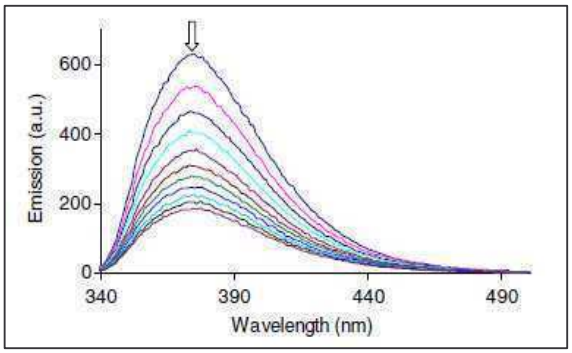

Figure 2.4: *Emission spectrum of receptor **bbp** (3.54 x 10^{-7} M in dry CH_3CN) during the titration with urea from 0 to 1 equiv (v/v).*

The formation of supramolecular complex between **bbp** and thiourea can be studied by the use fluorescence titration or quenching. The changes observed in the fluoresence spectra of a solution of **bbp** in acetonitrile on addition of up to 1.0 equivalents of thiourea are shown in figure 2.5. A large quenching in intensity of the 375 nm band was observed.

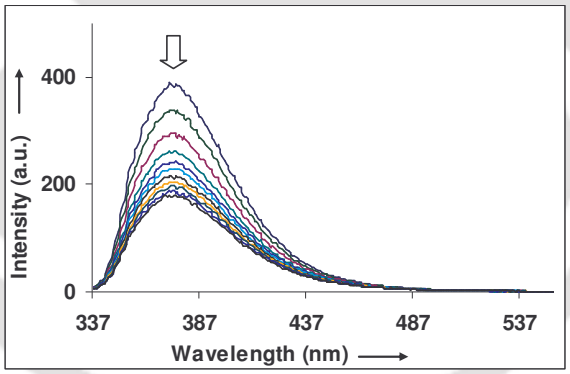

Figure 2.5: *Emission spectrum of receptor **bbp** (2.27 x 10^{-7} M in dry CH_3CN) during the titration with thiourea from 0 to 1 equiv (v/v).*

up to the addition of 1.0 equivalent of thiourea indicating that on formation of the donor-acceptor complex between thiourea and **bbp**, the excited state is modified leading to the quenching of fluorescence. Therefore, formation of donor-acceptor supramolecular complex modifies the optical properties of **bbp** in solution and could be employed for sensing neutral guests

2.2.3 Single Crystal X-ray analysis

The formation of supramolecular complex between **bbp** and urea in the solid state was confirmed by means of single crystal X-ray analysis. The crystal structures of the supramolecular complexes between **bbp** and urea in the ratios 1:1 and 2:1 are shown in Figure 2.6a. The crystallographic data are listed in table 2.1 and table 2.2 for the ratios 1:1 and 1:2 respectively. As observed from the ORTEP diagram, one receptor molecule and one urea molecule combine (left) forming a stable donor–acceptor complex in a 1:1 ratio (**bbp** : urea). The urea molecule fits into the cavity of **bbp** and is bound to the NH protons. In this complex, one receptor molecule donates two of its protons to the carbonyl oxygen of urea which is pointed inwards into its cavity. The donor–acceptor complex thus formed between the carbonyl oxygen of urea and NH protons of **bbp** is of the order (N2—H----O1) 2.85 Å and (N3—H----O1) 2.92 Å. Further, crystals of the 2:1 complex (**bbp** : urea) also successfully solved as represented in Figure 2.6a (right). It was again observed that the urea molecule prefers the cavity of **bbp** in order to form the hydrogen-bonded complex. The urea molecule acts like a bridge between two receptor molecules, accepting protons from one receptor and donating one of its NH_2 protons to another receptor forming a stable donor–acceptor complex involving two molecules of **bbp**. The bond distances between the carbonyl oxygen of urea and the NH protons of **bbp** are (N6—H----O5) 2.88 Å and (N10—H----O5) 2.93 Å, respectively, which are almost identical to the bond distances in the 1:1 complex. The distance between one of the urea NH_2 protons and the imine nitrogen of the second receptor was found to be (N15—H----N1) 2.99 Å. The cavity of this second molecule of receptor **bbp** is utilized to bind a water molecule having bond distances of 2.93 Å for (N2—H----O3) and (N5—H----O3). This evidence indicates good association of **bbp** with urea, leading to 1:1 and 2:1 adducts. This is the first crystallographic report on the formation of stable supramolecular complexes between a neutral receptor and urea.

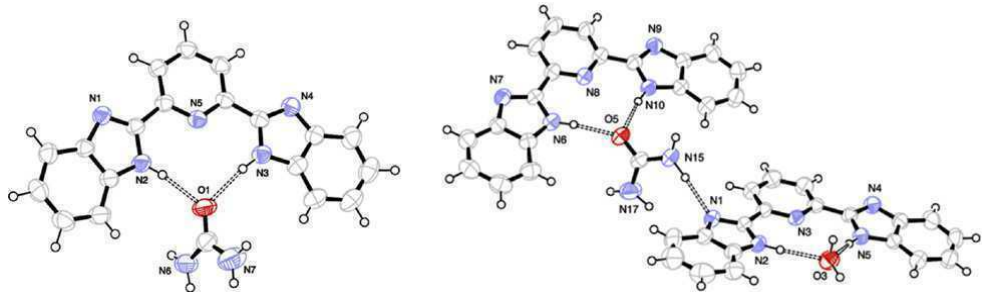

(a)

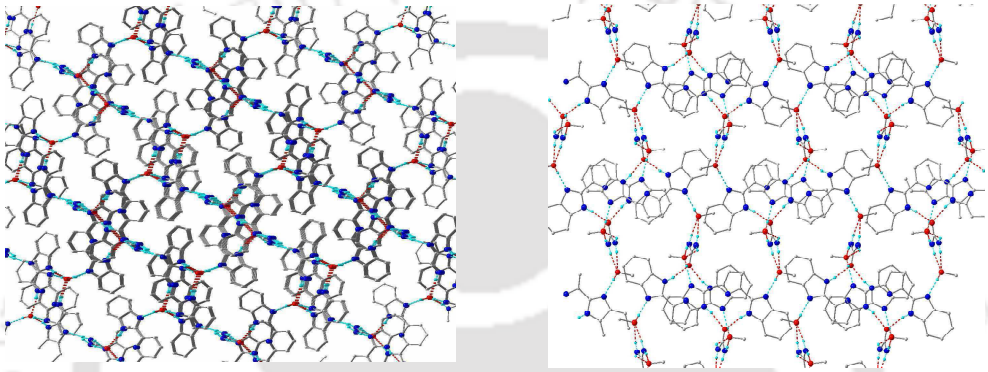

(b)

Figure 2.6: (a) *ORTEP diagrams of the hydrogen-bonded* ***bbp*** *: urea complex in the ratio 1:1 (left) and 2:1 (right). Solvent molecules omitted for clarity; (b) interlinking of* ***bbp*** *by urea using H-bonding.*

The X-ray structures of both 2:1 and 1:1 complexes along with the spectroscopic changes observed on the titration of urea and **bbp** are clear indications of the formation of supramolecular complexes in both solution and solid state. As the carbonyl oxygen of urea is pointed inwards into the cavity of receptor **bbp** in both the X-ray structures, the possibility of incorporating more substituted guests is greatly enhanced, which is usually very difficult with cyclic hosts. Both these hydrogen-bonded complexes are readily formed by simple mixing of **bbp** with urea in different ratios. The simple procedure to prepare **bbp** and its ability to form hydrogen-bonded complexes with amide linkages and water molecules opens up its utility for the recognition of several biologically relevant

molecules. Moreover, participation of the imine nitrogen in stabilizing the supramolecular structure is unique and enhances the recognition capabilities of receptor **bbp**.

Table 2.1: Crystallographic data for **bbp**:urea complex in methanol solvent.

	bbp:urea (1:1)
Formulae	$C_{22}H_{25}N_7O_3$
Mol. wt.	435.49
Crystal system	Monoclinic
Space group	*P*21/*n*
Temperature /K	298(2)
Wavelength /Å	0.71073
a /Å	7.4620(3)
b /Å	19.7030(9)
c /Å	15.0776(6)
α/°	90.00
β/°	97.583(3)
γ/°	90.00
V/ Å^3	2197.38(16)
Z	5
Density/g cm^{-3}	1.645
Abs. Coeff. /mm^{-1}	0.115
Refinement method	Full-matrix least-squares on F^2
WR_2(all data)	0.1420

Table 2.2: Crystallographic data for **bbp**:urea complex in acetonitrile solvent.

	bbp:urea (1:2)
Formulae	C_{39} H_{32} N_{12} O_2
Mol. wt.	700.77
Crystal system	Monoclinic
Space group	*P*21/*n*
Temperature /K	298(2)
Wavelength /Å	0.71073
a /Å	20.5454(6)
b /Å	7.5836(2)
c /Å	21.8464(6)
α/°	90.00
β/°	91.596(2)
γ/°	90.00
V/ $Å^3$	3402.53(16)
Z	4
Density/g cm^{-3}	1.368
Abs. Coeff. /mm^{-1}	0.090
Refinement method	Full-matrix least-squares on F^2
WR_2(all data)	0.1308

2.2.4 FT-IR Spectroscopy

The formation of supramolecular complexes was confirmed by FT-IR studies also. The FT-IR spectra of the complexes were recorded in KBr pellets. In the IR spectra characteristic absorptions are present for C=O or C=S stretching vibrations. Upon complexation these vibrations shift to a lower wave number ($\Delta\upsilon$ = 55 – 330 cm^{-1}), which is in agreement with the coordination of the oxygen or sulfur to N-H part of the **bbp** ligand.

The N-H peak of ligand at 3117 cm^{-1} shifted to 3447 cm^{-1} in the 1:1 complex and to 3208 cm^{-1} for 1:2 complex of urea:**bbp** complexes. Again, the C=O stretching frequency of urea (1678 cm^{-1}) shifts to a lower wave number of 1623 cm^{-1} upon complexation. Hence FT-IR can be applied to study the complex formation of **bbp** ligand with the neutral guests.

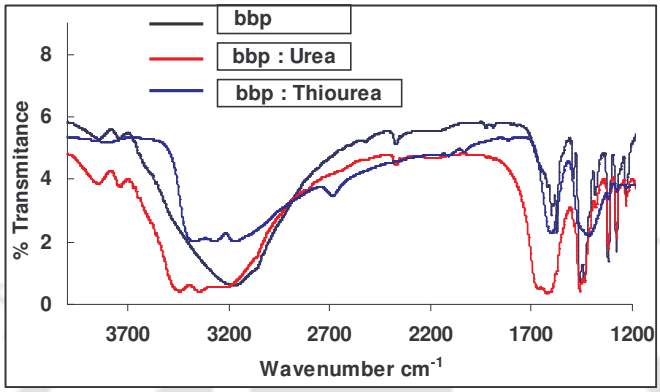

Figure 2.7: *FT-IR spectra of bbp:urea and bbp:thiourea complexes.*

2.2.5 Determination of association constant

The association constant (*K*a) calculated[10] for the 1:1 complex of **bbp** and urea and was found to be 44.38 M^{-1}, suggesting strong hydrogen bonding between **bbp** and urea. The association constant for **bbp** and thiourea was found to be 40.88 M^{-1}.

2.3 Conclusion

In summary, the present results demonstrate that 2,6-bis(2-benzimidazolyl)pyridine is an efficient receptor for binding urea with high affinity. Crystallographic analysis further revealed that receptor **bbp** utilizes its cavity and the imine nitrogen on its outer core to form stable supramolecular complexes with urea. Again, from the solution state properties of **bbp** ligand with thiourea also shows the utility of the ligand for the recognition of thiourea. The low concentration at which they operate and the low synthetic cost of preparing them make them ideal candidates for designing sensors and building supramolecular complexes with well-defined geometry.

2.4 Experimental Section

2.4.1 General

All reagents were used as received without further purification unless mentioned. These materials were of reagent grade or better. Acetonitrile was distilled from calcium hydride. UV/Vis spectra were recorded on a Perkin Elmer Lambda-25 spectrophotometer. Fluorescence spectra were recorded on a Varian Carry 25 spectrophotometer. FT-IR spectra were taken on a Perkin Elmer spectrophotometer with samples prepared as KBr pellets. ^{1}H-NMR spectra were obtained with a 400 MHz Varian FT spectrometer. Chemical shifts (ppm) were referenced to the residual solvent peaks. The data collections of single crystals were performed on a Bruker Nonius Smart Apex II X-ray single crystal diffractometer (CCD). Cell constants and orientation matrices for data collection were obtained from least-square refinement with a set of 45 narrow-frame (0.5º in ω) scans. The structure was solved by direct methods and refined by full-matrix least-squares calculations with SHELX97 software. All hydrogen atoms attached to heteroatoms were located in the difference fourier map and refined with isotropic displacement coefficients.

2.4.2 Preparation of bbp:urea complexs

The **bbp** ligand has been prepared by the known literature method.[8]

Preparation of bbp and urea complex in the ration 1:1:

A solution of urea (0.020 g, 33.3 mmol) in methanol was added dropwise to a methanolic solution of bbp (0.104 g, 33.3 mmol) and allowed to stir for 5 min. The vial containing the clear solution of the above mixture was allowed to stand (rt) for 48 h leading to the formation of crystals that were suitable for X-ray diffraction analysis.

Preparation of bbp and urea complex in the ration 2:1:

A solution of urea (0.010 g, 16.65 mmol) in acetonitrile was added dropwise to a solution of 1 (0.104 g, 33.3 mmol) in acetonitrile. The solution was allowed to stir for 5 min. The vial containing the clear solution of the above mixture was allowed to stand (rt) for 48 h leading to the formation of crystals that were suitable for X-ray diffraction analysis.

2.5 References:

1. (a) Martinez-Máñez, R.; Sancenón, F. *Chem. Rev*. **2003**, *103*, 4419–4476; (b) Sessler, J. L.; Camiolo, S.; Gale, P. A. *Coord. Chem. Rev*. **2003**, *240*, 17–55; (c) Beer, P. D.; Gale, P. A. *Angew. Chem., Int. Ed*. **2001**, *40*, 486–516; (d) *Lehn, J.-M. Supramolecular Chemistry, Concepts and Perspectives;VCH: Weinheim,Germany,* **1995**; pp 139–160.
2. (a) Lee, M.-E.; van der Vegt, F. A. N. 2006, 128, ; pp 4948–4949; (b) Cooke, I. J. *Nature* **1962**, *194*, 1262–1263; (c) Coombe, J. B.; Tribe, D. E. *Nature* **1958**, *182*, 116–117.
3. Morris, J. G.; Payne, E. J. Agri. Sci. 1970, 74, 259–271.
4. Johnson, D. *In Clinical Chemistry*; Taylor, E. H., Ed. Wiley: New York**, 1989**; pp 55–82.
5. (a) Bell, T.W.; Liu, J. *J. Am. Chem. Soc.* **1988**, *110*, 3673; (b) Ray, J.K.; Halder, M.K.; Gupta, S.; Kar, G.K. *Tetrahedron* **2000**, *56*, 909; (c) Goswami, S.; Mukherjee, R.; Ray, *J. Org. Lett*. **2005**, *7*, 1283.
6. *IARC,* **1974,** *7,* 95.
7. Ferrer, I.; and Durán, N. *Biotechnol. Lett*. **1987**, *5*, 361.
8. (a) Addison, A. W.; Burke, P. J. *J. Heterocycl. Chem*. **1981**, *18*, 803–805; (b) Addison, A. W.; Rao, T. N.; Wahlgren, C.G. *J. Heterocycl. Chem*. **1983**, *20*, 1481–1484.
9. (a) Cannon, W. R.; Madura, J. D.; Thummel, R. P.; McCammon, J. A. *J. Am. Chem. Soc.* **1993**, *115*, 879–884; (b) Hegde, V.; Hung, C. Y.; Madhukar, P.; Cunningham, R.; Hopfner, T.; Thummel, R. P. *J. Am. Chem. Soc*. **1993**, *115*, 872–878; (c) Hegde, V.; Madhukar, P.; Madura, J. D.; Thummel, R. P. *J. Am. Chem. Soc*. **1990**, *112*, 4549–4550.
10. Chou, P. T.; Wu, G. R.; Wei, C. Y.; Cheng, C. C.; Chang, C. P.; Hung, F. T. *J. Phys. Chem. B* **2000**, *104*, 7818–7829.

Abstract

2,6-*bis*(benzimidazol-2-yl)pyridine ligand has been demonstrated as a probe to detect toxic metabolites of benzene such as phenol, hydroquinone, resorcinol, catechol and p-benzoquinone. Supramolecular complex formation was studied by simple techniques like UV/Visible and fluorescence spectroscopy in solution state and by single crystal X-ray analysis in the solid state.

3.1 Introduction

Benzene and its metabolites which include phenols and quinones are carcinogens, known to cause the breakage and rearrangement of chromosomes in human, animal and yeast cells. Hydroquinone (benzene-1,4-diol) and catechol present in cigarette smoke are metabolites of benzene which result from the pyrolysis of naturally occurring flavonoids found in tobacco.[1] It has been demonstrated by several physiological studies that 'hydroquinone' and its oxidation product 'p-benzoquinone' are responsible for immunosuppression as well as myelotoxicity and are known to inhibit mitogen-stimulated activation of both T and B lymphocytes.[2] Besides their carcinogenic properties, these metabolites of benzene are present in several naturally occurring biomolecules such as Coenzyme Q (CoQ), in the form of hydroquinone or quinone fragments in their structures, due to which they are able to undergo redox interconversions in the living cells.[3] Among the several biochemical roles of CoQ, the most important one is in electron transport chain process, passing reduced species to the acceptors and in the direct electron transfer towards oxygen. CoQ also has structural resemblance with the vitamin K group of compounds that possess quinine rings. Thus, metabolites of benzene also play an important role in the biological cycles.

In spite of their important relevance to biology, there are very few synthetic receptors that form supramolecular adducts with all these small phenolic compounds.[4]

This chapter deals with the utilization of 2,6-*bis*(benzimidazol-2-yl)pyridine ligand, **bbp**, to detect various metabolites of benzene even in the presence of competitive solvent environment by the use UV/Visible and fluorescence spectroscopy and single crystal X–ray analysis, which is a proof of their potential application in chemical and biological sensing.

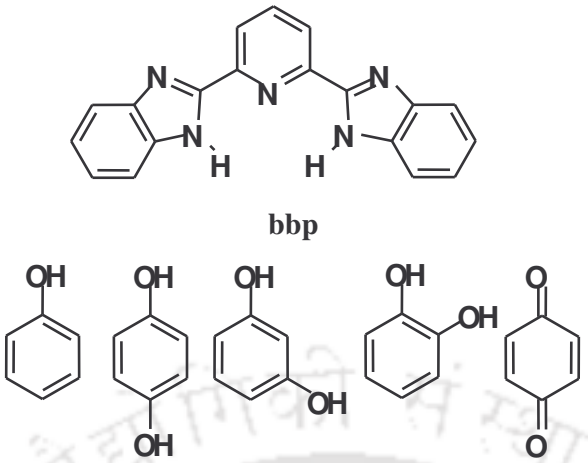

Figure 3.1: *2,6-Bis(2-benzimidazolyl)pyridine **bbp**, phenol, hydroquinone, resorcinol, catechol and p-benzoquinone.*

3.2 Results and Discussion

The **bbp** ligand has been prepared by the known literature method.[5]

3.2.1 UV/Visible Spectroscopy

Supramolecular complex formation was studied by simple technique of UV/Vis titration which was done in dry acetonitrile. The binding ability of receptor **bbp** was evaluated by titrating 0.1 equivalents of hydroquinone aliquots into a solution of **bbp** in acetonitrile at regular intervals and recording the changes in UV/Vis. It was observed that on increasing the concentration of hydroquinone, progressive decrease of intensity in the initial absorption band (Figure 3.2) having λ_{max} at 327 nm associated with the π-π^* transition of bbp resulted. Concurrently, a new peak at 294 nm with higher intensity develops which is due to the formation of stable complex between **bbp** and hydroquinone.

This family of spectra shows formation of an isosbestic point at 307 nm indicating the presence of at least one species at equilibrium. The inset in Figure 3.2 shows the changes in titration profile of the band at 327 nm corresponding to **bbp**: hydroquinone H-bonded complex. It was observed that the spectral features reached a limiting value only after the

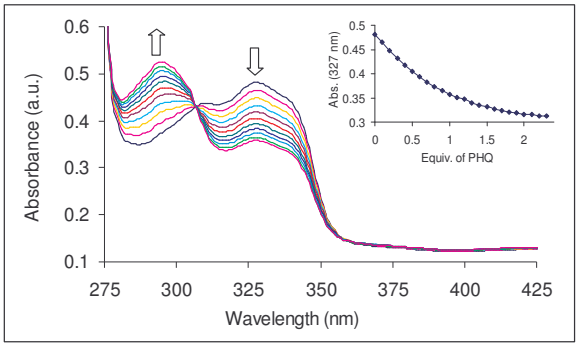

Figure 3.2: *UV/Vis spectra of **bbp** (8.46 x 10^{-6} M in dry CH_3CN) during titration with hydroquinone from 0-2 equivalents (v/v). Inset - Titration profile of the band at 327 nm corresponding to bbp: hydroquinone H-bonded complex.*

addition of 2.0 equivalents of hydroquinone (though the changes observed in the spectra on addition of 1.1 to 2.0 equivalents hydroquinone were very minor compared to the initial ten additions). Thus the gradual decrease in the band intensity at 327 nm and formation of a new higher intensity blue-shifted band at 294 nm with a clear isosbestic point is proof for the formation of hydrogen-bonded complex between **bbp** and hydroquinone. The association constant (K_a) for the 1:1 complex was calculated[6] to be 441 M^{-1} which is the highest value for the supramolecular adduct of any host with hydroquinone. The 33 nm blue shift in absorption spectra would not have occurred unless there were interactions between the hydroquinone and the imidazole ring of receptor **bbp**. The low concentrations at which these spectroscopic changes were observed clearly reveal that receptor **bbp** possesses excellent properties as a host material for recognizing phenolic guests in high affinity.

Similar UV/Vis (Figure 3.3) titration experiments of **bbp** were also performed with phenol, resorcinol, catechol and *p*-benzoquinone.

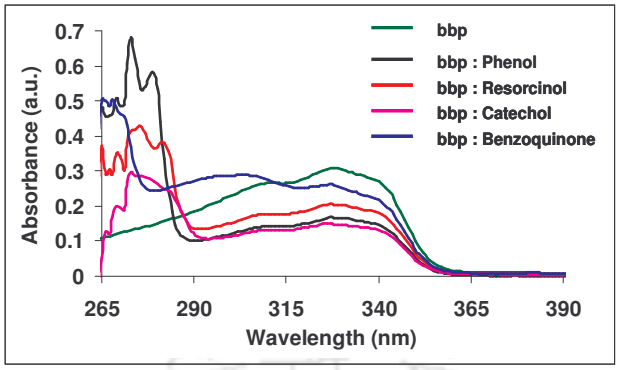

Figure 3.3: *UV/Vis spectra of **bbp** with phenol, resorcinol, catechol and benzoquinone in 1:1 ratio.*

The spectral variations observed for **bbp** on titrating with all these metabolites in a 1:1 ratio were unique for each guest, demonstrating the selective nature of **bbp** as a probe for recognizing different guest molecules.

3.2.2 Fluorescence Spectroscopy

The formation of supramolecular complex can be easily monitored by the use fluorescence titration or quenching. The changes observed in the fluoresence spectra of a solution of **bbp** in acetonitrile on addition of up to 2.0 equivalents of hydroquinone are shown in figure 3.4. A large quenching in intensity of the 375 nm band was observed up to the addition of 1.0 equivalent of hydroquinone indicating that on formation of the donor-acceptor complex between hydroquinone and **bbp**, the excited state is modified leading to the quenching of fluorescence.

The changes in the fluorescence spectra on adding further aliquots of hydroquinone to **bbp** were very minor, which is in agreement with the results of UV/Vis titration. Therefore, formation of donor-acceptor supramolecular complex modifies the optical properties of **bbp** in solution and could be employed for probing neutral guests.

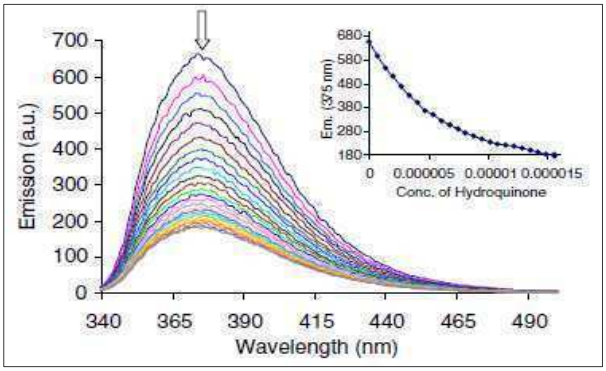

Figure 3.4: *Emission spectra of **bbp** (7.05 x 10^{-7} M in dry CH_3CN) during the titration with hydroquinone from 0-2 equivalents (v/v). Inset-plot of the emission intensity (375 nm) of **bbp** as a function of hydroquinone concentration*.

Similar fluorescence (Figure 3.5) titration experiments of **bbp** were also performed with phenol, resorcinol, catechol and *p*-benzoquinone.

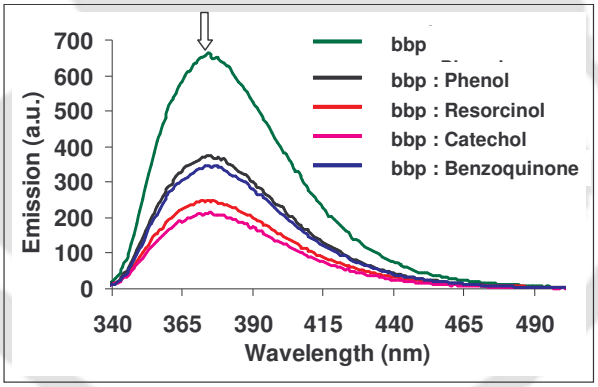

Figure 3.5: *Emission spectra of **bbp** with phenol, resorcinol, catechol and benzoquinone in 1:1 ratio*

The spectral variations observed for **bbp** on titrating with all these metabolites in a 1:1 ratio were unique for each guest, demonstrating the selective nature of **bbp** as a probe for recognizing different guest molecules.

3.2.3 Single Crystal X-ray analysis

The formation of supramolecular complex between **bbp** and hydroquinone in the solid state was confirmed by means of single crystal X-ray analysis. The ORTEP view (Figure 3.6) shows that **bbp** forms a stable supramolecular adduct with hydroquinone through the imine nitrogen located on its outer core via hydrogen-bonding. The O1—H·····N2 (imine) distance is found to be 2.67 Å, which indicates a fairly good association of **bbp** and hydroquinone. The hydroquinone molecule lies outside the cavity of **bbp** and seemed to deaggregate two receptor molecules by acting like a spacer between them. The inner cavity of **bbp** forms bonds with a molecule of water having bond distances of 3.00 Å for (N3—H·····O2) and 2.94 Å (N4—H····O2).

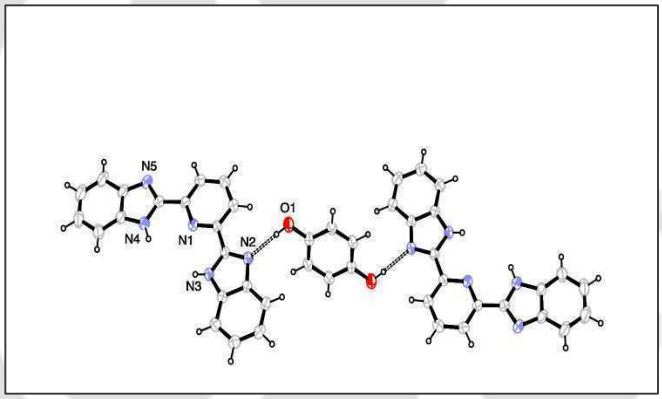

Figure 3.6: *ORTEP diagram of the hydrogen-bonded* ***bbp:****hydroquinone complex in the ratio 1:1. Solvent molecules are omitted for clarity.*

This is the first crystallographic report showing a novel supramolecular complex between imine nitrogen of receptor **bbp** with any phenolic guest. The supramolecular complex formation of **bbp** ligand with hydroquinone was also attempted in other solvents and good quality crystals of this complex could be obtained in several cases like ethanol, acetonitrile and the mixtures of any of these solvents with water indicating that even in competitive environments, **bbp** prefers to form a supramolecular complex with hydroquinone. The crystallographic data are listed in table 3.1 and table 3.2 for methanol and ethanol solvent

respectively. However, the bond distance of hydroquinone and **bbp** was shortest in the crystals that were grown in methanol. By acting as a spacer, hydroquinone seemed to also deaggregate molecules of receptor **bbp** in the solution state as observed by the increased intensity of the blue shifted peak until the formation of a stable supramolecular complex. These results are apparent indications that **bbp** is a smart receptor capable of recognizing different guest molecules having minor structural difference, depending on their size and nature, and by utilizing the NH groups on the inner cavity[7] and/or the nitrogen lone pairs on the outer core to form self-assembled supramolecular complexes with high affinity. It is important to note here that even in the presence of solvents like methanol and ethanol that would compete strongly with hydroquinone to form a supramolecular adduct, **bbp** is selective to hydroquinone and forms stable crystals that could be isolated and analyzed by x-ray diffraction.

Table 3.1: Crystallographic data for **bbp**:hydroquinone complex in methanol solvent

	bbp:hydroquinone
Formulae	$C_{23}H_{22}N_5O_3$
Mol. wt.	416.46
Crystal system	Monoclinic
Space group	*P*2(1)/*n*
Temperature /K	298(2)
Wavelength /Å	0.71073
a /Å	11.185(3)
b /Å	14.395(5)
c /Å	13.548(5)
α/°	90.00
β/°	103.03(2)
γ/°	90.00
V/ Å^3	2125.1(12)

Z	4
Density/g cm^{-3}	1.302
Abs. Coeff. /mm^{-1}	0.089
Refinement method	Full-matrix least-squares on F^2
WR_2(all data)	0.3102

Table 3.2: Crystallographic data for **bbp:**hydroquinone complex in ethanol solvent

	bbp:hydroquinone
Formulae	$C_{24}H_{24}N_5O_3$
Mol. wt.	430.48
Crystal system	Monoclinic
Space group	*P*2(1)/*n*
Temperature /K	298(2)
Wavelength /Å	0.71073
a /Å	11.3692(3)
b /Å	14.3746(5)
c /Å	13.6532(3)
α/°	90.00
β/°	102.425(2)
γ/°	90.00
V/ $Å^3$	2179.05(11)
Z	4
Density/g cm^{-3}	1.312
Abs. Coeff. /mm^{-1}	0.089
Refinement method	Full-matrix least-squares on F^2
WR_2(all data)	0.2284

3.3 Conclusion

In summary, **bbp** ligand has been shown to behave as an efficient receptor that performs recognition of several toxic metabolites of benzene with high sensitivity and selectivity. The value of binding constant calculated from the spectroscopic data showed that **bbp** is the highest affinity receptor that binds hydroquinone solely through hydrogen bonds. The formation of stable hydrogen-bonded supramolecular complex between **bbp** and hydroquinone is also shown by the X-ray structure analysis. In terms of simplicity, selectivity, binding strength and ease to perform molecular recognition, **bbp** is extremely efficient receptor that recognizes different metabolites of benzene with high efficiency, thereby extending its utility as a neutral receptor.

3.4 Experimental Section

3.4.1 General

All reagents were used as received without further purification unless mentioned. These materials were of reagent grade or better. Acetonitrile was distilled from calcium hydride. UV/Vis spectra were recorded on a Perkin Elmer Lambda-25 spectrophotometer. Fluorescence spectra were recorded on a Varian Cary Eclipse Fluorescence Spectrophotometer. The data collections of single crystals were performed on a Bruker Nonius Smart Apex II X-ray single crystal diffractometer (CCD). Cell constants and orientation matrices for data collection were obtained from least-square refinement with a set of 45 narrow-frame (0.5° in ω) scans. The structure was solved by direct methods and refined by full-matrix least-squares calculations with SHELX97 software. All hydrogen atoms attached to heteroatoms were located in the difference fourier map and refined with isotropic displacement coefficients.

3.4.2 Preparation of bbp:hydroquinone complex

The **bbp** ligand has been prepared by the known literature method.[5]

A solution of hydroquinone (0.030 g, 0.272 mmol) in methanol or ethanol was added dropwise to a methanolic or ethanolic solution of **bbp** (0.085 g, 0.272 mmol) and allowed to stir for 5 minutes. The vial containing the clear solution of the above mixture was allowed to stand (rt) for 24 hours leading to the formation of crystals that were suitable for X-ray diffraction analysis.

3.5 References:

1. (a) McCue, J.M.; Lazis, S.; Cohen, J.J.; Modiano, J.F.; Freed, B.M. *Mol. Immunology* **2003**, *39*, 995-1001. (b) Wallace, L. A. *Environ. Health Perspect* **1989**, *82*, 165-169.
2. Pyatt, D.W.; Stillman, W.S.; Irons, R.D. *Toxicology and Appl. Pharmacology* **1998**, *149(2)*, 178-184.
3. Ramasarma, T.; Lester, R.L. *J. Biol. Chem.* **1960**, *235*, 3309-3314.
4. (a) Kerckhoffs, J.M.C.A.; Ishi-I, T.; Paraschiv, V.; Timmerman, P.; Crego-Calama, M.; Shinkai, S.; Reinhoudt, D.N. *Org. Biomol. Chem.* **2003**, *1*, 2596-2603. (b) Krasowski, Matthew D.; Hong, Xuan; Hopfinger, A.J.; Harrison, Neil L. *J. Med. Chem.* **2002**, *45(15)*, 3210-3221.
5. (a) Addison, A. W.; Burke, P. J. *J. Heterocycl. Chem*. **1981**, *18*, 803–805. (b) Addison, A. W.; Rao, T. N.; Wahlgren, C G. *J. Heterocycl. Chem*. **1983**, *20*, 1481–1484.
6. Chou, P. T.; Wu, G.R.; Wei, C.Y.; Cheng, C.C.; Chang, C.P.; Hung, F.T. *J. Phys. Chem. B* **2000**, *104*, 7818-7829.
7. Chetia, B.; Iyer, P.K. *Tetrahedron Lett.* **2006,** *47*, 8115-8117.

Abstract

2,6-Bis(2-benzimidazolyl)pyridine, **bbp** a neutral tridentate ligand, is employed as a chemosensor for the detection of fluoride ions. The binding of anionic guest species with this ligand is studied using UV/Vis spectroscopy, fluorescence spectroscopy, and ^{1}H NMR techniques. The results indicate that **bbp** can be used as a chemical shift and optical modification based sensor for the detection of fluoride ions. Anion binding studies using ^{1}H NMR revealed that this receptor exhibits high selectivity for fluoride over chloride, bromide and iodide.

The interaction of this ligand with some of the other important anions e.g. acetate, bisulfate, perchlorate, tetrafluoroborate etc. also has been performed for comparison.

4a.1 Introduction

The development of synthetic receptors capable of selectively recognizing anions continues to attract a great deal of interest due to their significance in a plethora of biological, chemical, and environmental processes.[1] Despite their popularity, the design of 'substrate specific' synthetic receptors still remains a great challenge for supramolecular scientists due to (1) the large size of anions compared to the cations (Table 1.1) (2) the chemical environment that determines the strength of interaction and (3) the pH of the medium. Efforts to overcome the above challenges, foremost by Sessler,[2] Jeong,[3] Gale, and Beer[4] have led to considerable advancement of several classes of anion receptors and provided insight into newer host molecules. Numerous neutral receptors exist for anions; most of them containing –NH fragments which act as hydrogen bond donors for the anions.[5]

This chapter deals with the utilization of **bbp** towards the detection of anions by UV/Vis and fluorescence spectroscopy and ^{1}H NMR techniques.

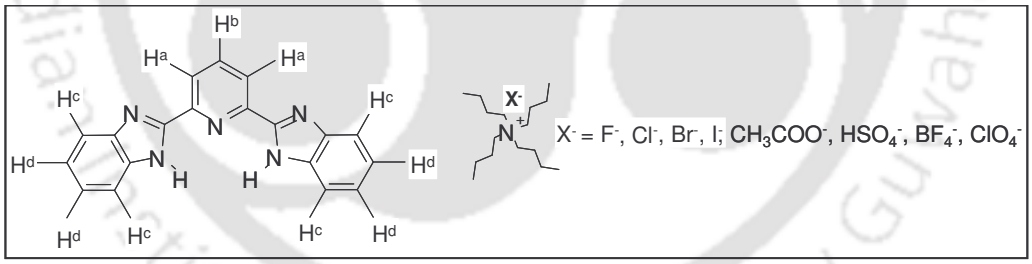

Figure 4a.1: *2,6-Bis(2-benzimidazolyl)pyridine,* ***bbp*** *and various anions.*

4a.2 Results and discussion

The ligand was prepared according to the known literature method.[6]

Ligand **bbp** has two –NH fragments that can form hydrogen bonded adducts with anions. It is structurally very simple, stable to heat / light and can be synthesized in one step from commercially cheap starting materials. Due to its well-defined internal cavity consisting of

two NH hydrogen atoms, **bbp** can function as an ideal host for the recognition of anions by hydrogen bonding interactions.

4a.2.1 ^{1}H-NMR Spectroscopy

Initial binding studies were carried out by adding the tetrabutyl-ammonium salts (TBAX) ($[Bu_4N]^+X^-$; $X^- = F^-, Cl^-, Br^-, I^-$) to a CD_3CN solution of **bbp**. The changes in the chemical shifts of **bbp** were examined by recording the ^{1}H NMR spectrum at room temperature (Figure 4a.2). The largest chemical shift for the aromatic protons of **bbp** was observed on adding the $[Bu_4N]^+$-fluoride salt, which indicated a strong interaction of **bbp** with F^-. Significant chemical shift changes (upon addition of the fluoride salt of $[Bu_4N]^+X^-$ to **bbp**), were observed for the H^c and H^d proton signals which were shifted upfield to 7.5 and 7.05 ppm, respectively, from the previous positions of 7.7 and 7.3 ppm. On the other hand, addition of the Cl^-, Br^- and I^- salts of $[Bu_4N]^+$ led to negligible changes in the chemical shifts of H^c and H^d protons (Figure 4a.2). Thus, it is safe to conclude that larger the anions, the more difficult it is to accommodate them within the cavity of **bbp**. The reason for the large chemical shift changes in **bbp**, on the addition of $[Bu_4N]^+F^-$ arises from the fact that F^- has a higher negative charge and better hydrogen bond acceptor properties compared to the other anions. When the fluoride anion and **bbp** form a complex adduct (with the –NH protons of the benzimidazole rings) a reasonably large conformational twist occurs to accommodate the fluoride in the cavity of **bbp**. This may be a further reason for the observed chemical shifts of the H^c and H^d protons. No chemical shift of the H^b protons present on the pyridine ring occurred while a negligible change in the position of the H^a proton position occurred after formation of a complex of **bbp** with fluoride anion, which rules out the possibility of the direct participation of the pyridine ring and its nitrogen in hydrogen bonding with the anions. Thus it could be easily predicted that fluoride ions form a hydrogen-bonded complex with the two – NH's present

at the inner cavity of **bbp** and in order to accommodate fluoride into this cavity, **bbp** undergoes a moderate twist. The smaller size of fluoride compared to chloride, bromide and iodide allows it to be accommodated in the cavity of **bbp**. Though, in all possibilities other anions form hydrogen bonded complexes with **bbp**, the larger diameter of these anions compared to fluoride may not allow them to enter the cavity of **bbp** due to steric reasons. These studies thus indicate that **bbp** can be used as a chemical sensor for the detection of fluoride anions among the halides and ^{1}H NMR could be employed as a chemical shift based probe.

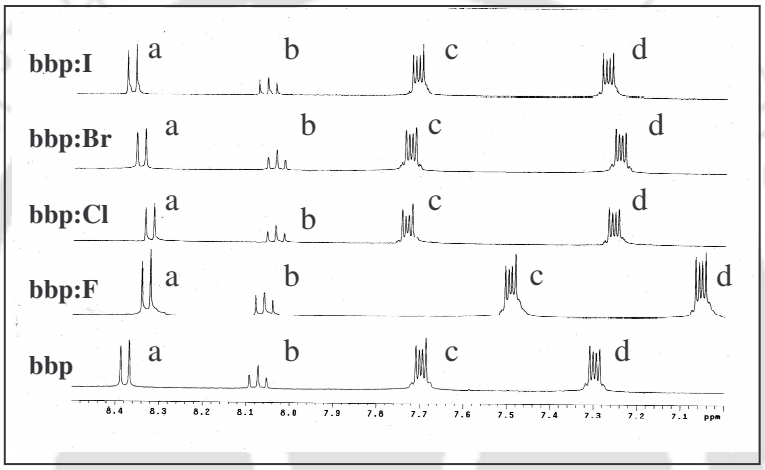

Figure 4a.2: *^{1}H NMR, 400 MHz spectra taken over the course of the titration of a CD_3CN solution of **bbp** with 1 equivalent of $[Bu_4N]^+F^-$, $[Bu_4N]^+Cl^-$, $[Bu_4N]^+Br^-$ and $[Bu_4N]^+I^-$.*

Similarly, ^{1}H-NMR titrations with other anions for example acetate, bisulfate, perchlorate, tetrafluoroborate etc. also has been done and their binding studies carried out by adding the tetrabutyl-ammonium salts (TBAX) ($[Bu_4N]^+X^-$; $X^- = CH_3COO^-$, HSO_4^-, BF_4^-, ClO_4^-) to a CD_3CN solution of **bbp**. The changes in the chemical shifts of **bbp** were examined by recording the ^{1}H NMR spectrum at room temperature (Figure 4a.3).

The largest chemical shift for the aromatic protons of **bbp** was observed on adding the $[Bu_4N]^+$-acetate salt, which indicated a strong interaction of **bbp** with CH_3COO^-. Significant chemical shift changes (upon addition of the acetate salt of $[Bu_4N]^+CH_3COO^-$ to **bbp**), were observed for the H^c and H^d proton signals. H^c protons were shifted

downfield to 7.82 from 7.7 ppm and H^d protons were shifted upfield to 7.2 from previous position of 7.3 ppm. Similarly, on addition of $[Bu_4N]^+HSO_4^-$ both H^c and H^d proton were also shifted. The H^c protons were shifted downfield to 7.75 from 7.7 ppm and H^d protons were shifted upfield to 7.16 from previous position 7.3 ppm. On the other hand, addition of the BF_4^- and ClO_4^- salts of $[Bu_4N]^+$ led to negligible changes in the chemical shifts of H^c and H^d protons.

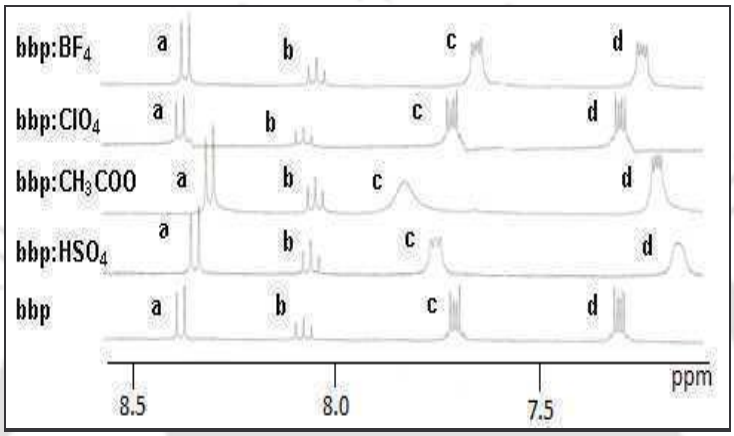

Figure 4a.3: *^1H NMR, 400 MHz spectra taken over the course of the titration of a CD_3CN solution of **bbp** with 1 equivalent of $[Bu_4N]^+CH_3COO^-$, $[Bu_4N]^+HSO_4^-$, $[Bu_4N]^+BF_4^-$ and $[Bu_4N]^+ClO_4^-$.*

4a.2.2 UV/Visible Spectroscopy

The interactions of **bbp** with the $[Bu_4N]^+X^-$ salts of fluoride, chloride, bromide and iodide were further investigated by spectrophotometric titration experiments in acetonitrile solution. The optical changes were evaluated by titrating 0.1 equivalents of anion aliquots into a solution of **bbp** at regular intervals and recording the changes in the UV/Visible spectra. In particular, a standard solution of $[Bu_4N]^+F^-$ was added as fixed aliquots to a standard solution of **bbp** (9.64×10^{-6} M) and the spectra are reported below (Figure 4a.4). Upon addition of fluoride, the band at 327 nm progressively decreased in intensity with broadening and a new peak at 311 nm appeared. Along with the above observation, a clear isosbestic point at 315 nm was observed. The formation of this isosbestic point indicates

that at least one stable species is present at equilibrium and that a stable complex forms between **bbp** and fluoride.

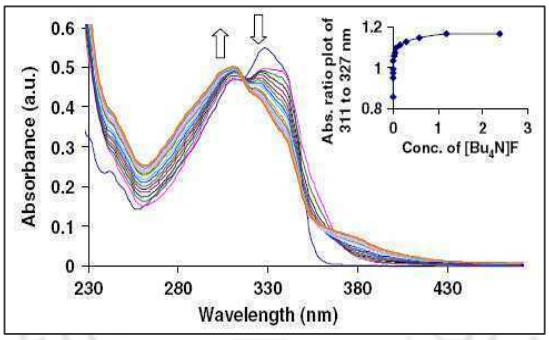

Figure 4a.4: *UV/Visible spectra of **bbp** (6.35 x 10^{-6} M in dry CH_3CN) during titration with $[Bu_4N]^+F^-$ from 0-2 equivalents (v/v). Inset-absorbance ratio plot of 311 nm to 327 nm as a function of fluoride ion concentration.*

The inset in Figure 4a.4 shows the changes in the titration profile of the band at 327 nm corresponding to the **bbp:**$[Bu_4N]^+F^-$, hydrogen bonded complex. On addition of 1 equivalent of fluoride, the band at 327 nm is totally quenched and a new peak corresponding to the **bbp**:fluoride complex appears at 311 nm. The association constant (*K*a) calculated[7] was found to be 439.49 M^{-1}, suggesting strong hydrogen bonding between **bbp** and fluoride.

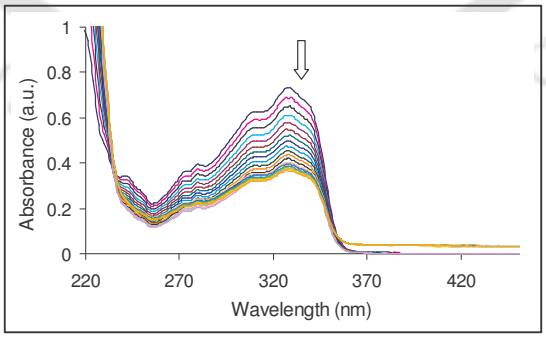

Figure 4a.5: *UV/Visible spectrum of **bbp** (7.87 x 10^{-6} M in dry CH_3CN) during the titration with $[Bu_4N]^+Cl^-$ from 0-2 equivalents.*

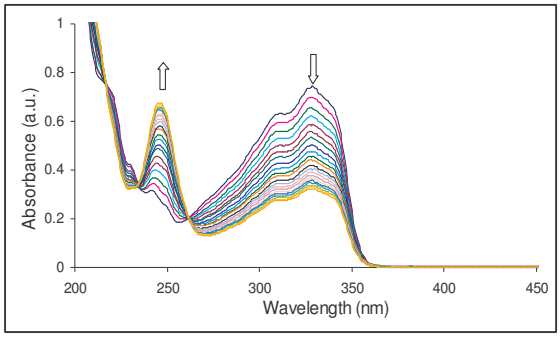

Figure 4a.6: *UV/Visible spectrum of **bbp** (7.32 x 10^{-6} M in dry CH_3CN) during the titration with $[Bu_4N]^+Br^-$ from 0-2 equivalents*

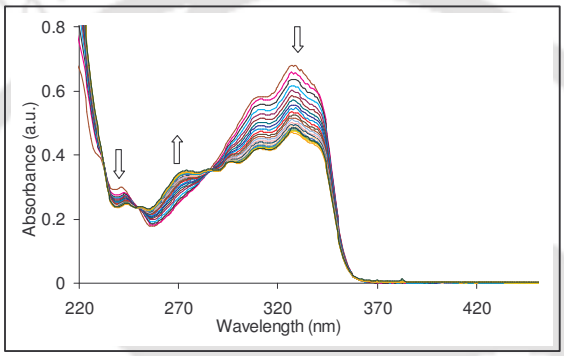

Figure 4a.7: *UV/Visible spectrum of **bbp** (8.53 x 10^{-6} M in dry CH_3CN) during the titration with $[Bu_4N]^+I^-$ from 0-2 equivalents*

Analogous investigations were carried out with Cl^-, Br^- and I^- and the titration experiments were monitored by UV/Visible spectroscopy (Figure 4a.5-7). An acetonitrile solution of **bbp** was titrated with a standard solution of tetrabutylammonium salt of the chosen anions. In all cases, a new absorption band developed on titration and sharp isosbestic points were observed in the recorded spectra. The spectral variations observed for **bbp** on titrating with the anions mentioned below is represented as a 1:1 ratio plot, where unique spectral features were observed for each anionic guest hydrogen bonded with **bbp**, thereby demonstrating the selective nature of **bbp** as a sensitive chemical sensor for recognizing different anionic guest molecules (Figure 4a.8).

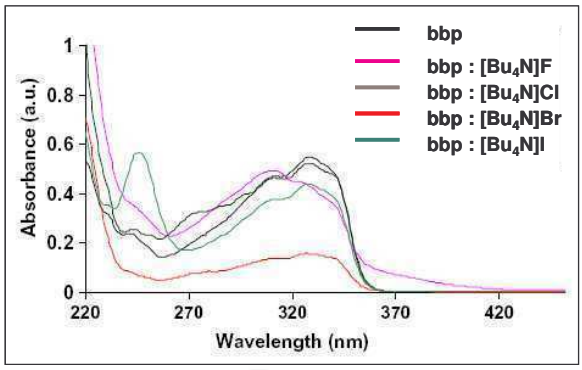

Figure 4a.8: *UV/Visible spectra of **bbp** with $[Bu_4N]^+F^-$, $[Bu_4N]^+Cl^-$, $[Bu_4N]^+Br^-$ and $[Bu_4N]^+I^-$ in 1:1 ratio.*

The interactions of **bbp** with the $[Bu_4N]^+$ salts of acetate, bisulfate, tetrafluoroborate, perchlorate were further investigated by spectrophotometric titration experiments in acetonitrile solution. The optical changes were evaluated by titrating 0.1 equivalents of anion aliquots into a solution of **bbp** at regular intervals and recording the changes in the UV/Vis spectra. In particular, a standard solution of $[Bu_4N]^+CH_3COO^-$ was added in fixed aliquots to a standard solution of **bbp** (8.62×10^{-6} M) and the spectra are reported below (Figure 4a.9). Upon addition of acetate, the band at 327 nm progressively decreased in intensity with broadening and a new peak of higher wavelength is formed at 368 nm.

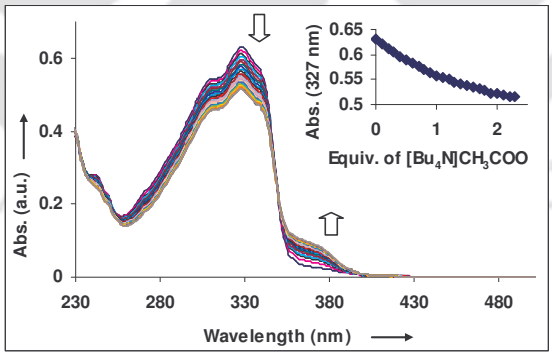

Figure 4a.9: *UV/Visible spectra of **bbp** (8.62×10^{-6} M in dry CH_3CN) during titration with $[Bu_4N]^+CH_3COO^-$ from 0-2 equivalents (v/v). Inset - Titration profile of the band at 327 nm corresponding to equivalent of $[Bu_4N]^+CH_3COO^-$.*

Along with the above observation, a clear isosbestic point at 350 nm was observed. The formation of this isosbestic point indicates that at least one stable species is present at equilibrium and that a stable complex forms between **bbp** and acetate.

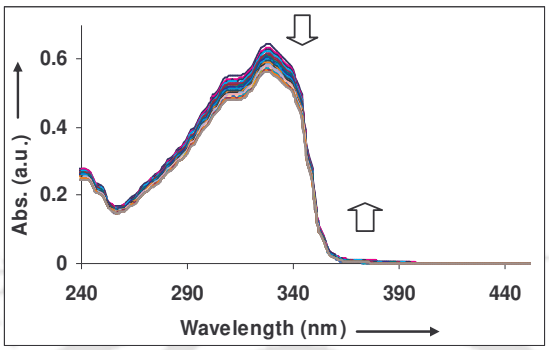

Figure 4a.10: *UV/Visible spectrum of **bbp** (8.32 x 10^{-6} M in dry CH_3CN) during the titration with $[Bu_4N]^+HSO_4^-$ from 0-2 equivalents.*

The inset in Figure 4a.9 shows the changes in the titration profile of the band at 327 nm corresponding to the **bbp:**$[Bu_4N]^+CH_3COO^-$, hydrogen bonded complex. On addition of 1 equivalent of acetate, the band at 327 nm is decreased and a new peak corresponding to the **bbp**:acetate complex appears at 368 nm. The association constant (K_a) calculated[7] was found to be 380.49 M^{-1}, suggesting strong hydrogen bonding between **bbp** and acetate

On addition of bisulfate anion, the peak at 327 nm is slightly decreased and red shifted. There is a formation of isosbestic point at 350 nm which is not so intense but indicating the presence of at least of one stable species at equilibrium and formation of stable complex between bbp and bisulfate (Fig. 4a.10).

Analogous investigations were carried out with ClO_4^- and BF_4^- and the titration experiments were monitored by UV/Visible spectroscopy (Figure 4a.11-12). An acetonitrile solution of **bbp** was titrated with a standard solution of

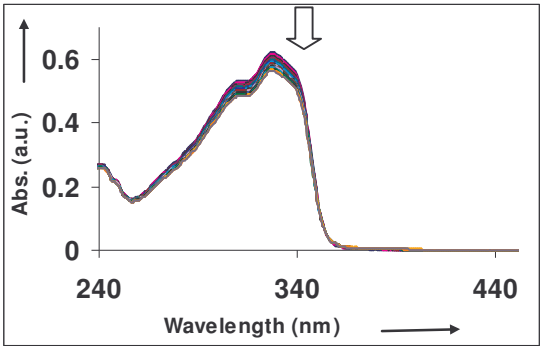

Figure 4a.11: *UV/Visible spectrum of **bbp** (7.58 x 10^{-6} M in dry CH_3CN) during the titration with $[Bu_4N]^+ClO_4^-$ from 0-2 equivalents.*

tetrabutylammonium salt of the chosen anions. In all cases, a new absorption band developed on titration and clear isosbestic points were observed in the recorded spectra. The spectral variations observed for **bbp** on titrating with the anions mentioned above is represented as a 1:1 ratio plot, where distinctive spectral features were observed for each anionic guest hydrogen bonded with **bbp**, thereby demonstrating the selective nature of **bbp** as a sensitive chemical sensor for recognizing different anionic guest molecules (Figure 4a.13).

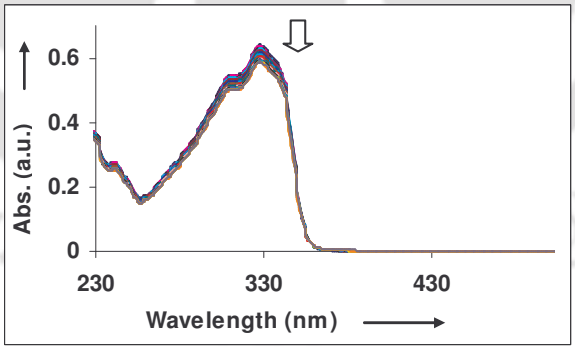

Figure 4a.12: *UV/Visible spectrum of **bbp** (7.62 x 10^{-6} M in dry CH_3CN) during the titration with $[Bu_4N]^+BF_4^-$ from 0-2 equivalents.*

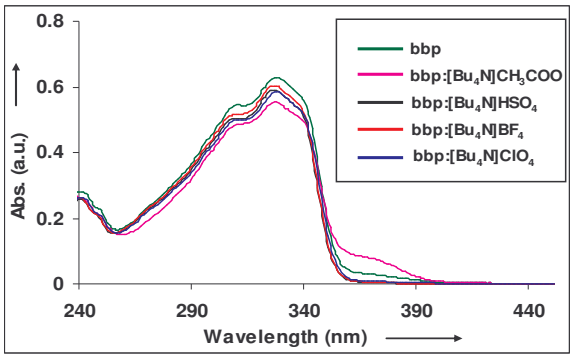

Figure 4a.13: *UV/Visible spectra of* ***bbp*** *with* $[Bu_4N]^+CH_3COO^-$, $[Bu_4N]^+HSO_4^-$, $[Bu_4N]^+ClO_4^-$ *and* $[Bu_4N]^+BF_4^-$ *in 1:1 ratio.*

4a.2.3 Fluorescence Spectroscopy

Fluorescence spectroscopy studies were also carried out in order to evaluate the ability of **bbp** to operate as a fluorescent anion sensor. Remarkable quenching of the fluorescence was observed on addition of anions. The changes observed in the fluorescence spectra of a solution of **bbp** in acetonitrile on adding up to 2.0 equivalents of $[Bu_4N]^+F^-$ are depicted in (Figure 4a.14). A large quenching (> 85%) in intensity of the 375 nm band was observed on the addition of 1.0 equivalent of $[Bu_4N]^+F^-$ indicating that on formation of the hydrogen bonded complex between $[Bu_4N]^+F^-$ and **bbp**, the excited state was modified considerably leading to the quenching of fluorescence. On continuous addition of $[Bu_4N]^+F^-$ to a solution of **bbp** the peak was slowly red shifted to 434 nm. The changes observed in the fluorescence spectra on adding more than 1 equivalent of $[Bu_4N]^+F^-$ aliquots to **bbp** were insignificant, which is in good agreement with the results of UV/visible titration. Figure 4a.14 inset shows the changes in the titration profile of the band at 373 nm corresponding to the **bbp :** $[Bu_4N]^+F^-$, hydrogen bonded complex.

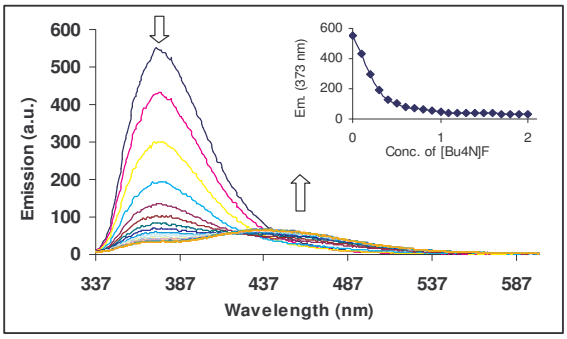

Figure 4a.14: *Emission spectra of **bbp** (7.05 x 10^{-7} M in dry CH_3CN) during the titration with $[Bu_4N]^+F^-$ from 0 to 2 equiv (v/v). Inset—plot of the emission intensity (373 nm) of **bbp** as a function of $[Bu_4N]^+F^-$ concentration.*

Analogous investigations were carried out with Cl^-, Br^- and I^- and the titration experiments were monitored by fluorescence spectroscopy (Figure 4a.15-17). An acetonitrile solution of **bbp** was titrated with a standard solution of tetrabutylammonium salt of the chosen anions. In all cases, a new band developed on quenching of fluorescence. The spectral variations observed for **bbp** on titrating with the anions mentioned above is represented as a 1:1 ratio plot, where unique spectral features were observed for each anionic guest hydrogen bonded with **bbp**, thereby demonstrating the selective nature of **bbp** as a sensitive chemical sensor for recognizing different anionic guest molecules (Figure 4a.18).

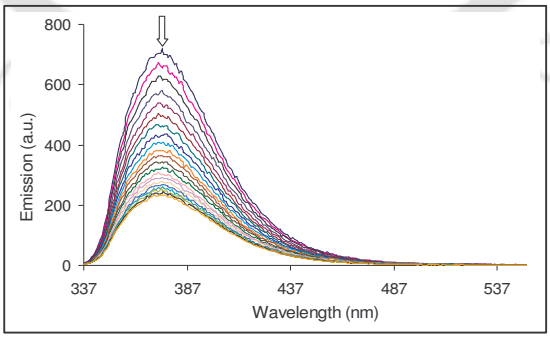

Figure 4a.15: *Emission spectra of **bbp** (8.99 x 10^{-7} M in dry CH_3CN) during the titration with $[Bu_4N]^+Cl^-$ from 0-2 equivalents.*

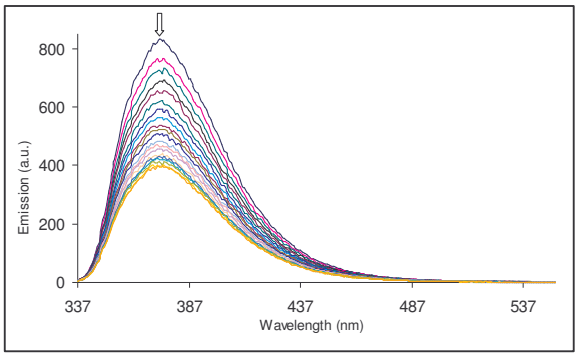

Figure 4a.16: *Emission spectra of **bbp** (7.32 x 10^{-7} M in dry CH_3CN) during the titration with $[Bu_4N]^+Br^-$ from 0-2 equivalents.*

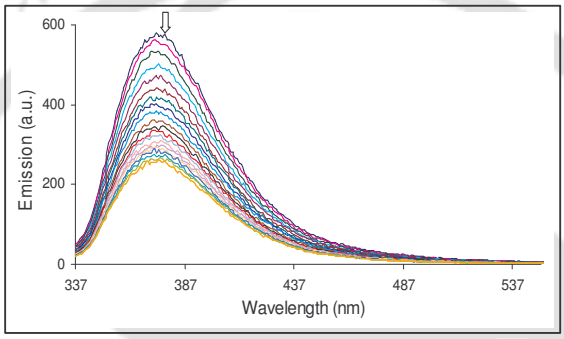

Figure 4a.17: *Emission spectra of **bbp** (1.052 x 10^{-6} M in dry CH_3CN) during the titration with $[Bu_4N]^+I^-$ from 0-2 equivalents.*

Fluorescence spectroscopy studies were further carried out with different anions such as acetate, bisulfate, perchlorate, tetrafluoroborate etc. in order to evaluate the ability of **bbp** to operate as a fluorescent anion sensor with these anions. Similarly, titration was performed by adding 0.1 equivalents of anion aliquots to the **bbp** solution at regular intervals to observe the fluorescence quenching of the receptor. In particular, a standard solution of $[Bu_4N]^+CH_3COO^-$ was added in fixed aliquots to a standard solution of **bbp** and the spectra are reported below (Figure 4a.19). A large quenching in intensity of the 375 nm band was observed on the addition of 1.0 equivalent of $[Bu_4N]^+CH_3COO^-$ indicating that on formation of the hydrogen bonded complex between $[Bu_4N]^+CH_3COO^-$

and **bbp**, the excited state was modified considerably leading to the quenching of fluorescence.

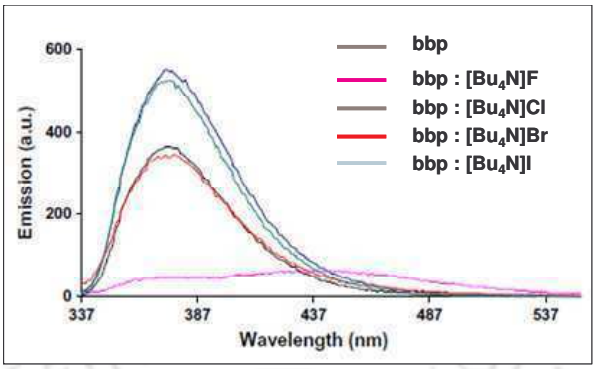

Figure 4a.18: *Emission spectra of **bbp** with $[Bu_4N]^+F^-$, $[Bu_4N]^+Cl^-$, $[Bu_4N]^+Br^-$ and $[Bu_4N]^+I^-$ in 1:1 ratio.*

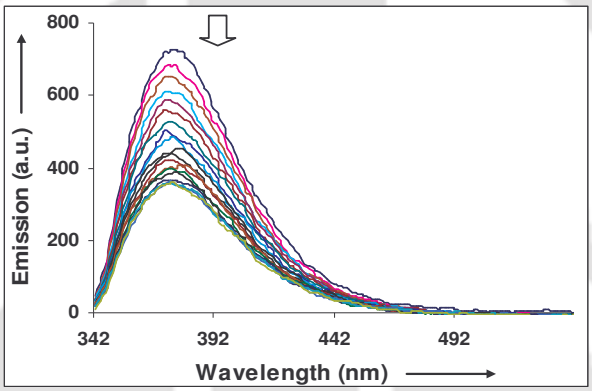

Figure 4a.19: *Emission spectra of **bbp** (7.2×10^{-7} M in dry CH_3CN) during the titration with $[Bu_4N]^+CH_3COO^-$ from 0-2 equivalents.*

Analogous investigations were carried out with HSO_4^-, ClO_4^- and BF_4^- and the titration experiments were monitored by fluorescence spectroscopy (Figure 4a.20-22). An acetonitrile solution of **bbp** was titrated with a standard solution of tetrabutylammonium salt of the chosen anions.

Among these, maximum quenching was observed for acetate in comparison to other anions which was also supported from UV/Vis and ^{1}H NMR titration values. The titrations of bbp with other anions are reported below (Figure 4a.20-22).

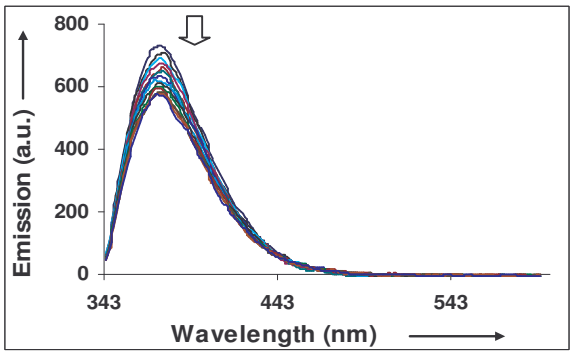

Figure 4a.20: *Emission spectra of **bbp** (7.2 x 10^{-7} M in dry CH_3CN) during the titration with $[Bu_4N]^+HSO_4^-$ from 0-2 equivalents.*

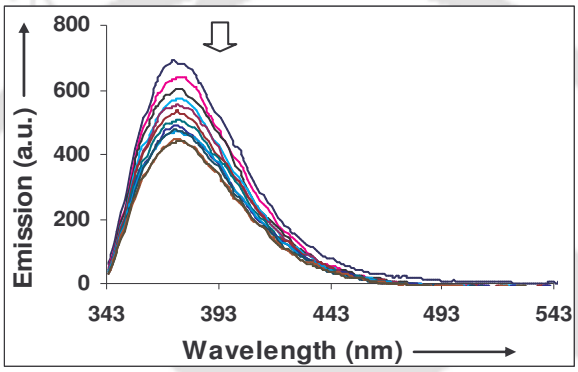

Figure 4a.21: *Emission spectra of **bbp** (6.8 x 10^{-7}M in dry CH_3CN) during the titration with $[Bu_4N]^+ClO_4^-$ from 0-2 equivalents.*

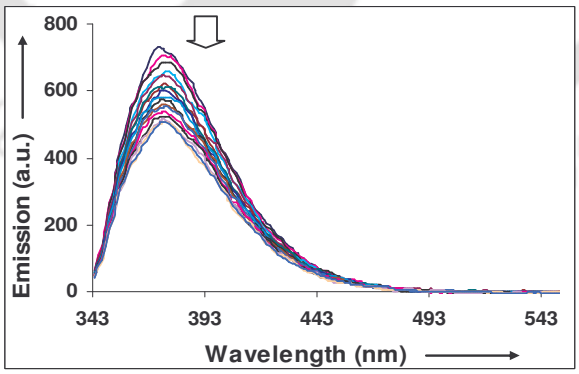

Figure 4a.22: *Emission spectra of **bbp** (7.8 x 10^{-7} M in dry CH_3CN) during the titration with $[Bu_4N]^+BF_4^-$ from 0-2 equivalents.*

In all cases, a new band developed on quenching of fluorescence but it is less prominent in comparison to acetate. The spectral variations observed for **bbp** on titrating with the anions mentioned below is represented as a 1:1 ratio plot, where unique spectral features were observed for each anionic guest, hydrogen bonded with **bbp**, thereby demonstrating the selective nature of **bbp** as a sensitive chemical sensor for recognizing different anionic guest molecules (Figure 4a.23).

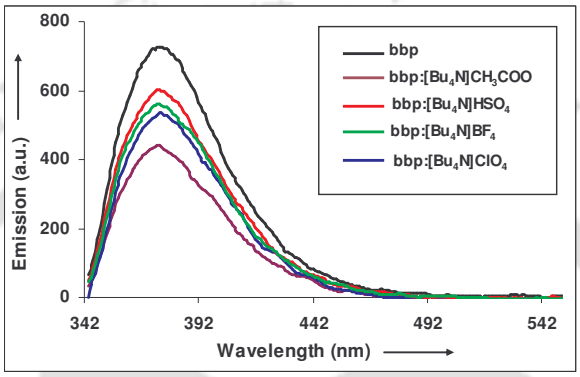

Figure 4a.23: *Emission spectra of* ***bbp*** *with* $[Bu_4N]^+CH_3COO^-$, $[Bu_4N]^+HSO_4^-$, $[Bu_4N]^+ClO_4^-$ *and* $[Bu_4N]BF_4$ *in 1:1 ratio.*

4a.2.4 Determination of Association constant

The association constants (K_a) calculated[7] from the UV/Vis plot at 327 nm show very strong binding of **bbp** with fluoride ions as compared with other anions studied here. (Table 4a.1) The UV/Vis and fluorescence data shows clearly that bbp can be used as a chemical sensor to detect fluoride anions.

Table 4a.1: Association constants (K_a) of **bbp** with anions in CH_3CN

Anions	K_a (M^{-1})
F^-	439.49
Cl^-	41.18
Br-	21.96
I^-	24.46
CH_3COO^-	380.49
HSO_4^-	102.18
ClO_4^-	32.96
BF_4^-	29.46

4a.3 Conclusion

In summary, anion sensing behavior of 2,6-bis(2-benzimidazolyl)pyridine, **bbp**, ligand has been studied. It shows high selectivity for fluoride over other anions at concentrations as low as 10^{-7} M. The binding of the above tridentate ligand with a series of anions was monitored by changes in ^{1}H NMR chemical shifts, as well as by UV/Visible and fluorescence spectroscopy. In the fluorescence titration large quenching was observed for fluoride anion in comparison to other anions that leads to **bbp** as a chemosensor for fluoride ion in comparison to other anions. Similar UV/Visible and ^{1}H NMR titrations of **bbp** with different anions also shows maximum binding with fluoride anion in comparison to other anion that also support for the chemosensor behavior of **bbp** for fluoride anion. The calculated binding constant was observed maximum for fluoride ion. In terms of simplicity and selectivity **bbp** can be used as a chemosensor for fluoride ion.

4a.4 Experimental Section

4a.4.1 General

All reagents were used as received without further purification unless mentioned. These materials were of reagent grade or better. Acetonitrile was distilled from calcium hydride. UV/Vis spectra were recorded on a Perkin Elmer Lambda-25 spectrophotometer. Fluorescence spectra were recorded on a Varian Cary Eclipse Fluorescence spectrophotometer. ^{1}H-NMR spectra were obtained with a 400 MHz Varian FT spectrometer. Chemical shifts (ppm) were referenced to the residual solvent peaks.

4a.5 References

1. (a) Martinez-Máñez, R.; Sancenón, F. *Chem. Rev*. **2003**, *103*, 4419–4476; (b) Beer, P. D.; Gale, P. A. *Angew. Chem. Int. Ed*. **2001**, *40*, 486–516; (c) Lehn, J.-M. *Supramolecular Chemistry, Concepts and Perspectives; VCH: Weinheim, Germany*, **1995**; pp. 139–160.
2. (a) Sessler, J. L.; Gross, D. E.; Cho, W.-S.; Lynch, V. M.; Schmidtchen, F. P.; Bates, G. W.; Light, M. E.; Gale, P. A. *J. Am. Chem. Soc.* **2006**, *128*, 12281–12288; (b) Miyaji, H.; Kim, H.-K.; Sim, E.-K.; Lee, C.-K.; Cho, W.-S.; Sessler, J. L.; Lee, C.-H. *J. Am. Chem. Soc.* **2005**, *127*, 12510–12512; (c) Sessler, J. L.; An, D.; Cho, W.-S.; Lynch, V.; Marquez, M. *Chem. Commun*. **2005**, *4*, 540–542; (d) Shevchuk, S. V.; Lynch, V. M.; Sessler, J. L. *Tetrahedron* **2004**, *60*, 11283–11291; (e) Miyaji, H.; Sessler, J. L. *Angew. Chem., Int. Ed.* **2001**, *40*, 154–157; (f) Anzenbacher, P., Jr.; Try, A. C.; Miyaji, H.; Jursikova, K.; Lynch, V. M.; Marquez, M.; Sessler, J. L. *J. Am. Chem. Soc*. **2000**, *122*, 10268–10272; (g) Anzenbacher, P., Jr.; Jursikova, K.; Sessler, J. L. *J. Am. Chem. Soc*. **2000**, *122*, 9350–9351; (h) Black, C. B.; Andrioletti, B.; Try, A. C.; Ruiperez, C.; Sessler, J. L. *J. Am. Chem. Soc*. **1999**, *121*, 10438–10439; (i) Shionoya, M.; Furuta, H.; Lynch, V.; Harriman, A.; Sessler, J. L. *J. Am. Chem. Soc*. **1992**, *114*, 5714–5722.
3. (a) Kim, N.-K.; Chang, K.-J.; Moon, D.; Lah, M. S.; Jeong, K.-S. *Chem. Commun*. **2007**, 3401–3403; (b) Lee, J.-Y.; Lee, M.-H.; Jeong, K.-S. *Supramol. Chem.* **2007**, *19*, 257–263; (c) Chang, K.-J.; Kang, B.-N.; Lee, M.-H.; Jeong, K.-S. *J. Am. Chem. Soc.* **2005**, *127*, 12214–12215; (d) Chang, K.-J.; Moon, D.; Lah, M. S.; Jeong, K.-S. *Angew. Chem., Int. Ed.* **2005**, *44*, 7926–7929.
4. (a) Bates, G. W.; Gale, P. A.; Light, M. E. *Chem. Commun.* **2007**, 2121–2123; (b) Garcia-Garrido, S. E.; Caltagirone, C.; Light, M. E.; Gale, P. A. *Chem. Commun*. **2007**, 1450–1452; (c) Gale, P. A.; Quesada, R. *Coord. Chem. Rev*. **2006**, 3219–3244;

(d) Vickers, M.; Martindale, K. S.; Beer, P. D. *J. Mater. Chem.* **2005**, *15*, 2784–2790; (e) Wong, W. W. H.; Vickers, M. S.; Cowley, A. R.; Paul, R. L.; Beer, P. D. *Org. Biomol. Chem*. **2005**, *3*, 4201–4208; (f) Curiel, D.; Cowley, A.; Beer, P. D. *Chem. Commun*. **2005**, 236–238; (g) Beer, P. D.; Gale, P. A. *Angew. Chem., Int. Ed*. **2001**, *40*, 486–516; (h) Beer, P. D.; Drew, M. G. B.; Gradwell, K. *J. Chem. Soc., Perkin Trans*. 2 **2000**, 511–519; (i) Beer, P. D.; Szemes, F.; Balzani, V.; Sala, C. M.; Drew, M. G. B.; Dent, S. W.; Maestri, M. *J. Am. Chem. Soc*. **1997**, *119*, 11864–11875.

5. Bianchi, A.; Bowman-J., K.; Garcia-Espana, E. *Supramolecular Chemistry of Anions,* Wiley-VCH, New York, **1997**.
6. (a) Addison, A. W.; Burke, P. J. *J. Heterocycl. Chem*. **1981**, *18*, 803–805. (b) Addison, A. W.; Rao, T. N.; Wahlgren, C G. *J. Heterocycl. Chem.* **1983**, *20*, 1481–1484.
7. Chou, P. T.; Wu, G. R.; Wei, C. Y.; Cheng, C. C.; Chang, C. P.; Hung, F. T. *J. Phys. Chem. B* **2000**, *104*, 7818-7829.

Abstract

1,3-bis(5,6-dimethyl-1H-benzo[d]imidazol-2-yl)benzene, **bbb** a neutral tridentate ligand, is employed as a chemosensor for the detection of different anions. The binding of anionic guest species with this ligand is studied using UV/Vis spectroscopy, fluorescence spectroscopy, and ^{1}H NMR techniques. The results indicate that **bbb** can be used as a chemical shift and optical modification based sensor for the detection of different anions. Anion binding studies using ^{1}H NMR and fluorescence spectroscopy revealed that this receptor exhibits high selectivity for fluoride over other anions.

4b.1 Introduction

The development of synthetic receptors capable of selectively recognizing anions continues to attract a great deal of interest due to their significance in a plethora of biological, chemical, and environmental processes.[1] In spite of recent advances and the variety of anion receptors developed so far, the problem of achieving strong and selective anion recognition has not yet been solved. Despite their popularity, the design of 'substrate specific' synthetic receptors still remains a great challenge for supramolecular scientists due to (1) the large size of anions compared to the cations (2) the chemical environment that determines the strength of interaction and (3) the pH of the medium. A number of researchers[2-4] tried to overcome the above challenges and have led to considerable advancement of several classes of anion receptors and provided insight into newer host molecules. Numerous neutral receptors exist for anions; most of them containing –NH fragments which act as hydrogen bond donors for the anions.[5] Isophthalamides are excellent anion receptors in organic solution and have been used by different groups in anion receptors.[6] Anthraquinones containing hydrogen bond donor groups have already been reported by different groups that bind and sense anions by color change.[7] But ligands having without fluorophore or additional signal part that can easily detect anions are very rare and is a research field of considerable interest.

This chapter deals with the utilization of 1,3-bis(5,6-dimethyl-1H-benzo[d]imidazol-2-yl)benzene, **bbb** ligand towards the detection of anions by UV/Vis and fluorescence spectroscopy and ^{1}H NMR techniques.

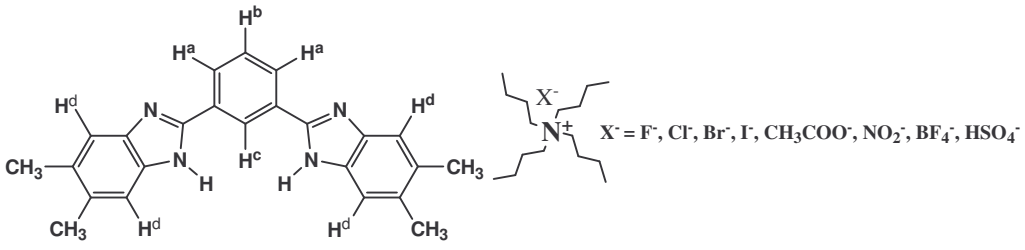

Figure 4b.1: *1,3-bis(5,6-dimethyl-1H-benzo[d]imidazol-2-yl)benzene,* ***bbb*** *and various anions.*

4b.2 Results and discussion

Ligand **bbb** has two –NH fragments and one –CH fragment that can form hydrogen bonded adducts with anions. It is structurally very simple, stable to heat / light and can be synthesized in one step from commercially cheap starting materials. In comparison to the 2,6-Bis(2-benzimidazolyl)pyridine, **bbp** ligand, **bbb** ligand contains four methyl groups in the benzimidazol part, because of the steric factor of the methyl groups **bbb** becomes more selective and that also enhances the solubility of the ligand. Again, as the "middle part" of the host ligand contains benzene ring instead of pyridine, the interaction of benzene –CH fragment with the anions can be well studied. So, its well-defined internal cavity consisting of two NH hydrogen atoms and CH hydrogen atoms, **bbb** can function as an ideal host for the recognition of anions by hydrogen bonding interactions.

4b.2.1 ^{1}H-NMR Spectroscopy

^{1}H NMR spectroscopy has been widely used to investigate receptor–substrate interactions and it can provide details of the interactions between the host and the guest. Initial binding studies were carried out by adding the tetrabutyl-ammonium salts (TBAX) ($[Bu_4N]^+X^-$; X^- = F^-, Cl^-, Br^-, I^-, CH_3COO^-, NO_2^-, BF_4^-, HSO_4^-) to a CD_3CN solution of **bbb**. The changes in the chemical shifts of **bbb** were examined by recording the ^{1}H NMR spectrum at room temperature (Figure 4b.2). The largest chemical shift for the aromatic protons of **bbb** was observed on adding the $[Bu_4N]^+$-fluoride salt, which indicated a strong interaction of **bbb** with F^-. Significant chemical shift changes (upon addition of the fluoride salt of $[Bu_4N]^+X^-$ to **bbb**), were observed for the H^a, H^b and H^c proton signals which were shifted upfield to 8.12, 7.92 and 7.86 ppm, respectively, from the positions of 8.2, 7.96 and 7.77 ppm. On the addition of chloride salt of $[Bu_4N]^+X^-$ to **bbb** no significant changes occur for H^a, H^b and H^d proton signals, however H^c proton signal shifted to 7.85 ppm from 7.77 ppm which is to some extent similar to F^-. On the other hand, addition of the Br^-, I^- and NO_2^- salts of

$[Bu_4N]^+$ led to negligible changes in the chemical shifts of all the protons. Again, on the addition of BF_4^-, no significant changes occur with the other protons except for H^c proton signal which is shifted to 7.71 ppm from 7.77 ppm. But, the addition of HSO_4^- anion shows significant spectral changes where all H^a, H^b and H^c proton signals shifted to downfield except for H^d proton signal. The values changed to 8.24, 8.02 and 7.84 from the original positions of 8.2, 7.96 and 7.77 ppm respectively. This shows that a very strong complex was formed between **bbb** and HSO_4^- also. It is likely that these strong interactions may be due to the protonation of the receptor by the anions which was observed in the ^1H NMR spectra the peak for H^c and H^d protons which became somewhat broader than the original peaks. Again, on the addition of CH_3COO^- salt of $[Bu_4N]^+X^-$ to **bbb**, H^a, H^b and H^c proton signals were shifted to 8.12, 7.88 and 7.76 ppm, respectively, from the positions of 8.2, 7.96 and 7.77 ppm. From the above chemical shift changes, we can conclude that larger the anions, the more difficult it is to accommodate them within the cavity of **bbb**. The other reason for the large chemical shift changes in **bbb**, on the

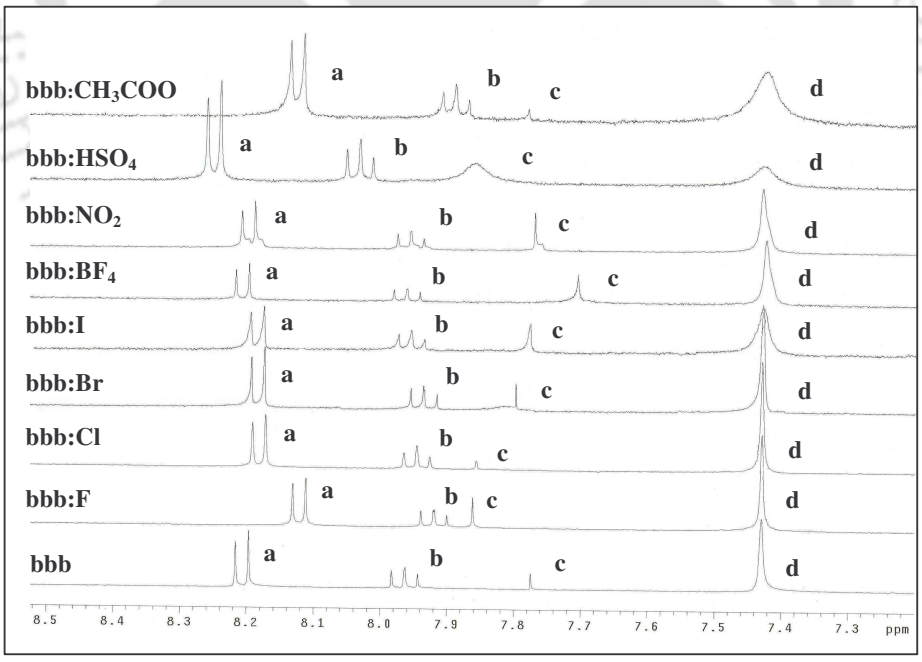

Figure 4b.2: *^1H NMR, 400 MHz spectra taken over the course of the titration of a CD_3CN solution of **bbb** with 1 equivalent of $[Bu_4N]^+F^-$, $[Bu_4N]^+Cl^-$, $[Bu_4N]^+Br^-$, $[Bu_4N]^+I$, $[Bu_4N]^+CH_3COO^-$, $[Bu_4N]NO_2^-$, $[Bu_4N]^+BF_4^-$, $[Bu_4N]^+HSO_4^-$.*

addition of $[Bu_4N]^+F^-$ is attributed to the fact that F^- has a higher negative charge and better hydrogen bond acceptor properties compared to the other anions. Although, Cl^- ion shows chemical shift changes similar to F^- ion for H^c proton signals, it does not show any significant changes with other protons, which clearly shows that the cavity may not be enough to accommodate the Cl^- ion in its cavity. When the fluoride anion and **bbb** form a complex adduct (with the –NH protons of the benzimidazole rings and –CH protons of the benzene ring) a reasonably large conformational twist occurs to accommodate the fluoride in the cavity of **bbb** as well as the –CH protons of the benzene ring also bind to the F^- ion through hydrogen bonding, because of which large chemical shifts was observed for the H^a and H^b protons. These chemical shift changes also rules out the possibility of the direct participation of the benzene ring –CH protons in hydrogen bonding with the anions. Thus, it could be easily predicted that fluoride ions form a hydrogen-bonded complex with the two – NH's and one –CH protons of the benzene ring present at the inner cavity of **bbb**, and in order to accommodate fluoride into its cavity, **bbb** undergoes a moderate twist. The smaller size of fluoride compared to other anions allows it to be accommodated in the cavity of **bbb**. Though, in all possibilities other anions form hydrogen bonded complexes with **bbb**, the larger diameter of these anions compared to fluoride may not allow them to enter the cavity of **bbb** due to steric reasons. These studies thus indicate that **bbb** can be used as a chemical sensor for the detection of fluoride anions among the halides and ^1H NMR could be employed as a chemical shift based probe.

4b.2.2 UV/Visible Spectroscopy

The interactions of **bbb** with the tetrabutyl-ammonium salts (TBAX) ($[Bu_4N]^+X^-$; $X^- = F^-$, Cl^-, Br^-, I^-, CH_3COO^-, NO_2^-, BF_4^-, HSO_4^-) were further investigated by spectrophotometric titration experiments in acetonitrile solution. The optical changes were evaluated by titrating 0.1 equivalents of anion aliquots into a solution of **bbb** at regular intervals and

recording the changes in the UV/Vis spectra. In particular, a standard solution of $[Bu_4N]^+F^-$ was added in fixed aliquots to a standard solution of **bbb** (8.24 x 10^{-6} M) and the spectra are reported below.(Figure 4b.3) Upon addition of fluoride, the band at 339 nm progressively decreased in intensity with broadening and a clear isosbestic point at 368 nm was observed. The formation of this isosbestic point indicates that at least one stable species is present at equilibrium and that a stable complex forms between **bbb** and fluoride.

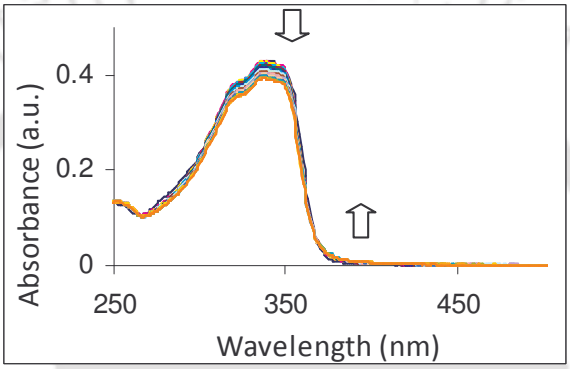

Figure 4b.3: *UV/Visible spectra of **bbb** (8.24 x 10^{-6} M in dry CH_3CN) during titration with $[Bu_4N]^+F^-$ from 0-2 equivalents (v/v)*

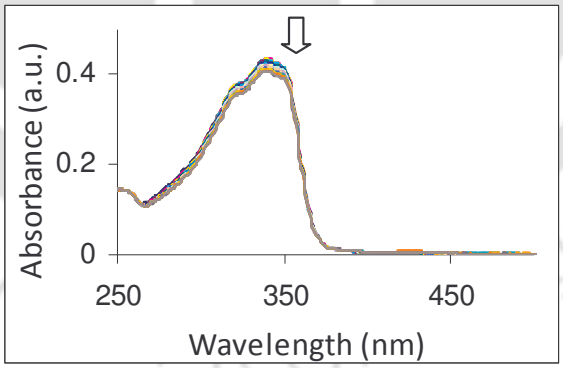

Figure 4b.4: *UV/Visible spectrum of **bbb** (8.30 x 10^{-6} M in dry CH_3CN) during the titration with $[Bu_4N]^+CH_3COO^-$ from 0-2 equivalents.*

Analogous investigations were carried out with Cl^-, Br^-, I^-, CH_3COO^-, NO_2^-, BF_4^- and HSO_4^- and the titration experiments were monitored by UV/Visible spectroscopy (Figure 4b.4-5). An acetonitrile solution of **bbb** was titrated with a standard solution of

tetrabutylammonium salt of the chosen anions. In all cases, the peak at 339 nm was decreased on titration and a new peak was observed in the recorded spectra but the shift was very minor.

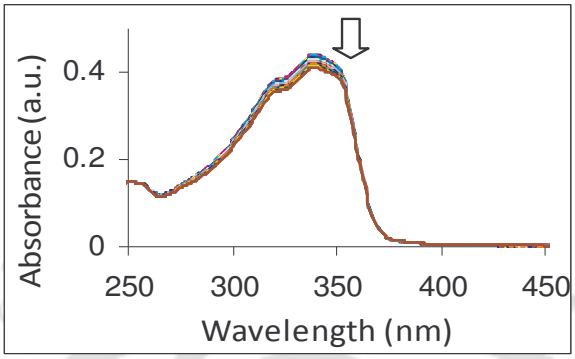

Figure 4b.5: *UV/Visible spectrum of **bbb** (8.44 x 10^{-6} M in dry CH_3CN) during the titration with $[Bu_4N]^+HSO_4^-$ from 0-2 equivalents.*

The spectral variations observed for **bbb** on titrating with the anions mentioned below is represented as a 1:1 ratio plot, where unique spectral features were observed for each anionic guest bonded with **bbb**, thereby demonstrating the selective nature of **bbb** as a sensitive chemical sensor for recognizing different anionic guest molecules (Figure 4b.6).

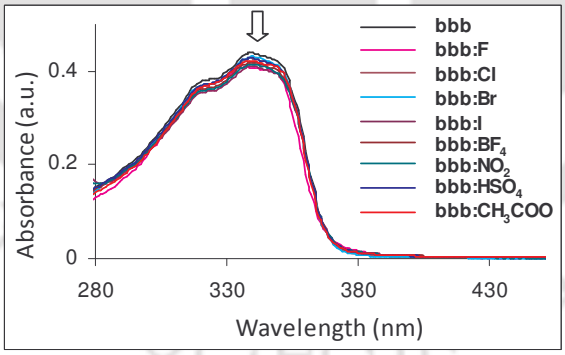

Figure 4b.6: *UV/Visible spectra of **bbb** with $[Bu_4N^+]F^-$, $[Bu_4N]^+Cl^-$, $[Bu_4N]^+Br^-$, $[Bu_4N]^+I^-$. $[Bu_4N]^+CH_3COO^-$, $[Bu_4N]^+NO_2^-$,$[Bu_4N]^+BF_4^-$, $[Bu_4N]^+HSO_4^-$ in 1:1 ratio.*

4b.2.3 Fluorescence Spectroscopy

Fluorescence spectroscopy studies were also carried out in order to evaluate the ability of **bbb** to operate as a fluorescent anion sensor. Remarkable quenching of the fluorescence

was observed on addition of anions. The changes observed in the fluorescence spectra of a solution of **bbb** in acetonitrile on adding up to 2.0 equivalents of $[Bu_4N]^+F^-$ are depicted in (Figure 4b.7). A large quenching (> 75%) in intensity of the 393 nm band was observed on the addition of 1.0 equivalent of $[Bu_4N]^+F^-$ indicating that on formation of the hydrogen bonded complex between $[Bu_4N]^+F^-$ and **bbb**, the excited state was modified considerably leading to the quenching of fluorescence. On continuous addition of $[Bu_4N]^+F^-$ to a solution of **bbb** the peak was slowly red shifted to 403 nm. The changes observed in the fluorescence spectra on adding more than 1 equivalent of $[Bu_4N]^+F^-$ aliquots to **bbb** were insignificant, which is in good agreement with the results of UV/Vis titration. Figure 4b.7 inset shows the changes in the titration profile of the band at 393 nm corresponding to the **bbb :** $[Bu_4N]^+F^-$, hydrogen bonded complex.

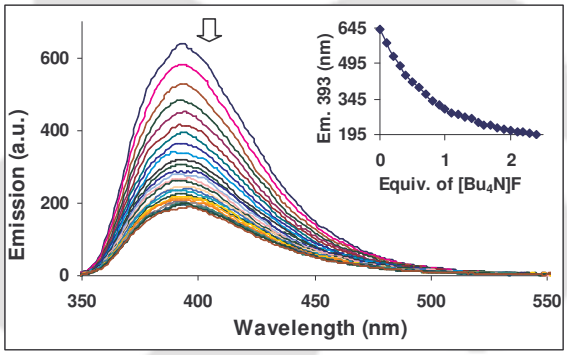

Figure 4b.7: *Emission spectra of **bbb** (6.24 x 10^{-7} M in dry CH_3CN) during the titration with $[Bu_4N]^+F^-$ from 0 to 2 equiv (v/v). Inset—plot of the emission intensity (393 nm) of **bbb** as a function of $[Bu_4N]^+F^-$ equivalent..*

Analogous investigations were carried out with Cl^-, Br^-, I^-, CH_3COO^-, NO_2^-, BF_4^- and HSO_4^- and the titration experiments were monitored by fluorescence spectroscopy (Figure 4b.8-9). An acetonitrile solution of **bbb** was titrated with a standard solution of tetrabutylammonium salt of the chosen anions. In particular, a standard solution of $[Bu_4N]^+CH_3COO^-$ was added as fixed aliquots to a standard solution of **bbb** and the spectra are reported below (Figure 4b.8). A large quenching in intensity of the 393 nm

band was observed on the addition of 1.0 equivalent of $[Bu_4N]^+CH_3COO^-$ indicating that on formation of the hydrogen bonded complex between $[Bu_4N]^+CH_3COO^-$ and **bbb**, the excited state was modified considerably leading to the quenching of fluorescence. Again, on the addition of 1.0 equivalent of $[Bu_4N]^+Cl^-$, large quenching in intensity of the 393 nm band was observed but that was less in comparison to F^- or CH_3COO^-.

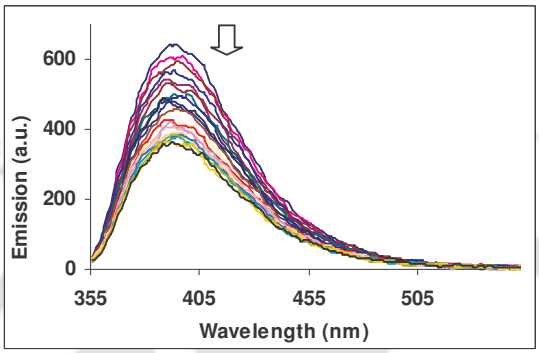

Figure 4b.8: *Emission spectra of **bbb** (6.26 x 10^{-7} M in dry CH_3CN) during the titration with $[Bu_4N]^+CH_3COO^-$ from 0-2 equivalents.*

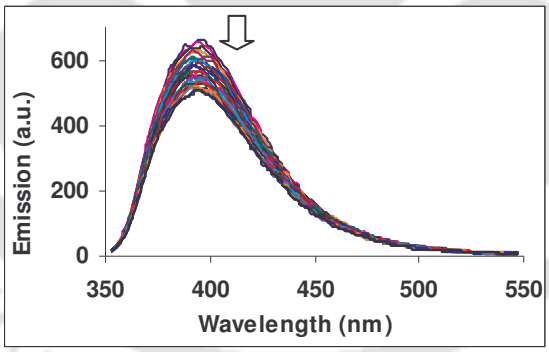

Figure 4b.9: *Emission spectra of **bbb** (6.49 x 10^{-7} M in dry CH_3CN) during the titration with $[Bu_4N]^+Cl^-$ from 0-2 equivalents.*

Similarly with the other anions also, a new band developed on quenching of fluorescence and the quenching intensity by the anions is maximum of 60% which is less in comparison to $[Bu_4N]^+F^-$. The spectral variations observed for **bbb** on titrating with the anions mentioned below is represented as a 1:1 ratio plot, where unique spectral features were observed for each anionic guest bonded with **bbb**, thereby demonstrating the selective

nature of **bbb** as a sensitive chemical sensor for recognizing different anionic guest molecules (Figure 4b.10).

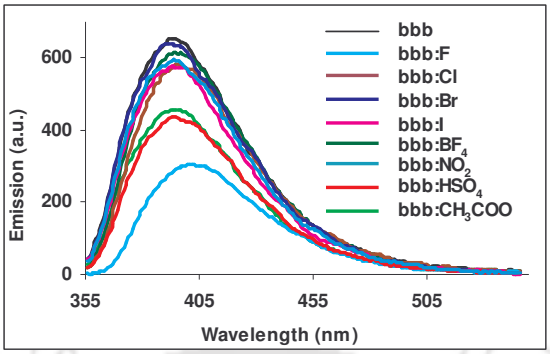

Figure 4b.10: *Emission spectra of **bbb** with $[Bu_4N]^+F^-$, $[Bu_4N]^+Cl^-$, $[Bu_4N]^+Br^-$, $[Bu_4N]^+I^-$ $[Bu_4N]^+CH_3COO^-$, $[Bu_4N]^+NO_2^-$,$[Bu_4N]^+BF_4^-$, $[Bu_4N]^+HSO_4^-$ in 1:1 ratio.*

4b.2.4 Determination of Association constant

The association constants (K_a) calculated[8] from the UV/Visible plot at 339 nm show very strong binding of **bbb** with fluoride ions as compared with other anions studied here. (Table 4b.1) The UV/Visible and fluorescence data shows clearly that **bbb** can be used as a chemical sensor to detect fluoride anions.

Table 4b.1: Association constants (K_a) of **bbb** with anions in CH_3CN

Anions	K_a (M^{-1})
F^-	502.79
Cl^-	61.12
Br-	20.63
I^-	18.22
CH_3COO^-	186.32
HSO_4^-	242.16
NO_2^-	29.46
BF_4^-	32.96

4b.3 Conclusion

In summary, a new ligand 1,3-bis(5,6-dimethyl-1H-benzo[d]imidazol-2-yl)benzene, **bbb** was synthesized and anion sensing behavior of this ligand has been studied carefully. The binding of the above tridentate ligand with a series of anions was monitored by changes in ^{1}H NMR chemical shifts, as well as by UV/Vis and fluorescence spectroscopy. The interaction of -CH fragment of benzene part as well as –NH fragment of imidazol part with different anions has been well studied. From ^{1}H NMR data it was clear that the position of –CH fragment (H^c proton) was modified on the addition of different anions which confirmed the hydrogen bonding interaction of this –CH unit with the anions. The sequence of binding constants of the different anions with the receptor decreases from F^- to I^-. The receptor also binds with acetate and bisulfite anions although their strength is less in comparison to fluoride and as confirmed from fluorescence and ^{1}H NMR data. **bbb** shows high selectivity for fluoride over other anions at concentrations as low as 10^{-7} M. Among all the anions, F^- establishes the strongest H-bond interaction with both –NH and –CH fragment of the benzimidazol moiety. From both selectivity and ease of use, it is clear that **bbb** can be used as a sensor for fluoride anion.

4b.4 Experimental Section

4b.4.1 General

All reagents were used as received without further purification unless mentioned. These materials were of reagent grade or better. Acetonitrile was distilled from calcium hydride. UV/Vis spectra were recorded on a Perkin Elmer Lambda-25 spectrophotometer. Fluorescence spectra were recorded on a Varian Cary Eclipse Fluorescence spectrophotometer. ^{1}H-NMR spectra were obtained with a 400 MHz Varian FT spectrometer. Chemical shifts (ppm) were referenced to the residual solvent peaks.

Preparation of bbb ligand

Isophthalic acid (Aldrich, 0.50 g) and 4,5-Dimethyl-benzene-1,2-diamine (Aldrich, 0.90 g) were dispersed in orthophosphoric acid (Aldrich, 10cm^3), and heated for 4h at 220°C. Whilst still hot, the resulting solution was poured into cold distilled water (1 dm^3) with vigorous stirring. The resulting blue precipitate was collected by filtration, then dispersed in 500cm^3 of hot 10% (w/v) Na_2CO_3 (aq) and stirred for 30min. The insoluble material was collected by filtration, dispersed in cold distilled water (800cm^3), and adjusted to pH 4 using 10% (v/v) HCl (aq) then recovered by filtration and recrystallized from the minimum amount of methanol. The final product obtained was a white powder (90%, 0.90 g) with a melting point in excess of 250°C.

4b.5 References

1. (a) Martinez-Máñez, R.; Sancenón, F. *Chem. Rev*. **2003**, *103*, 4419–4476; (b) Beer, P. D.; Gale, P. A. *Angew. Chem. Int. Ed*. **2001**, *40*, 486–516; (c) Lehn, J.-M. *Supramolecular Chemistry, Concepts and Perspectives; VCH: Weinheim, Germany*, **1995**; pp. 139–160.

2. (a) Sessler, J. L.; Gross, D. E.; Cho, W.-S.; Lynch, V. M.; Schmidtchen, F. P.; Bates, G. W.; Light, M. E.; Gale, P. A. *J. Am. Chem. Soc.* **2006**, *128*, 12281–12288; (b) Miyaji, H.; Kim, H.-K.; Sim, E.-K.; Lee, C.-K.; Cho, W.-S.; Sessler, J. L.; Lee, C.-H. *J. Am. Chem. Soc.* **2005**, *127*, 12510–12512; (c) Sessler, J. L.; An, D.; Cho, W.-S.; Lynch, V.; Marquez, M. *Chem. Commun*. **2005**, *4*, 540–542; (d) Shevchuk, S. V.; Lynch, V. M.; Sessler, J. L. *Tetrahedron* **2004**, *60*, 11283–11291; (e) Miyaji, H.; Sessler, J. L. *Angew. Chem., Int. Ed.* **2001**, *40*, 154–157; (f) Anzenbacher, P., Jr.; Try, A. C.; Miyaji, H.; Jursikova, K.; Lynch, V. M.; Marquez, M.; Sessler, J. L. *J. Am. Chem. Soc*. **2000**, *122*, 10268–10272; (g) Anzenbacher, P., Jr.; Jursikova, K.; Sessler, J. L. *J. Am. Chem. Soc*. **2000**, *122*, 9350–9351; (h) Black, C. B.; Andrioletti, B.; Try, A. C.; Ruiperez, C.; Sessler, J. L. *J. Am. Chem. Soc*. **1999**, *121*, 10438–10439; (i) Shionoya, M.; Furuta, H.; Lynch, V.; Harriman, A.; Sessler, J. L. *J. Am. Chem. Soc*. **1992**, *114*, 5714–5722.

3. (a) Kim, N.-K.; Chang, K.-J.; Moon, D.; Lah, M. S.; Jeong, K.-S. *Chem. Commun*. **2007**, 3401–3403; (b) Lee, J.-Y.; Lee, M.-H.; Jeong, K.-S. *Supramol. Chem.* **2007**, *19*, 257–263; (c) Chang, K.-J.; Kang, B.-N.; Lee, M.-H.; Jeong, K.-S. *J. Am. Chem. Soc.* **2005**, *127*, 12214–12215; (d) Chang, K.-J.; Moon, D.; Lah, M. S.; Jeong, K.-S. *Angew. Chem., Int. Ed.* **2005**, *44*, 7926–7929.

4. (a) Bates, G. W.; Gale, P. A.; Light, M. E. *Chem. Commun.* **2007**, 2121–2123; (b) Garcia-Garrido, S. E.; Caltagirone, C.; Light, M. E.; Gale, P. A. *Chem. Commun*. **2007**, 1450–1452; (c) Gale, P. A.; Quesada, R. *Coord. Chem. Rev*. **2006**, 3219–3244;

(d) Vickers, M.; Martindale, K. S.; Beer, P. D. *J. Mater. Chem.* **2005**, *15*, 2784–2790; (e) Wong, W. W. H.; Vickers, M. S.; Cowley, A. R.; Paul, R. L.; Beer, P. D. *Org. Biomol. Chem*. **2005**, *3*, 4201–4208; (f) Curiel, D.; Cowley, A.; Beer, P. D. *Chem. Commun*. **2005**, 236–238; (g) Beer, P. D.; Gale, P. A. *Angew. Chem., Int. Ed*. **2001**, *40*, 486–516; (h) Beer, P. D.; Drew, M. G. B.; Gradwell, K. *J. Chem. Soc., Perkin Trans*. 2 **2000**, 511–519; (i) Beer, P. D.; Szemes, F.; Balzani, V.; Sala, C. M.; Drew, M. G. B.; Dent, S. W.; Maestri, M. *J. Am. Chem. Soc*. **1997**, *119*, 11864–11875.

5. Bianchi, A.; Bowman-J., K.; Garcia-Espana, E. *Supramolecular Chemistry of Anions,* Wiley-VCH, New York, **1997**.
6. (a) Kavallieratos, K.; Gala, S. R. de.; Austin, D. J.; Crabtree, R. H. *J. Am. Chem. Soc*., **1997**, *119*, 2325; (b) Kavallieratos, K.; Bertao, C. Crabtree, R.H. *J. Org. Chem*., **1999**, *64*, 1675; (c) Hossain, M.A.; Llinares, J.M.; Powell, D.; Bowman-James, K. *Inorg. Chem*., **2001**, *40*, 2936; (c) Deetz, M.J.; Shang, M.; Smith, B.D. *J. Am. Chem. Soc*., **2000**, *122*, 6201.
7. (a) Miyaji, H.; Sessler, J. L.; *Angew. Chem., Int. Ed*., **2001**, *40*, 154; (b) Kang, S.O.; Jeon, S.; Nam, K.C. *Supramol. Chem*., **2002**, *14*, 405; (c) Jiménez, D.; Martinez-Máñez, R.; Sancenón, F.; Soto, J.; *Tetrahedron Lett*., **2002**, *43*, 2823.
8. Chou, P. T.; Wu, G. R.; Wei, C. Y.; Cheng, C. C.; Chang, C. P.; Hung, F. T. *J. Phys. Chem. B* **2000**, *104*, 7818-7829.

Abstract

Metal-ligand binding is used as a driving force for the formation of organic/inorganic hybrid materials. The formation of metallo-supramolecular complexes with different metal ions (e.g. Zn^{2+}, Co^{2+}, Cd^{2+} etc.) was studied for two ditopic ligands having hexyl chain as a spacer, where one monomer ligand formed the coordinate bond and the other formed the organometallic bond. The optical and thermal properties of the new materials were investigated by a variety of analytical techniques, including UV/Visible, photoluminescence spectroscopy and thermogravimetric analysis. Viscosity studies demonstrate the formation of self-assembling aggregates.

5.1 Introduction

Metallo-supramolecular chemistry is a topic of great current interest. Metallo-supramolecular complexes have been studied intensively due to their outstanding optical, thermal and mechanical properties and potential applications in various fields including light-emitting diodes, field effect transistors, photovoltaic cells, sensors etc. There has been a lot of recent interest that uses the metal ligand binding as the driving force for the self-assembly of ditopic ligands into supramolecular polymers.[1] Different groups have reported a number of ditopic ligands that possess diverse spacers capable of forming metallo-supramolecular complexes with several metal ions, thus, providing a new avenue for research that displayed appreciable mechanical properties[2] in addition to other well-explored properties. One of the easiest methods for supramolecular polymerization i.e. the self-assembly of monomers into polymeric structures, is through the utilization of the non covalent bond by using metal/ligand interactions which offers a large diversity not only for thermodynamic stability but also kinetic lability. Thus simple addition of metal ions to a monomer that has ligand units placed at either end should result in the self-assembly of metallo-polymeric aggregates. Interestingly, however, reports of metallo-supramolecular complexes with appreciable mechanical properties appear to be rare. With the objective to develop new organic/inorganic hybrid materials, which combine good mechanical properties and other attractive properties (e.g., high stability at elevated temperatures, specific opto/electronic functions) with ease of processing, we embarked on the exploration of various new classes of metallo-supramolecular complexes.

This chapter deals with the preparation of ditopic ligands having hexyl chain as a spacer from simple tridentate ligands of 2,6-bis(1´-methylbenzimidazoyl)-4-hydroxypyridine and 2,6-bis(1´-methylbenzimidazoyl)-4-hydroxybenzene, detailed characterization followed by the study of their metallo-supramolecular complex forming ability with different metal

ions using UV/Visible and fluorescence spectroscopy, viscosity measurement and thermal stability of the complexes have been studied.

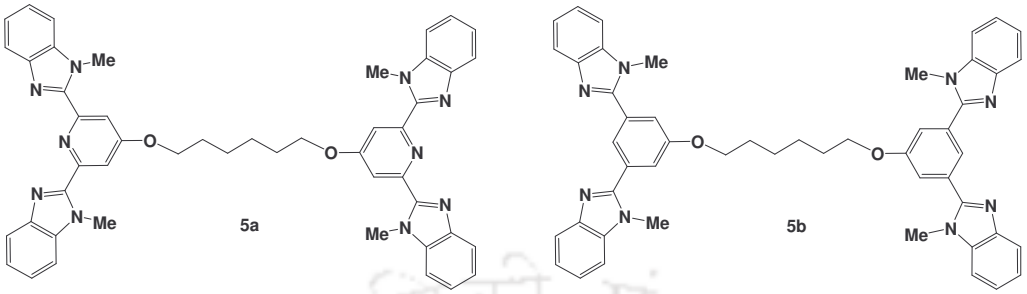

Figure 5.1: *Ditopic ligands **5a** and **5b***

5.2 Results and Discussion

The synthesis of 4-hydroxy-2,6-bis(1´-methylbenzimidazoyl)pyridine and 4-hydroxy-2,6-bis(1´-methylbenzimidazoyl)benzene ligands was achieved in one step, from commercially available starting materials, using the well known Phillips condensation method.[3]

5.2.1 UV/Visible Spectroscopy

Metallo-supramolecular complex formation was studied by simple technique of UV/Visible titration which was done in a mixture of dry acetonitrile and chloroform. The formation of the metallo-supramolecular materials, $[\mathbf{5a}MX_2]_n$ and $[\mathbf{5b}MX_2]_n$ can be achieved by simple addition of 1 equiv. of the appropriate metal ion salt to a solution of the ditopic monomer, **5a**, or **5b**. We have found that a variety of ions (e.g., Cd^{2+}, Zn^{2+}, Co^{2+}) can be utilized to interact with the ditopic ligands. The complexation of these metal ions to the ligand can be followed by UV/Vis spectroscopy.

The ditopic ligands **5a** and **5b** show the ligand absorption band at 314 nm and 296 nm respectively, which is assigned to the π-π* transitions of the ditopic ligands. Addition of 1 equiv. of the salts of Cd^{2+}, Zn^{2+}, Co^{2+} ions to any of these monomers in acetonitrile and chloroform solvent mixture resulted in a red shift of this band with the clear formation of

isosbestic point, broadening and a clear change in the color of the solution with different metal ions. Addition of the metal ions to the ditopic ligand **5a** forms gel like morphology

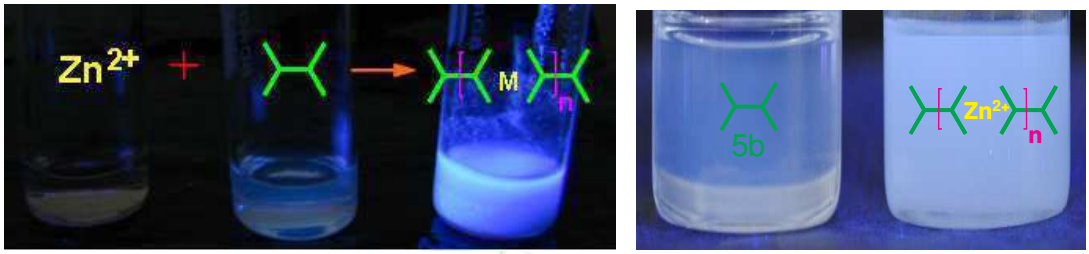

. ***(a)*** ***(b)***

Figure 5.2: *(a) Ditopic ligand **5a**, Zn^{2+} and complex; (b) Ditopic ligand **5b** and complex with, Zn^{2+} under UV light.*

which precipitate with time and show high brightness under UV illumination (Figure 5.2). Contrarily ditopic ligand **5b**, on the addition of the metal ions did not form any precipitates but a minor color change was observed. Figure 5.3 clearly shows the formation of metallo-supramolecular complexes between the ditopic ligand **5a** and Zn^{2+} metal ions. This red shift in the absorption and the significant broadening nature of the peaks confirm the formation of metallo-supramolecular complexes.

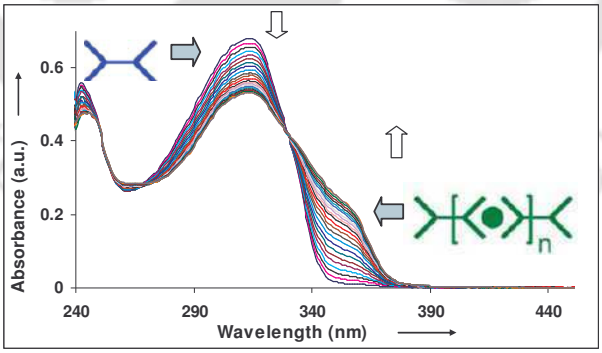

Figure 5.3: *UV/Vis spectra of **5a** (6.45 x 10^{-6} M in dry $CHCl_3$: CH_3CN = 4 : 1) during the titration with $Zn(ClO_4)_2$ from 0-2 equivalents*

The binding ability of the ditopic ligand **5a** was evaluated by titrating 0.1 equivalents of $Zn(ClO_4)_2$ aliquots into a solution of **5a** in acetonitrile at regular intervals and recording

the changes in UV/Vis spectral data. It was observed that on increasing the concentration of the metal ion, progressive decrease of intensity in the initial absorption band (Figure 5.3) having λ_{max} at 314 nm associated with the π-π^* transition of **5a** resulted. Concurrently, a new peak at 355 nm develops which is due to the formation of stable complex between **5a** and $Zn(ClO_4)_2$. This family of spectra shows formation of an isosbestic point at 330 nm indicating the presence of at least one intermediate species at equilibrium. It was observed that the spectral features reached a limiting value only after the addition of 2.0 equivalents of metal ions (though the changes observed in the spectra on addition of 1.1 to 2.0 equivalents metal were very minor compared to the initial ten additions). Thus the gradual decrease in the band intensity at 314 nm and formation of a new higher intensity blue-shifted band at 350 nm with a clear isosbestic point is proof for the formation of metallo-supramolecular complex between monomer **5a** and metal.

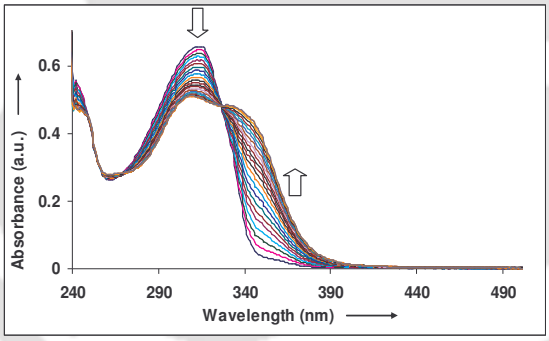

Figure 5.4: *UV/Vis spectra of **5a** (6.24 x 10^{-6} M in dry $CHCl_3$: CH_3CN = 4 : 1) during the titration with $Co(ClO_4)_2$ from 0-2 equivalents.*

Similarly, on the addition of Co^{2+} and Cd^{2+} metal salts resulted in the peaks to be red shifted with the clear formation of isosbestic point. Figure 5.4 shows the changes of spectral properties on the addition of Co^{2+} metal ions, where the initial absorption band having λ_{max} at 314 nm progressively decreases with broadening and a new red shifted peak

is seen at 344nm and formation of a clear isosbestic point at 326 nm which shows that there is at least one species at equilibrium.

Figure 5.5 shows the changes of spectral properties on the addition of Cd^{2+} metal ions, where the initial absorption band having λ_{max} at 314 nm progressively decreases and the peak is red shifted also with a clear formation of an isosbestic point at 326 nm which shows that there is at least one species at equilibrium.

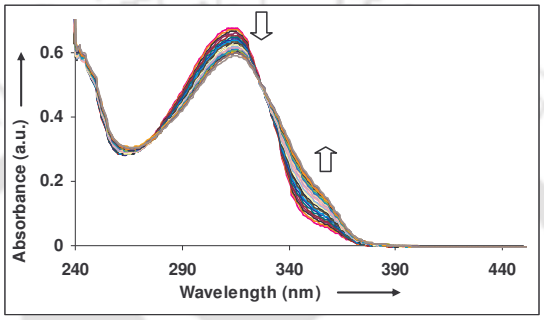

Figure 5.5: *UV/Vis spectra of* ***5a*** *(6.46 x* 10^{-6} *M in dry* $CHCl_3$ *:* CH_3CN *= 4 : 1) during the titration with* $Cd(ClO_4)_2$ *from 0-2 equivalents.*

On the other hand, ditopic ligand **5b** shows different optical properties on the addition of metal ions. Fig. 5.6 clearly shows the spectral changes that occur on the addition of $Zn(ClO_4)_2$. It was observed that on increasing the concentration of the metal ion, progressive decrease of intensity in the initial absorption band (Figure 5.6) having λ_{max} at 296 nm associated with the π-π^* transition of **5b** resulted. The peak is red shifted with a clear formation of isosbestic point at 325 nm which is due to the formation of stable complex between **5b** and $Zn(ClO_4)_2$. The formation of an isosbestic point indicates the presence of at least one species at equilibrium.

Similarly, on the addition of Co^{2+} and Cd^{2+} metal ions the peaks were red shifted with the clear formation of isosbestic point. Figure 5.7 shows the changes of spectral properties on the addition of Co^{2+} metal ions, where the initial absorption band having λ_{max} at 296 nm

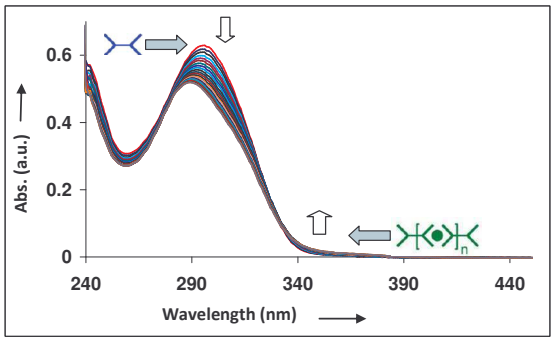

Figure 5.6: *UV/Vis spectra of* ***5b*** *(6.50 x 10^{-6} M in dry $CHCl_3$: CH_3CN = 4 : 1) during the titration with $Zn(ClO_4)_2$ from 0-2 equivalents.*

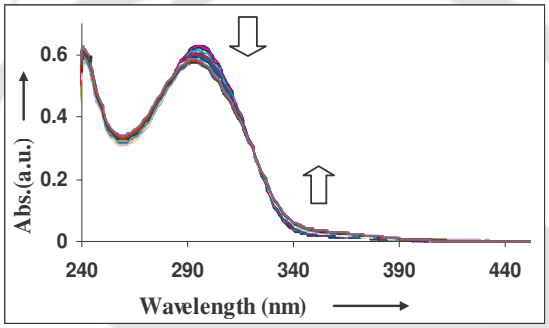

Figure 5.7: *UV/Vis spectra of* ***5b*** *(6.52 x 10^{-6} M in dry $CHCl_3$: CH_3CN = 4 : 1) during the titration with $Co(ClO_4)_2$ from 0-2 equivalents.*

progressively decreases and the peak is red shifted and there is a formation of an isosbestic point at 321 nm which shows that there is at least one species at equilibrium and confirms the formation of the supramolecular complex between the two compounds.

Figure 5.8 shows the changes of spectral properties on the addition of Cd^{2+} metal ions, where the initial absorption band having λ_{max} at 296 nm progressively decreases (minor) and the peak is red shifted with a clear formation of an isosbestic point at 325 nm which shows that there is at least one species at equilibrium and that also confirms the formation of the supramolecular complex between the ditopic ligand and metal ions.

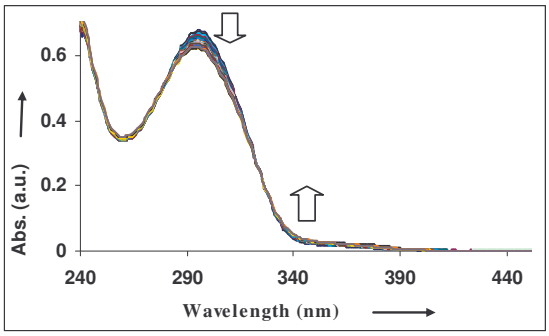

Figure 5.8: *UV/Vis spectra of **5b** (7.00 x 10^{-6} M in dry $CHCl_3$: CH_3CN = 4 : 1) during the titration with $Cd(ClO_4)_2$ from 0-2 equivalents.*

5.2.3 Fluorescence Spectroscopy

Fluorescence spectroscopy studies were also carried out in order to evaluate the ability of the two ditopic ligands **5a** and **5b** to form the metallo-supramolecular complexes with different metal ions. Remarkable quenching of the fluorescence was observed on addition of different metal ions. It was observed that monomer **5a** shows more quenching in comparison to **5b** which may be due to the formation of stronger coordination bond with monomer **5a** while with the monomer **5b** it will form weaker organometallic bond using the C-H part of the benzene ring.

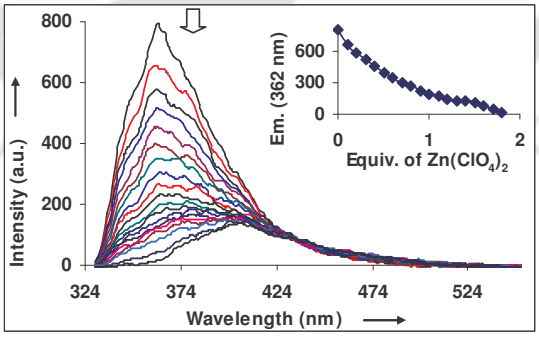

Figure 5.9: *Emission spectra of **5a** (9.20 x 10^{-7} M in dry $CHCl_3$: CH_3CN = 4 : 1) during the titration with $Zn(ClO_4)_2$ from 0-2 equivalents.*

The changes observed in the fluorescence spectra of a solution of **5a** in acetonitrile and chloroform solvent mixture on adding up to 2.0 equivalents of Zn^{2+} are depicted in Figure 5.9. A large quenching (> 95%) in intensity of the 362 nm band was observed on the addition of 1.0 equivalent of $Zn(ClO_4)_2$ indicating that on formation of the metallo-supramolecular complex between $Zn(ClO_4)_2$ and **5a**, the excited state was modified considerably leading to the quenching of fluorescence. On continuous addition of $Zn(ClO_4)_2$ to a solution of **5a** the peak was slowly red shifted to 407 nm. The changes observed in the fluorescence spectra on adding more than 1 equivalent of $Zn(ClO_4)_2$ aliquots to **5a** were insignificant, which is in good agreement with the results of UV/Vis titration. Figure 5.9 inset shows the changes in the titration profile of the band at 362 nm corresponding to the **5a** : $Zn(ClO_4)_2$ metallo-supramolecular complex.

Analogous investigations were carried out with $Cd(ClO_4)_2$ and $Co(ClO_4)_2$ and the titration experiments were monitored by fluorescence spectroscopy (Figure 5.10-11). An acetonitrile and chloroform solution of **5a** was titrated with a solution of those chosen metal ions. In all cases, a new band developed on quenching of fluorescence. Figure 5.10 shows the changes in fluorescence spectra on the addition of $Co(ClO_4)_2$ to a solution of **5a** in acetonitrile and chloroform solvent mixture. On the addition of the metal ions, the emission peak of the ditopic ligand which was at 362 nm slowly decreases due to the quenching by the metal ions and was red shifted to about 405 nm. Here also the maximum quenching was observed up to the addition of the one equivalent of the metal ions, whereas changes observed in the fluorescence spectra on adding more than 1 equivalent of $Co(ClO_4)_2$ aliquots to **5a** were insignificant. Figure 5.10 inset shows the changes in the titration profile of the band at 362 nm corresponding to the **5a**:$Co(ClO_4)_2$ metallo-supramolecular complex.

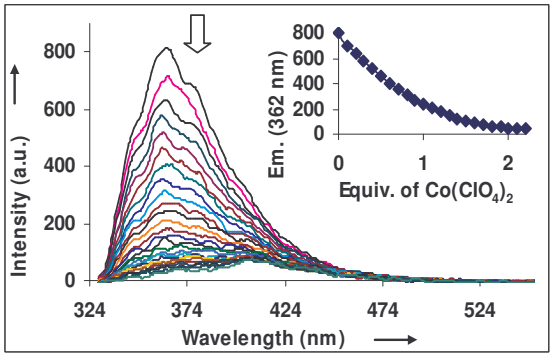

Figure 5.10: *Emission spectra of **5a** (9.32 x 10^{-7} M in dry $CHCl_3$: CH_3CN = 4 : 1) during the titration with $Co(ClO_4)_2$ from 0-2 equivalents.*

Similar fluorescence titration of **5a** was carried out with $Cd(ClO_4)_2$ in acetonitrile and chloroform solvent mixture. Figure 5.10 shows the changes of the emission spectra, where the intensity of the fluorescence emission peak of 362 nm gradually decreased on the addition of the metal ions due to the formation of the metallo-supramolecular complex between the ditopic ligand and the metal ions leading to quenching.

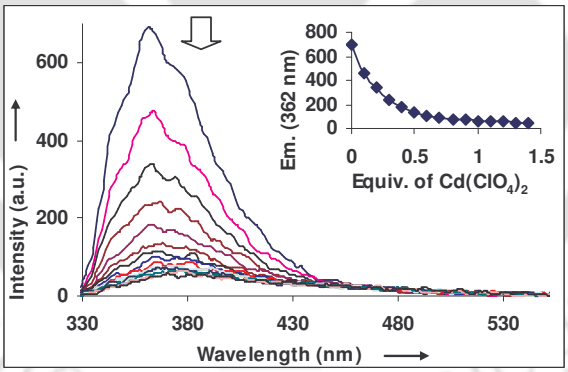

Figure 5.11: *Emission spectra of **5a** (8.00 x 10^{-7} M in dry $CHCl_3$: CH_3CN = 4 : 1) during the titration with $Cd(ClO_4)_2$ from 0-2 equivalents.*

Fluorescence spectroscopy studies were also carried out in order to evaluate the ability of the ditopic ligands **5b** to form the metallo-supramolecular complexes with different metal ions. The changes observed in the fluorescence spectra of a solution of **5b** in acetonitrile and chloroform solvent mixture on adding up to 2.0 equivalents of Zn^{2+} are depicted in

Figure 5.12. A large quenching (> 60%) in intensity of the 361 nm band was observed on the addition of 1.0 equivalent of $Zn(ClO_4)_2$ indicating that on formation of the metallo-supramolecular complex between $Zn(ClO_4)_2$ and **5b**, the excited state was modified considerably leading to the quenching of fluorescence. On continuous addition of $Zn(ClO_4)_2$ to a solution of **5b** the peak decreases gradually but in comparison to **5a** it was less where the quenching was (> 95%) which may be due to the formation of the weaker organometallic bond between the C-H part of the benzene ring of the monomer. The changes observed in the fluorescence spectra on adding more than 1 equivalent of $Zn(ClO_4)_2$ aliquots to **5b** were insignificant, which is in good agreement with the results of UV/visible titration. Figure 5.12 inset shows the changes in the titration profile of the band at 361 nm corresponding to the **5b** : $Zn(ClO_4)_2$ metallo-supramolecular complex.

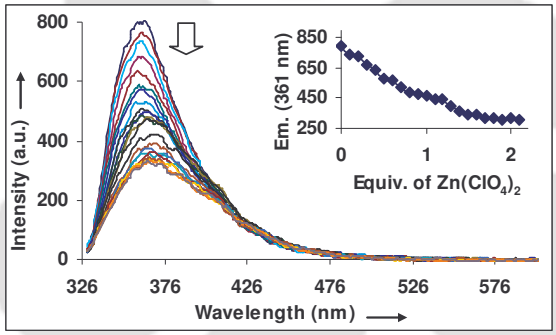

Figure 5.12: *Emission spectra of **5b** (9.50 x 10^{-7} M in dry $CHCl_3$: CH_3CN = 4 : 1) during the titration with $Zn(ClO_4)_2$ from 0-2 equivalents.*

Similar fluorescence titration experiments were carried out with $Cd(ClO_4)_2$ and $Co(ClO_4)_2$. (Figure 5.13-14). An acetonitrile and chloroform solution of **5b** was titrated with a solution of those chosen metal ions. In all cases, a new band developed on quenching of fluorescence. Figure 5.13 shows the changes in fluorescence spectra on the addition of $Co(ClO_4)_2$ to a solution of **5b** in acetonitrile and chloroform solvent mixture. On the addition of the metal ions, the emission peak of the ditopic ligand which was at 361 nm slowly decreases due to the quenching by the metal ions. Here also the maximum

quenching was observed up to the addition of one equivalent of the metal ions, changes observed in the fluorescence spectra on adding more than 1 equivalent of $Co(ClO_4)_2$ aliquots to **5b** were insignificant. Figure 5.12 inset shows the changes in the titration profile of the band at 361 nm corresponding to the **5b** : $Co(ClO_4)_2$ metallo-supramolecular complex.

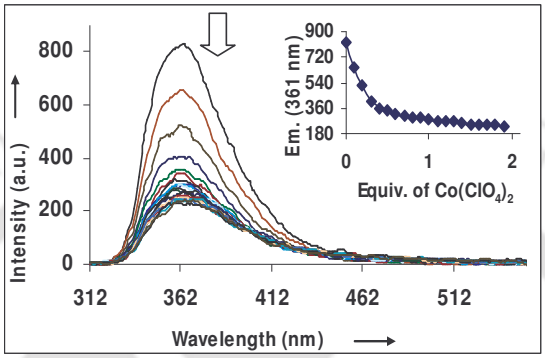

Figure 5.13: *Emission spectra of **5b** (9.80 x 10^{-7} M in dry $CHCl_3$: CH_3CN = 4 : 1) during the titration with $Co(ClO_4)_2$ from 0-2 equivalents.*

.

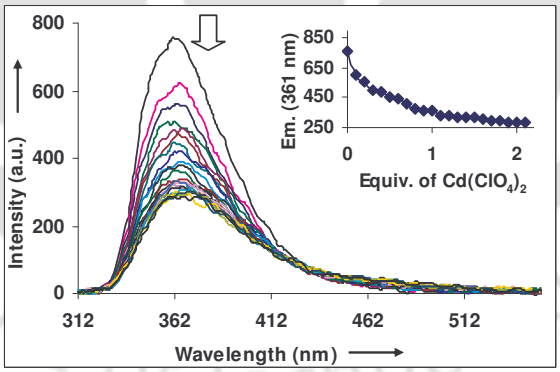

Figure 5.14: *Emission spectra of **5b** (8.80 x 10^{-7} M in dry $CHCl_3$: CH_3CN = 4 : 1) during the titration with $Cd(ClO_4)_2$ from 0-2 equivalents.*

Again fluorescence titration of **5b** was carried out with $Cd(ClO_4)_2$ in acetonitrile and chloroform solvent mixture. Figure 5.14 shows the changes in the emission spectra, where the intensity of the fluorescence emission peak of 361 nm showed minor decrease on the

addition of the metal ions due to the formation of the metallo-supramolecular complex between the ditopic ligand and the metal ions leading to quenching.

5.2.4 Study of thermal behaviour

The thermal properties of the metallo-supramolecular complexes and the parent monomers **5a** and **5b** were investigated by means of thermogravimetric analysis (TGA). A solution containing 25 mg (0.031 mmol) of **5a** in 300 µL of chloroform was mixed with a 1:1 stoichiometric amount of 11.74 mg (0.031 mmol) of zinc perchlorate hexahydrate in 150 µL of acetonitrile. This mixed solvent solution was then stirred for 2 hrs and the complex was allowed to air-dry and then was vacuum-dried in an oven for 12 hrs at room temperature.

Similarly, all other metallo-supramolecular complexes were prepared maintaining 1:1 ratio of the monomer and metal salts. A series of experiments were carried out in order to understand the thermal properties of these metallo-supramolecular complexes. The thermograms were recorded in atmospheric conditions. The working temperature range of the instrument is from ambient to 1300°C.

TGA traces of monomer (neat) **5a** (Figure 5.15) acquired under normal atmosphere and shows the onset of significant weight loss (3%) at 272 °C, corresponding to the loss of the water molecule present in the monomer. The Zn^{2+} and Cd^{2+} metallo-supramolecular complexes of **5a** show a rather similar thermal behavior, but the 4% weight loss occurs at somewhat lower temperatures. We ascribe this situation to the thermal degradation of the perchlorate counterions.

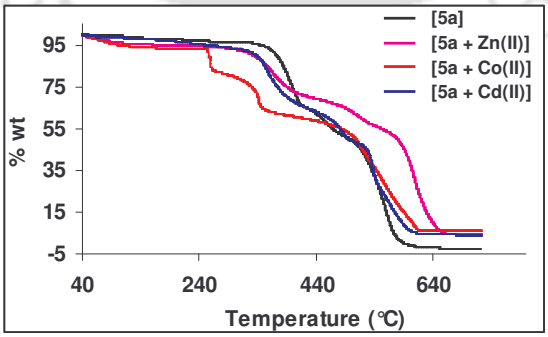

Figure 5.15: *Thermogravimetric analysis (TGA) traces of monomer **5a** and its supramolecular complexes with Zn^{2+}, $Co^{2+}$and Cd^{2+}.*

Similar behaviour was also observed in case of monomer **5b** and its metal complexes.

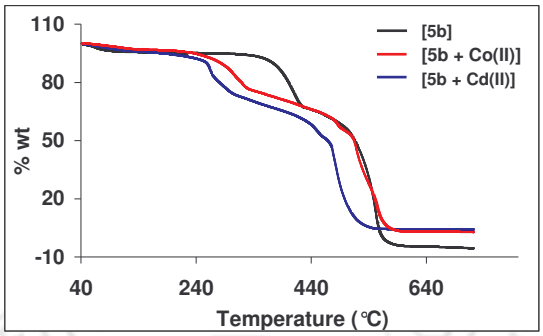

Figure 5.16: *Thermogravimetric analysis (TGA) traces of monomer **5b** and supramolecular complexes with* Co^{2+} *and* Cd^{2+}.

5.2.5 FT-IR Spectroscopy

The FT-IR spectra of all the complexes were recorded in KBr pellets. In the case of complexes of **5a** and **5b** with different metal ions the characteristic perchlorate vibrations appear at ~1089 cm^{-1} which are absent in case of the monomers. Again, the C=N vibration peak which appear at ~ 1593 cm^{-1} slightly shifted after addition of the metal ions (Fig. 5.17)

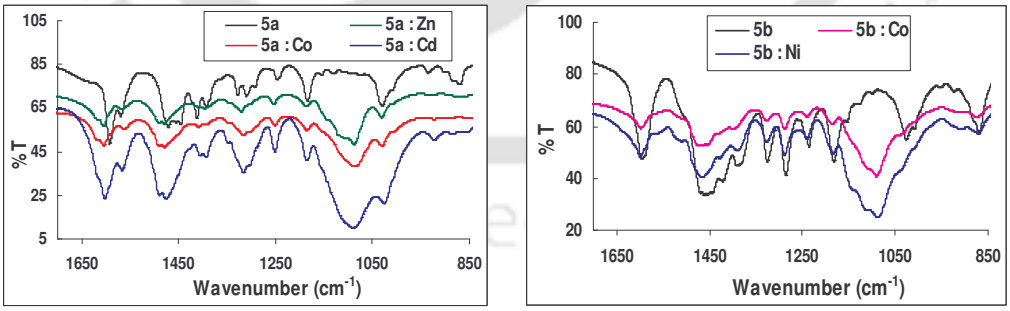

Figure 5.17: *FT-IR spectra for metal complexes of (a) monomer **5a** and (b) monomer **5b** in KBr pellets*

5.2.6 Viscosity measurement

Having demonstrated the formation of metallo-supramolecular complexes from a combination of UV/Vis, photoluminescence, and FT-IR studies this complex formation can be studied by viscosity measurement in solution state. The intrinsic viscosity, [η], of a sample is related to the molecular weight M of the polymer through the Mark-Houwink-Sakurada equation: $[\eta] = KM^a$, where *K* and *a* are experimentally determined polymer and environmentally specific constants. Viscosity studies were carried out using a Cannon-Ubbelohde microdilution viscometer, and the relative viscosities of the complexes were measured at a variety of different concentrations. Figure 5.18 shows the Huggins plot (reduced viscosity vs concentration) for Zn^{2+} complexes of the monomers **5a** and **5b**. Keeping the total solute concentration constant, the data show a steady increase of the reduced viscosity on dilution.

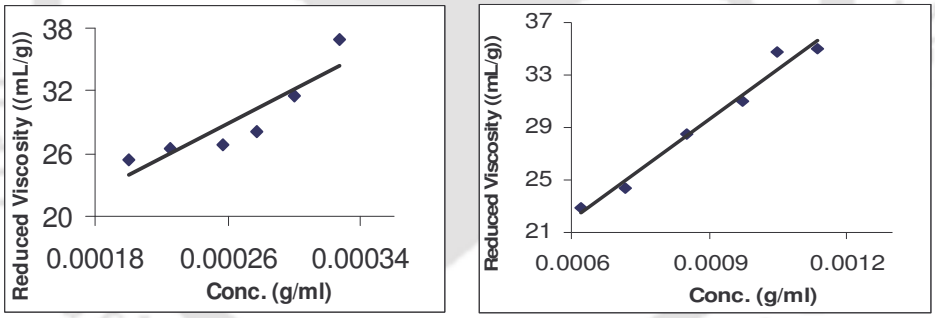

(a) **(b)**

Figure 5.18: *Plot of reduced viscosity vs concentration for the Zn^{2+} complexes of ditopic monomers (a)* ***5a*** *and (b)* ***5b.***

5.3 Conclusion

We have synthesized two ditopic ligands having hexyl chain as a spacer from simple tridentate ligands of 2,6-bis(1´-methylbenzimidazoyl)-4-hydroxypyridine and 2,6-bis(1´-methylbenzimidazoyl)-4-hydroxybenzene attached to either end. The products were well

characterized by ^{1}H NMR, ^{13}C NMR, FT-IR and mass spectroscopy. The metallo-supramolecular complex formation of these monomers has been studied with different metal ions e.g. Zn^{2+}, Co^{2+}, Cd^{2+} etc. using UV/Vis, fluorescence and ^{1}H NMR spectroscopy. UV/Vis spectra showed that on continuous addition of the different metal ions the absorption maximum decreases and the peak slowly red shifted with a clear formation of isosbestic point in both the monomers. Again from the fluorescence titration it was clear that on the addition of the metal ions to **5a** the emission peak was quenched due to the formation of the metallo-supramolecular complex and the peak was red shifted, while addition of the metal ions to **5b** showed less quenching due to the weaker organometallic bond formation by the C-H part of the benzene ring of the monomer with metal salts. Thermal studies showed that these complexes were highly stable at elevated temperature. The wide range of possible cores that can be studied, in accordance with the metal ions availability and their binding capability, which would not only exhibit different binding kinetics and thermodynamics but also can impart functionality, e.g., catalysis, luminescence, etc., opens the door to the creation of easy to process organic/inorganic hybrid materials in which the functionality and mechanical properties can easily be tailored as per requirement and application.

5.4 Experimental section

5.4.1 General

All reagents were used as received without further purification unless mentioned. These materials were of reagent grade or better. Acetonitrile was distilled from calcium hydride. UV/visible spectra were recorded on a Perkin Elmer Lambda-25 spectrophotometer. Fluorescence spectra were recorded on a Varian Cary Eclipse Fluorescence spectrophotometer. ^{1}H-NMR spectra were obtained with a 400 MHz Varian FT spectrometer. Chemical shifts (ppm) were referenced to the residual solvent peaks.

Thermogravimetric analyses (TGA) were carried out on a Shimadzu DT-30 thermal analyzer.

5.4.2 Preparation of different ligands and monomers

Preparation of 2,6-bis(1´-methylbenzimidazoyl)-4-hydroxypyridine ligand (OHBIP)

The 2,6-bis(1´-methylbenzimidazoyl)-4-hydroxypyridine ligand has been prepared by the known literature method.[3]

Preparation of 2,6-bis(1´-methylbenzimidazoyl)-4-hydroxybenzene ligand (OHBIB)

5-hydroxyisophthalic acid (0.728 g, 3.99 mmol) and N-methyl-1,2-phenylenediamine (1.07 g, 8.7 mmol) were dispersed in 10 ml orthophosphoric acid. The mixture was stirred and refluxed at 220°C for 12 hrs. After cooling to about 100°C, the hot mixture was poured to ice cold water and stirred for half an hour. The precipitate formed was filtered and poured to hot 10 % Na_2CO_3 solution and stirred. The product was filtered and acidified to pH 4. The precipitate was again filtered, washed with water and recrystalised from methanol to yield 1.3 grams of white needle type crystals. (> 90% yield)

Preparation of ditopic ligand 5a

HOBIP (2.0 g, 5.63 mmol) and 1,6-diiodohexane (0.63 g, 1.87 mmol) were dissolved into a solution of K_2CO_3 (4.2 g) in 10 mL of DMSO and stirred at 90°C for 24 hrs. After removing heat, the mixture was poured into 200 mL of half-saturated NH_4Cl and washed with 100 ml of chloroform. The organics were collected and extracted again from a mixture of water and chloroform. The organics were evaporated and the residue dried under vacuum. The material was purified via column chromatography (100:0 $CHCl_3$:MeOH $\rightarrow$ 95:05 $CHCl_3$:MeOH) to yield 1.1 grams of product as a solid. (74% yield)

^{1}H NMR (400 MHz, $CDCl_3$): δ 8.01 (s, 4H), 7.88 (d, 4H), 7.45 (d, 4H), 7.36 (m, 8H), 4.32 (t, 4H), 4.23 (s, 12H), 2.24 (s, 4H), 1.93 (s, 4H).

^{13}C NMR (100 MHz, $CDCl_3$): δ 166.6, 150.8, 150.2, 142.1, 137.0, 123.7, 123.0, 120.1, 112.1, 110.0, 68.8, 32.8, 29.1, 25.9.

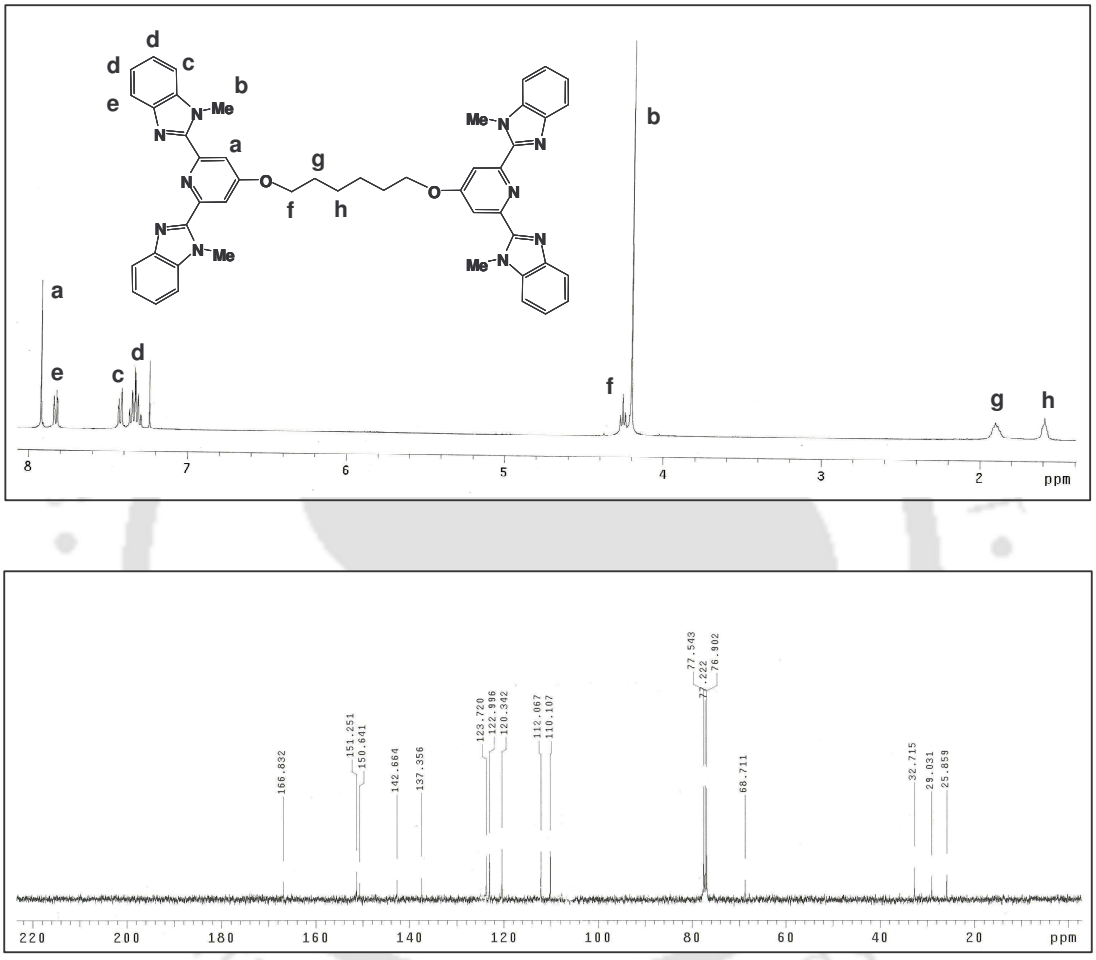

Figure 5.19: *^{1}H-NMR and ^{13}C-NMR spectra of monomer **5a** in $CDCl_3$ solvent.*

Preparation of ditopic ligand 5b

HOBIB (1.5 g, 4.23 mmol) and 1,6-diiodohexane (0.47 g, 1.41 mmol) were dissolved into a solution of K_2CO_3 (4.2 g) in 10 mL of DMSO and stirred at 90°C for 24 hrs. After removing heat, the mixture was poured into 200 mL of half-saturated NH_4Cl and washed with 100 ml of chloroform. The organics were collected and extracted again from a

mixture of water and chloroform. The organics were evaporated and the residue dried under vacuum. The material was purified via column chromatography (100:0 $CHCl_3$:MeOH ⟶ 95:04 $CHCl_3$:MeOH) to yield 0.68 grams of product as a solid. (62% yield)

^{1}H NMR (400 MHz, $CDCl_3$): δ 7.81 (d, 4H), 7.61 (s, 2H), 7.43 (s, 4H), 7.38 (d, 4H), 7.30 (m, 8H), 4.14 (t, 4H), 3.88 (s, 12H), 1.87 (s, 4H), 1.70 (s, 4H).

^{13}C NMR (100 MHz, $CDCl_3$): δ 159.7, 153.0, 142.9, 136.7, 132.0, 123.3, 122.8, 122.4, 120.0, 17.2, 109.9, 68.6, 32.0, 29.3 25.9.

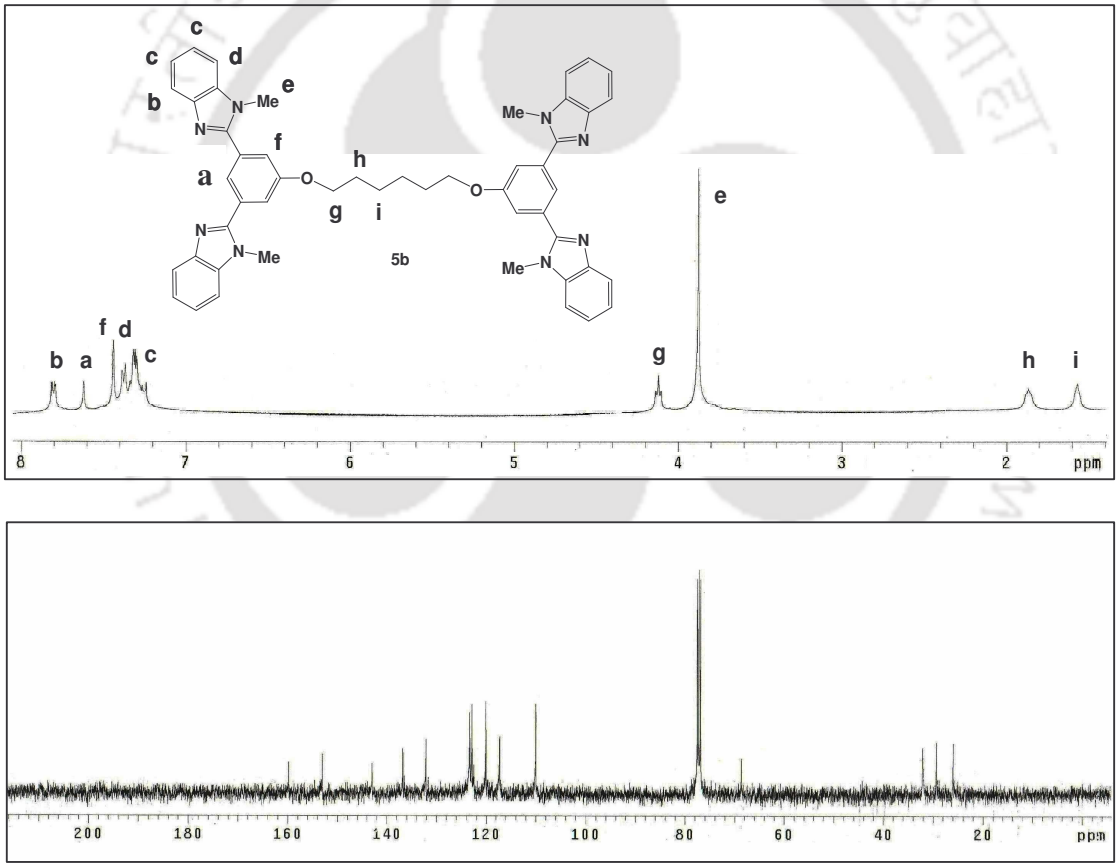

Figure 5.20: *^{1}H-NMR and ^{13}C-NMR spectra of monomer **5b** in $CDCl_3$ solvent.*

5.4.3 Mass Spectroscopy

The electrospray mass spectra for all the complexes were recorded in CH_3CN with (0.1%) formic acid. The (M+H) molecular ion peaks for the ditopic ligands **5a** and **5b** appear at 793.32 and 791.24 respectively (Figure 5.21).

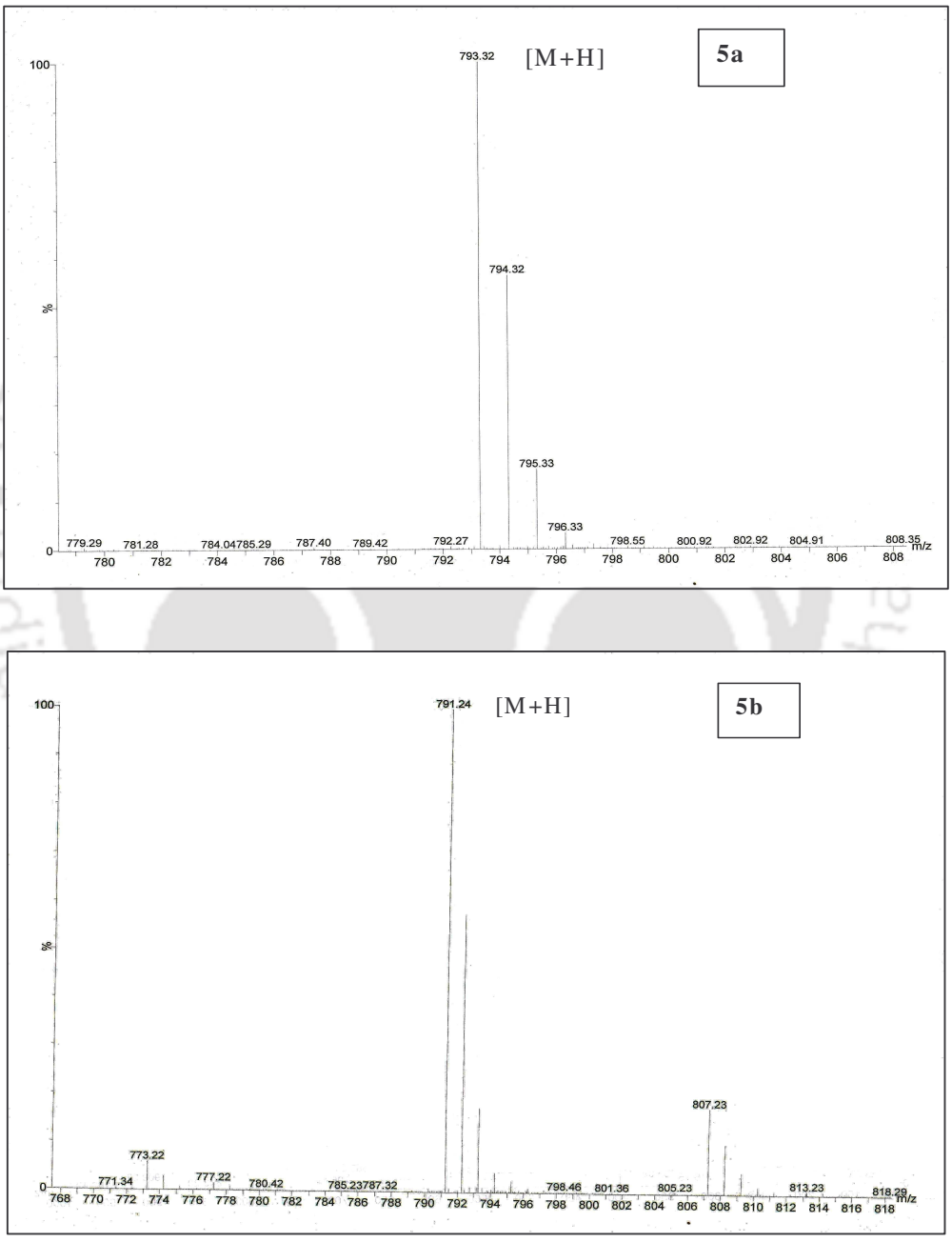

Figure 5.21: *ESI-Mass spectra for the monomers (a)* ***5a*** *and (b)* ***5b*** *in CH_3CN with (0.1%) formic acid.*

5.5 References

1. (a) Lohmeijer, B. G. G.; Schubert, U. S. *J. Polym. Sci., Part A: Polym. Chem.* **2003**, *41*, 1413. (b) Dobrawa, R.; Würthner, F. *J. Polym. Sci., Part A: Polym. Chem.* **2005**, *43*, 4981-4995. (c) Holliday, B. J.; Swager, T. M. *Chem. Commun.* **2005**, 23. (d) Friese, V. A.; Kurth, D. G. *Coord. Chem. Rev.* **2008**, *252*, 199.
2. (a) Iyer, P. K.; Beck, J. B.; Weder, C.; Rowan, S. J. *Chem. Commun.***2005**, 319. (b) Knapton, D.; Burnworth, M.; Rowan, S. J.; Weder, C. *Angew. Chem., Int. Ed.* **2006**, *45*, 5825. (c) Burnworth, M.; Rowan, S. J.; Weder, C. *Chem.sEur. J.* **2007**, *13*, 7828. (d) Knapton, D.; Rowan, S. J.; Weder, C. *Macromolecules* **2006**, *39*, 651. (e) Burnworth, M.; Knapton, D.; Rowan, S. J.; Weder, C. *J. Inorg. Organomet. Polym. Mater.* **2007**, *17*, 40, 91.
3. (a) Addison, A. W.; Burke, P. J. *J. Heterocycl. Chem*. **1981**, *18*, 803–805. (b) Addison, A. W.; Rao, T. N.; Wahlgren, C G. *J. Heterocycl. Chem.* **1983**, *20*, 1481–1484.

Abstract

Metal-ligand binding is used as a driving force for the formation of organic/inorganic hybrid materials. The formation of metallo-supramolecular complexes with different metal ions (e.g. Zn^{2+}, Co^{2+}, Cd^{2+} etc.) was studied for total four benzoxazol and benzothiazol ditopic ligands having pentaethylene glycol chain as a spacer, where formation of both non-covalent bond and organometallic bond take place. The optical and thermal properties of the new materials were investigated by a variety of analytical techniques, including UV/visible and photoluminescence spectroscopy, viscosity as well as thermogravimetric analysis. Viscosity studies demonstrate the formation of self-assembling aggregates.

6.1 Introduction

Metallo-supramolecular chemistry is a topic of great current interest. Metallo-supramolecular complexes have been studied intensively due to their outstanding optical, thermal and mechanical properties and reported a plenty of applications in various fields including light-emitting diodes, field effect transistors, photovoltaic cells, sensors etc. There has been a lot of recent interest that uses the metal ligand binding as the driving force for the self assembly of ditopic ligands into supramolecular polymers.[1] Monomers having long chain spacers are already reported to form foldamers that have been used in different applications like molecular recognition and sensing.[2] Different groups reported a number of ditopic ligands having novel spacers and binding sites that form metallo-supramolecular complexes with several metal ions, thus, providing newer avenues for research that displayed appreciable mechanical properties.[3] One of the easiest methods for supramolecular polymerization i.e. the self-assembly of monomers into polymeric structures through the utilization of the non covalent bond, is the use of metal/ligand interactions which offers a large diversity in not only thermodynamic stability but also kinetic lability. Thus simple addition of metal ions to a monomer that has ligand units placed at either end should result in the self-assembly of metallo-polymeric aggregates. In the previous chapter a combination of different metal salts with two monomeric ligands was combined to show that metallo-supramolecular complexes can be easily prepared. Interestingly, however, reports of metallo-supramolecular complexes having benzthaizol and benzoxazol based ligands appear to be rare and uncommon. With the objective to develop new organic/inorganic hybrid materials having benzthaizol and benzoxazol based ligands, which combine good mechanical properties and other attractive properties (e.g., high stability at elevated temperatures, specific opto/electronic functions) with ease of processing, we embarked on the exploration of various new classes of metallo-supramolecular complexes.

This chapter deals with the preparation of four ditopic ligands namely (**6a**), (**6b**), (**6c**), and (**6d**) having pentaethylene glycol chain as a spacer from simple tridentate ligands of 2,6-bis-benzothiazol-2-yl-pyridin-4-ol, 2,6-bis-benzoxazol-2-yl-pyridin-4-ol, 3,5-bis-benzothiazol-2-yl-phenol and 3,5-bis-benzoxazol-2-yl-phenol respectively, characterization and study of the metallo supramolecular complex formation with different metal ions using UV/Visible and fluorescence spectroscopy and thermal stability of the complexes have been studied.

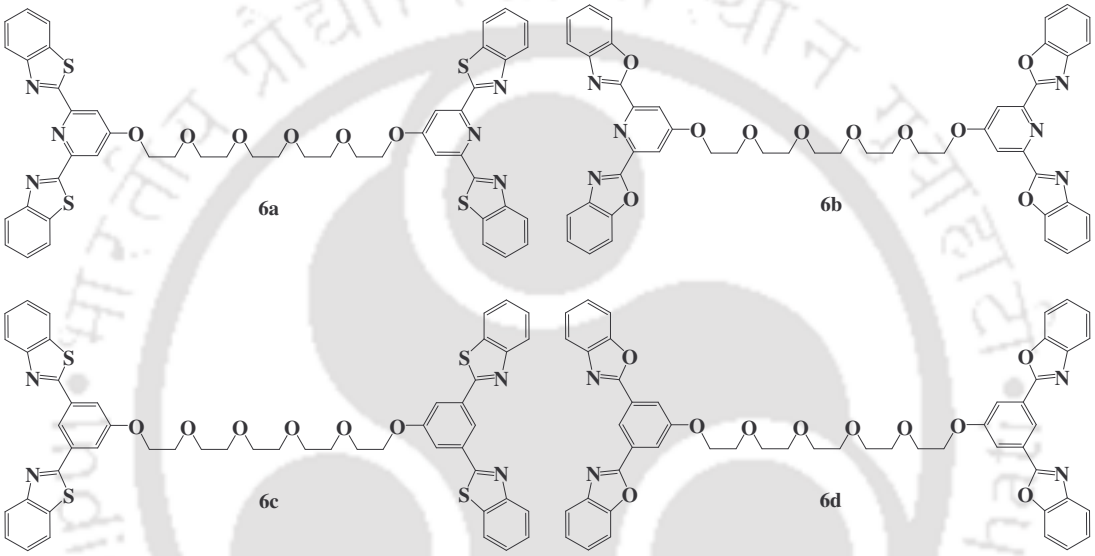

Figure 6.1: *Ditopic ligands **6a, 6b, 6c** and **6d.***

6.2 Results and Discussion

The synthesis of the ligands mentioned above was achieved in one step, from commercially available starting materials, using the well known Phillips condensation method.[4] The ditopic ligands **6a-6d** have been synthesized by the reaction of benzoxazol and benzothiazol ditopic ligands with bisiodopenta(ethylene glycol) using potassium carbonate in dimethyl sulfoxide.

6.2.1 UV/Visible Spectroscopy

Metallo-supramolecular complex formation was studied as in earlier chapter, by simple technique of UV/Visible titration performed in a mixture of dry acetonitrile and chloroform. The formation of the metallo-supramolecular materials, [**6a**MX_2]$_n$, [**6b**MX_2]$_n$, [**6c**MX_2]$_n$ and [**6d**MX_2]$_n$ can be achieved by simple addition of 1 equivalent of the appropriate metal ion salt to a solution of the above mentioned ditopic monomer, **6a**, **6b**, **6c** or **6d**. We have found that a variety of ions (e.g., Cd^{2+}, Zn^{2+}, Co^{2+}) can be utilized to interact with the ditopic lignads. The complexation of these representative metal ions with the above monomers can be followed by UV/Vis spectroscopy. Addition of the metal ions to the monomers formed different colored solution that can be distinguished easily by naked eye and under UV illumination, where all the monomers and complexes showed different color. The difference in color of all the monomers with Zn^{2+} ion is shown below.

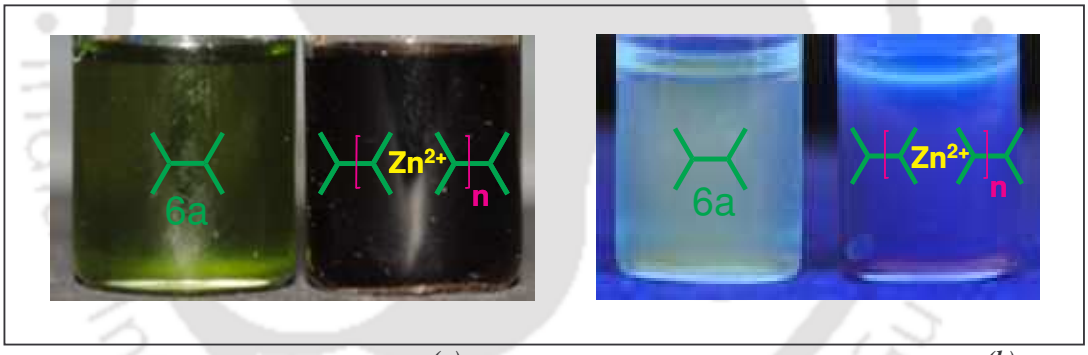

Figure 6.2: *Ditopic ligand **6a** and complex with Zn^{2+} (a) under white light and (b) under UV light.*

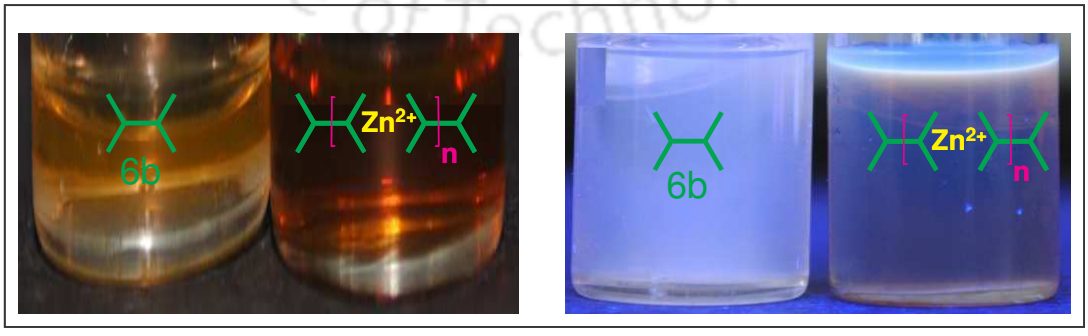

Figure 6.3: *Ditopic ligand **6b** and complex with Zn^{2+} (a) under white light and (b) under UV light.*

(a) *(b)*

Figure 6.4: *Ditopic ligand* ***6c*** *and complex with* Zn^{2+} *(a) under white light and (b) under UV light.*

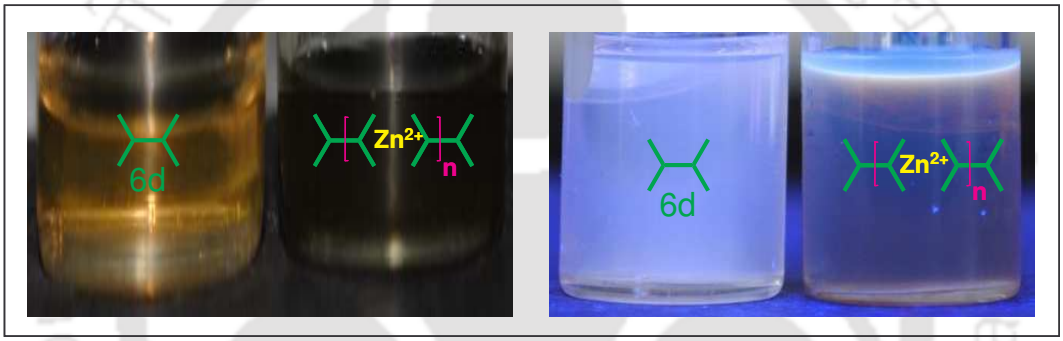

(a) *(b)*

Figure 6.5: *Ditopic ligand* ***6c*** *and complex with* Zn^{2+} *(a) under white light and (b) under UV light.*

The ditopic ligands **6a, 6b, 6c** and **6d** show the ligand absorption band at 323 nm, 309 nm, 302 nm and 296 nm respectively, which may be assigned to the π-π* transitions of the ditopic ligands. Addition of 1 equiv of the metals of Cd^{2+}, Zn^{2+}, Co^{2+} ions to any of these monomers in acetonitrile and chloroform solvent mixture results in a red shift of the absorption band with the clear formation of an isosbestic point and the colour of the solution also changes with different metal ions. Figure 6.6, clearly shows the formation of metallo-supramolecular complexes between the ditopic ligand **6a** and Zn^{2+} metal ions.

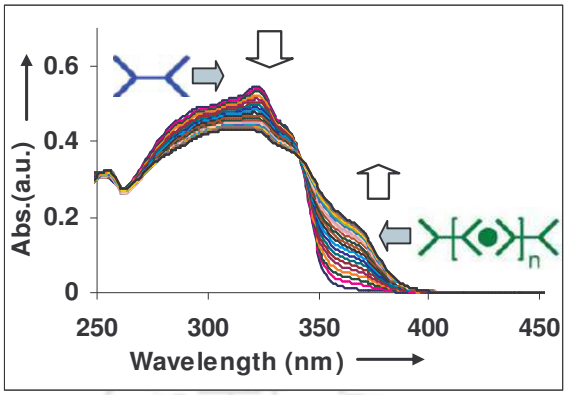

Figure 6.6: *UV/Vis spectra of* ***6a*** *(8.45 x 10^{-6} M in dry $CHCl_3$: CH_3CN = 4 : 1) during the titration with $Zn(ClO_4)_2$ from 0-2 equivalents.*

The binding ability of the ditopic ligand **6a** was evaluated by titrating 0.1 equivalent of $Zn(ClO_4)_2$ aliquots into a solution of **6a** in acetonitrile and chloroform solvent mixture at regular intervals and recording the changes in UV/visible. It was observed that on increasing the concentration of the metal ion, progressive decrease of intensity in the initial absorption band (Figure 6.6) having λ_{max} at 323 nm associated with the π-π^* transition of **6a** resulted and the peak is red shifted which is due to the formation of stable supramolecular complex between **6a** and $Zn(ClO_4)_2$. This family of spectra shows formation of an isosbestic point at 341 nm indicating the presence of at least one species at equilibrium. It was observed that the spectral features reached a limiting value only after the addition of 2.0 equivalents of metal ions (though the changes observed in the spectra on addition of 1.1 to 2.0 equivalents metal were very minor compared to the initial ten additions). Thus the gradual decrease in the band intensity at 323 nm and formation of a new higher intensity blue-shifted band at 365 nm with a clear isosbestic point is proof for the formation of metallo-supramolecular complex between monomer **6a** and metal.

Similarly, on the addition of Co^{2+} and Cd^{2+} metal ions the peaks also red shifted with the clear formation of isosbestic point. Figure 6.7 shows the changes of spectral properties on

the addition of Co^{2+} metal ions, where the initial absorption band having λ_{max} at 323 nm progressively decreases and the peak is red shifted and there is a formation of an isosbestic point at 326 nm which shows that there is at least one species at equilibrium.

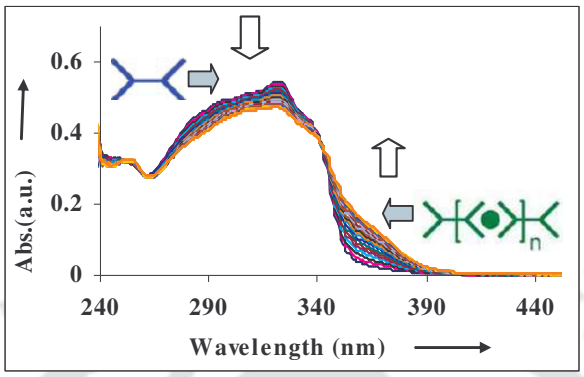

Figure 6.7: *UV/Vis spectra of **6a** (8.46 x 10^{-6} M in dry $CHCl_3$: CH_3CN = 4 : 1) during the titration with $Co(ClO_4)_2$ from 0-2 equivalents.*

Figure 6.8 depicts the changes in the spectral properties of 6a on the addition of Cd^{2+} metal ions, where the initial absorption band having λ_{max} at 323 nm progressively decreases and the peak is red shifted with a clear formation of an isosbestic point at 343 nm which shows that there is at least one species at equilibrium.

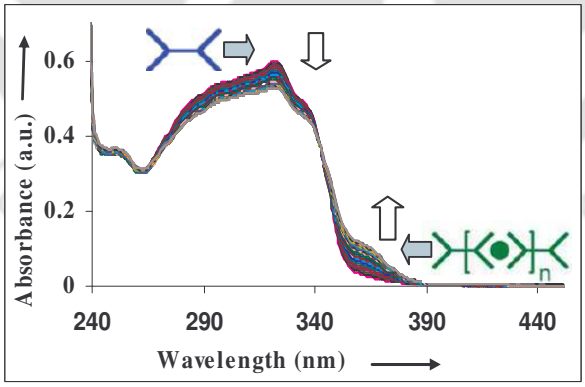

Figure 6.8: *UVVis spectra of 6**a** (9.38 x 10^{-6} M in dry $CHCl_3$: CH_3CN = 4 : 1) during the titration with $Cd(ClO_4)_2$ from 0-2 equivalents.*

On the other hand, ditopic ligand **6b** shows different optical properties on the addition of metal ions. Fig. 6.9 depicts the spectral changes that occur on the addition of $Zn(ClO_4)_2$. It was observed that on increasing the concentration of the metal ion, progressive

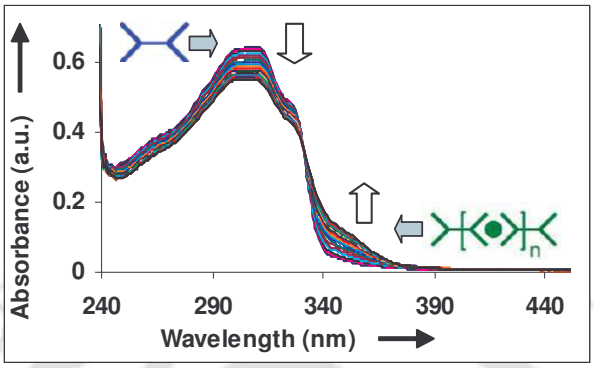

Figure 6.9: *UV/Vis spectra of* ***6b*** *(9.2 x 10^{-6} M in dry $CHCl_3$: CH_3CN = 4 : 1) during the titration with $Zn(ClO_4)_2$ from 0-2 equivalents.*

decrease of intensity in the initial absorption band (Figure 6.9) having λ_{max} at 309 nm associated with the π-π* transition of **6b** resulted. The peak is red shifted with a clear formation of isosbestic point at 331 nm which is due to the formation of stable complex between **6b** and $Zn(ClO_4)_2$. The formation of an isosbestic point indicates the presence of at least one species at equilibrium.

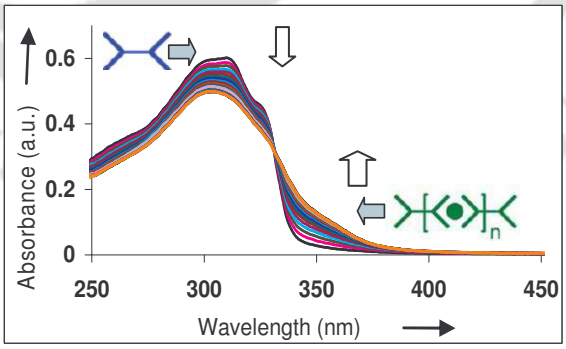

Figure 6.10: *UV/Vis spectra of* ***6b*** *(8.59 x 10^{-6} M in dry $CHCl_3$: CH_3CN = 4 : 1) during the titration with $Co(ClO_4)_2$ from 0-2 equivalents.*

Similarly, on the addition of Co^{2+} and Cd^{2+} metal ions the peaks were red shifted with the clear formation of isosbestic point. Figure 6.10 shows the changes of spectral properties on the addition of Co^{2+} metal ions, where the initial absorption band having λ_{max} at 309 nm progressively decreases and the peak is red shifted with a clear formation of an isosbestic point at 331 nm which shows that there is at least one species at equilibrium and also establishes the formation of supramolecular complexes between the two compounds.

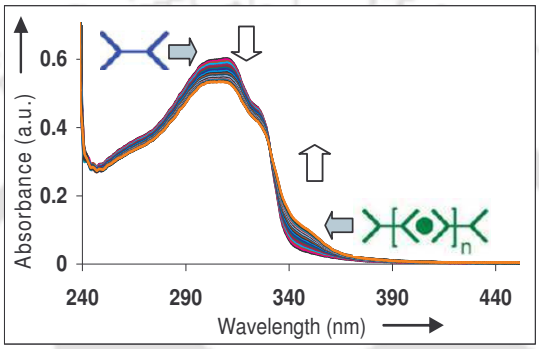

Figure 6.11: *UV/Vis spectra of* ***6b*** *(8.6 x 10^{-6} M in dry $CHCl_3$: CH_3CN = 4 : 1) during the titration with $Cd(ClO_4)_2$ from 0-2 equivalents.*

Figure 6.11 shows the changes of spectral properties on the addition of Cd^{2+} metal ions to the monomer **6b**, where the initial absorption band having λ_{max} at 309 nm progressively decreases and the peak is red shifted with a clear formation of an isosbestic point at 330 nm. This indicates that there is at least one species at equilibrium and also establishes the formation of the supramolecular complex between the ditopic ligand and metal ions.

Again formation of metallo-supramolecular complexes between the monomer **6c** and other metal ions has been monitored by UV/Visible titration. Monomer **6c** shows absorption maximum at 302 nm (Figure 6.12) and on the addition of metal ions the peak is red shifted but the changes were very less in comparison to the monomer **6a** and **6b.** That may be due to the low binding ability of the C-H part of the benzene ring in comparison to the earlier two monomers having pyridine ring. Figure 6.12 shows the spectral variations of monomer **6c** on the addition of the Zn^{2+} metal ion. On the addition of the metal ions, the

initial peak at 302 nm shows minor decrease and the peak is red shifted. Here also the formation of isosbestic point takes place at 341 nm but the changes were negligible in comparison to the monomers **6a** and **6b**. The observed minor changes and formation of isosbestic point shows the formation of metallo-supramolecular complex between the monomer **6c** and Zn^{2+} metal ion.

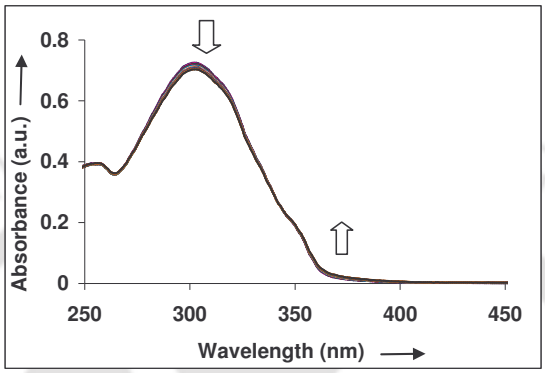

Figure 6.12: *UV/Vis spectra of* ***6c*** *(6.4 x* 10^{-6} *M in dry* $CHCl_3$ *:* CH_3CN *= 4 : 1) during the titration with* $Zn(ClO_4)_2$ *from 0-2 equivalents.*

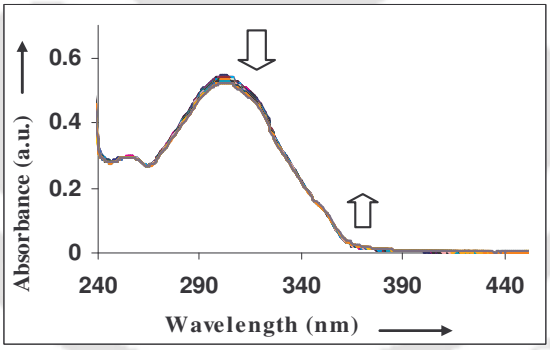

Figure 6.13: *UV/Vis spectra of* ***6c*** *(4.8 x* 10^{-6} *M in dry* $CHCl_3$ *:* CH_3CN *= 4 : 1) during the titration with* $Co(ClO_4)_2$ *from 0-2 equivalents.*

Similar titrations of monomer **6c** were performed with Co^{2+} and Cd^{2+} metal ions. Figure 6.13 and 6.14 shows the spectral changes of monomer **6c** on the addition of Co^{2+} and Cd^{2+} metal ions and in both the cases the absorption peaks were red shifted with a clear formation of isosbestic point at 345 nm and 352 nm respectively. The shifting of peak

position as well as formation of isosbestic point shows the formation of metallo-supramolecular complexes.

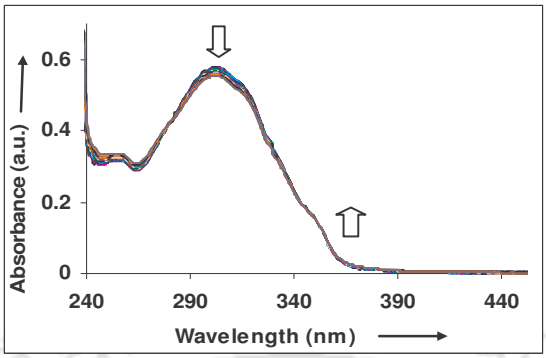

Figure 6.14: *UV/Vis spectra of* ***6c*** *(5.1 x 10^{-6} M in dry $CHCl_3$: CH_3CN = 4 : 1) during the titration with $Cd(ClO_4)_2$ from 0-2 equivalents.*

Again, ditopic ligand **6d** shows different optical properties on the addition of metal ions compared to **6a** and **6b**. Figure 6.15 depicts the spectral changes that occur on the addition of $Zn(ClO_4)_2$. It was observed that on increasing the concentration of the metal ion, progressive decrease of intensity in the initial absorption band (Figure 6.15) having λ_{max} at 296 nm associated with the π-π^* transition of **6d** resulted. The peak is red shifted with clear formation of isosbestic points at 281 nm and 347 nm which is due to the formation of a stable

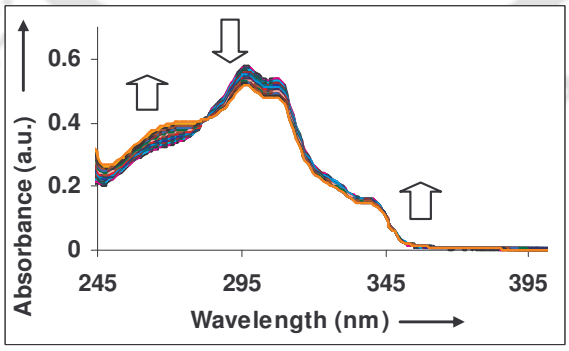

Figure 6.15: *UV/Vis spectra of* ***6d*** *(7.6 x 10^{-6} M in dry $CHCl_3$: CH_3CN = 4 : 1) during the titration with $Zn(ClO_4)_2$ from 0-2 equivalents.*

complex between **6d** and $Zn(ClO_4)_2$. The formation of an isosbestic point indicates the presence of at least one species at equilibrium. The shifting of peak position as well as formation of isosbestic point confirms the formation of metallo-supramolecular complex between the monomer **6d** and Zn^{2+} metal ion. The spectral changes observed here were more prominent in comparison to the monomer **6c** although here also organometallic bond formation takes place between the C-H of benzene ring and the metal.

Similarly, titrations of Co^{2+} and Cd^{2+} metal ions with monomer **6d** were also performed. On the addition of the metal ions, the absorption maximum peak of the monomer **6d** also red shifted with the clear formation of isosbestic point.

Figure 6.16 shows the changes of spectral properties on the addition of Co^{2+} metal ions, where the initial absorption band having λ_{max} at 296 nm progressively decreases and the peak is red shifted with clear formation of isosbestic points at 281 nm and 349 nm, which shows that there is at least one species at equilibrium and also establishes the formation of metallo-supramolecular complex between the two compounds.

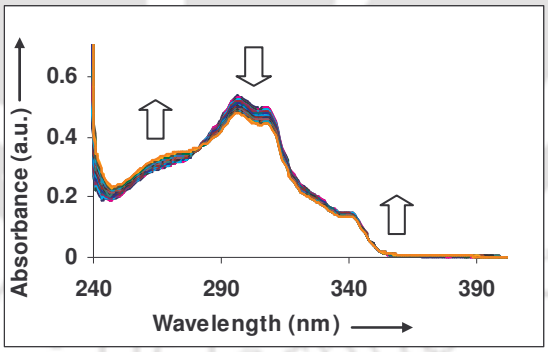

Figure 6.16: *UV/Vis spectra of **6d** (7.05×10^{-6} M in dry $CHCl_3$: CH_3CN = 4 : 1) during the titration with $Co(ClO_4)_2$ from 0-2 equivalents.*

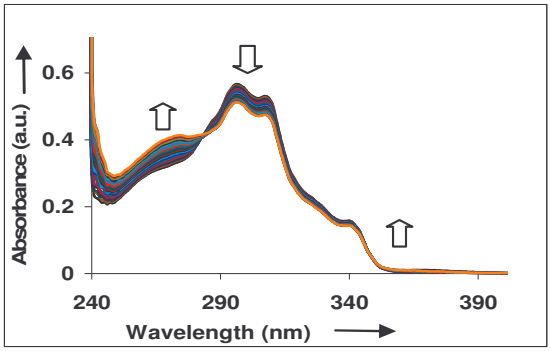

Figure 6.17: *UV/Vis spectra of* ***6d*** *(7.46 x 10^{-6} M in dry $CHCl_3$: CH_3CN = 4 : 1) during the titration with $Cd(ClO_4)_2$ from 0-2 equivalents.*

Again, Figure 6.17 shows the changes in the spectral properties on the addition of Cd^{2+} metal ions to the monomer **6d.** The initial absorption band having λ_{max} at 296 nm progressively decreases and the peak is red shifted with clear formation of isosbestic points at 283 nm and 347 nm which shows that there is at least one species at equilibrium. These spectral changes also establish the formation of the supramolecular complex between the ditopic ligand and metal ions.

6.2.3 Fluorescence Spectroscopy

Fluorescence spectroscopy studies were also carried out in order to evaluate the ability of the four ditopic ligands **6a**, **6b**, **6c** and **6d** to form the metallo-supramolecular complexes with different metal ions. Remarkable quenching of the fluorescence was observed on addition of different metal ions. It was observed that **6a** and **6b** shows more quenching in presence of metal salts in comparison to **6c** and **6d** which may be due to the formation of stronger coordination bond of metal salts with the centre pyridine ring of **6a** and **6b** while **6c** and **6d** will form weaker organometallic bond having the C-H part of the benzene ring. The fluorescence titrations of the monomers with different metal ions e.g. Zn^{2+}, Co^{2+}, Cd^{2+} have been performed in acetonitrile and chloroform solvent mixture.

The changes observed in the fluorescence spectra of a solution of **6a** in acetonitrile and chloroform solvent mixture on adding up to 2.0 equivalents of Zn^{2+} are depicted in (Figure 6.18). A large quenching (> 68%) in intensity of the 384 nm band was observed on the

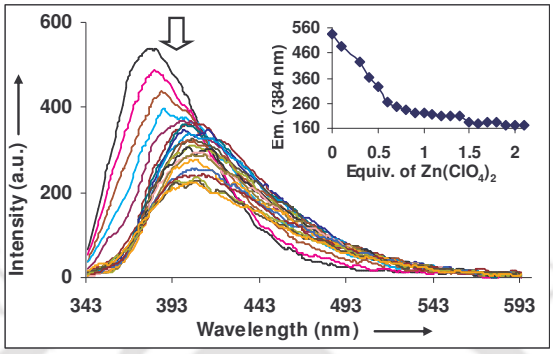

Figure 6.18: *Emission spectra of* ***6a*** *(6.4 x 10^{-7} M in dry $CHCl_3$: CH_3CN = 4 : 1) during the titration with $Zn(ClO_4)_2$ from 0-2 equivalents.*

addition of 1.0 equivalent of $Zn(ClO_4)_2$ indicating that on formation of the metallo-supramolecular complex between $Zn(ClO_4)_2$ and **6a**, the excited state was modified considerably leading to the quenching of fluorescence. On continuous addition of $Zn(ClO_4)_2$ to a solution of **6a** the peak was gradually red shifted to 407 nm. The changes observed in the fluorescence spectra on adding more than 1 equivalent of $Zn(ClO_4)_2$ aliquots to **6a** were insignificant, which is in good agreement with the results of UV/visible titration. Figure 6.18 inset shows the changes in the titration profile of the band at 384 nm corresponding to the **6a** : $Zn(ClO_4)_2$ metallo-supramolecular complex.

Analogous investigations were carried out with $Cd(ClO_4)_2$ and $Co(ClO_4)_2$ and the titration experiments were monitored by fluorescence spectroscopy (Figure 6.19-20). An acetonitrile and chloroform solution of **6a** was titrated with a solution of these metal ions. In both cases, a new band developed on quenching of fluorescence. Figure 6.19 shows the changes in fluorescence spectra on the addition of $Cd(ClO_4)_2$ to a solution of **6a** in acetonitrile and chloroform solvent mixture. The emission peak of the ditopic ligand

which was at 384 nm slows a gradual decrease on continuous addition of the metal ions and the peak was red

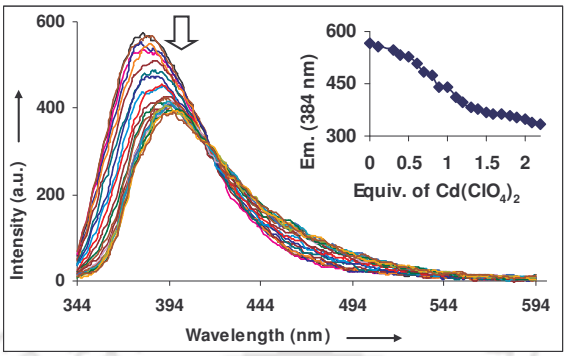

Figure 6.19: *Emission spectra of* ***6a*** *(6.65 x 10^{-7} M in dry $CHCl_3$: CH_3CN = 4 : 1) during the titration with $Cd(ClO_4)_2$ from 0-2 equivalents.*

shifted to about 397 nm. Here also the maximum quenching was observed up to the addition of 1 equivalent of the metal ions. Changes observed in the fluorescence spectra on adding more than 1 equivalent of $Cd(ClO_4)_2$ aliquots to **6a** were insignificant. Figure 6.19 inset shows the changes in the titration profile of the band at 384 nm corresponding to the **6a** : $Cd(ClO_4)_2$ metallo-supramolecular complex.

Similar fluorescence titration of **6a** was carried out with $Co(ClO_4)_2$ in acetonitrile and chloroform solvent mixture. Figure 6.20 shows the quenching of the emission spectra, where the intensity of the fluorescence emission peak of 384 nm was gradually decreased on the addition of the metal ions due to the formation of the metallo-supramolecular complex between the ditopic ligand and the metal ions leading to quenching.

Fluorescence spectroscopy studies were also carried out in order to evaluate the ability of the ditopic ligands **6b** to form the metallo-supramolecular complexes with different metal ions. It was observed that the quenching for this monomer is higher in comparison to monomer **6a** that is because of the high binding capacity of the oxazol part in comparison to thiazol part which takes part in bonding with the metal ions.

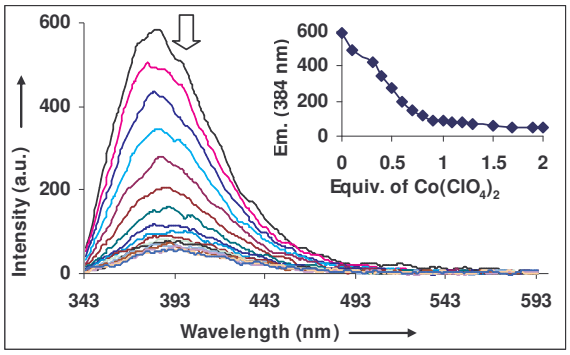

Figure 6.20: *Emission spectra of* ***6a*** *(6.97 x 10^{-7} M in dry $CHCl_3$: CH_3CN = 4 : 1) during the titration with $Co(ClO_4)_2$ from 0-2 equivalents.*

The changes observed in the fluorescence spectra of a solution of **6b** in acetonitrile and chloroform solvent mixture on adding up to 2.0 equivalents of Zn^{2+} are depicted in Figure 6.21. A large quenching (> 90%) in intensity of the 354 nm band was observed on the addition of 1.0 equivalent of $Zn(ClO_4)_2$ indicating that on formation of the metallo-supramolecular complex between $Zn(ClO_4)_2$ and **6b**, the excited state was modified considerably leading to the quenching of fluorescence. On continuous addition of $Zn(ClO_4)_2$ to a solution of **6b** the intensity of the peak decreased and was red shifted to 380 nm. The changes observed in the fluorescence spectra on adding more than 1 equivalent of $Zn(ClO_4)_2$ aliquots to **6b** were insignificant and the peak is red shifted, which is in good agreement with the results of UV/visible titration. Figure 6.21 inset shows the changes in the titration profile of the band at 361 nm corresponding to the **6b** : $Zn(ClO_4)_2$ metallo-supramolecular complex.

Similar fluorescence titration experiments were carried out with $Cd(ClO_4)_2$ and $Co(ClO_4)_2$. (Figure 6.22-23). An acetonitrile and chloroform solution of **6b** was titrated with a solution of those chosen metal ions. In all cases, a new band developed on quenching of fluorescence. Figure 6.22 shows the changes in fluorescence spectra on the addition of $Cd(ClO_4)_2$ to a

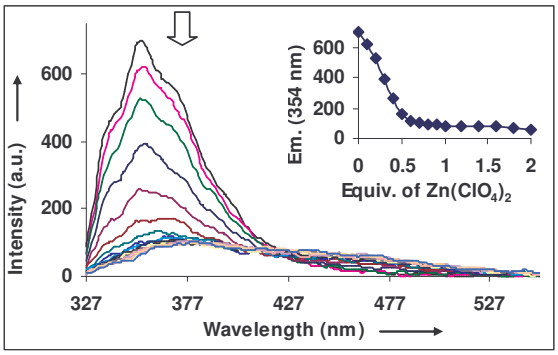

Figure 6.21: *Emission spectra of **6b** (8.6 x 10^{-7} M in dry $CHCl_3$: CH_3CN = 4 : 1) during the titration with $Zn(ClO_4)_2$ from 0-2 equivalents.*

solution of **6b** in acetonitrile and chloroform solvent mixture. On the addition of the metal ions, the emission peak of the ditopic ligand which was at 354 nm gradually decreases due to the quenching by the metal ions. Here also the maximum quenching was observed up to

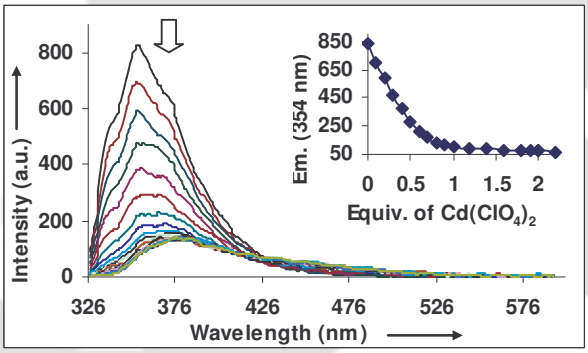

Figure 6.22: *Emission spectra of **6b** (9.4 x 10^{-7} M in dry $CHCl_3$: CH_3CN = 4 : 1) during the titration with $Cd(ClO_4)_2$ from 0-2 equivalents.*

addition of the one equivalent of the metal ions, changes observed in the fluorescence spectra on adding more than 1 equivalent of $Cd(ClO_4)_2$ aliquots to **6b** were insignificant and the emission peak is red shifted to 384 nm. Figure 6.22 inset shows the changes in the titration profile of the band at 354 nm corresponding to the **6b** : $Cd(ClO_4)_2$ metallo-supramolecular complex. Again fluorescence titration of **6b** was carried out with $Co(ClO_4)_2$ in acetonitrile and chloroform solvent mixture. Figure 6.23 shows the changes

in the emission spectra of 6b, where the intensity of the fluorescence emission peak at 354 nm gradually decreased on the addition of the metal ions due to the formation of the metallo-supramolecular complex

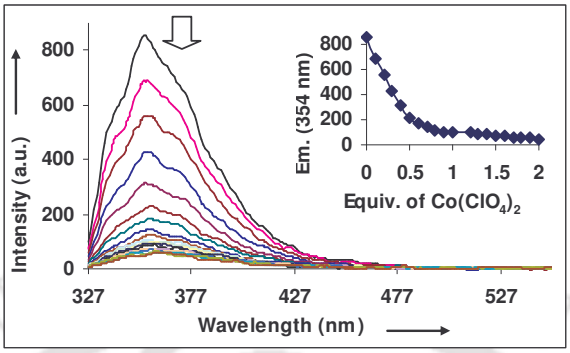

Figure 6.23: *Emission spectra of* ***6b*** *(9.8 x* 10^{-7} *M in dry* $CHCl_3$ *:* CH_3CN *= 4 : 1) during the titration with* $Co(ClO_4)_2$ *from 0-2 equivalents.*

between the ditopic ligand and the metal ions that leads to the quenching of the complex. Figure 6.23 inset shows the changes in the titration profile of the band at 354 nm corresponding to the **6b** : $Co(ClO_4)_2$ metallo-supramolecular complex.

Again, fluorescence titrations of monomer **6c** with different metals have been performed in acetonitrile and chloroform solvent mixture. Monomer **6c** shows fluorescence emission peak at 376 nm. It was observed that the quenching in case of monomer **6c** was very less (< 20%) in comparison to the monomers **6a** and **6b.** On continuous addition of $Zn(ClO_4)_2$ to a solution of **6c** (Fig. 6.24) the peak decreases but in comparison to monomers **6a** and **6b** it was less significant where the quenching was (> 90%) that may be due to the formation of the weaker organometallic bond between the C-H part of the benzene ring of the monomer which take part in the bond formation along with the coordinating bond and because of the bigger size of the benzthiazol part which take part in bonding. The changes observed in the fluorescence spectra on adding more than 1 equivalent of $Zn(ClO_4)_2$ aliquots to **6c** were also insignificant. Figure 6.24 inset shows the changes in the titration

profile of the band at 376 nm corresponding to the **6c** : $Zn(ClO_4)_2$ metallo-supramolecular complex.

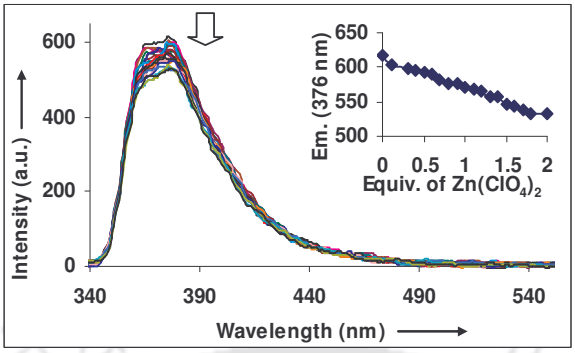

Figure 6.24: *Emission spectra of* ***6c*** *(7.8 x 10^{-7} M in dry $CHCl_3$: CH_3CN = 4 : 1) during the titration with $Zn(ClO_4)_2$ from 0-2 equivalents.*

Similar fluorescence titration was carried out with other metal ions e.g. Cd^{2+} and Co^{2+}. In both the cases the amount of quenching was less like the Zn^{2+} metal ion. In all the cases quenching was less in comparison to the other monomers **6a** and **6b.** Fig. 6.25 and 6.26 inset shows the changes in the titration profile of the band at 376 nm corresponding to the **6c** : $Cd(ClO_4)_2$ and **6c** : $Co(ClO_4)_2$ metallo-supramolecular complex respectively.

.

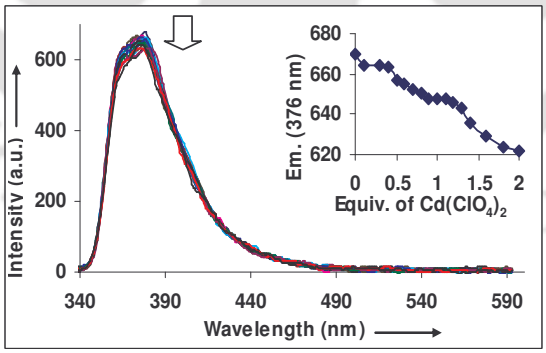

Figure 6.25: *Emission spectra of* ***6c*** *(8.47 x 10^{-7} M in dry $CHCl_3$: CH_3CN = 4 : 1) during the titration with $Cd(ClO_4)_2$ from 0-2 equivalents.*

Finally, fluorescence titrations of monomer **6d** with different metal have been done in acetonitrile and chloroform solvent mixture. Monomer **6d** shows fluorescence emission

peak at 365 nm. It was observed that the quenching in case of monomer **6d** was less (< 28 %) in comparison to the monomers **6a** and **6b** but somewhat higher in comparison to monomer **6c.**

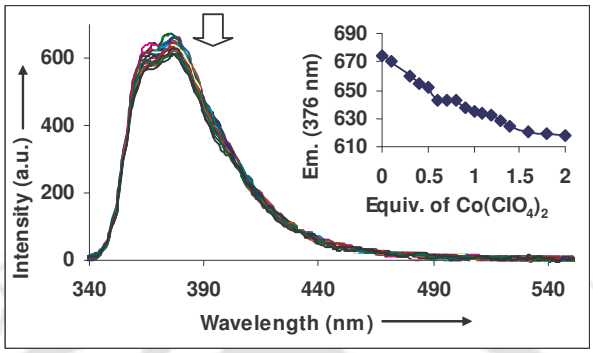

Figure 6.26: *Emission spectra of* ***6c*** *(8.54 x 10^{-7} M in dry $CHCl_3$: CH_3CN = 4 : 1) during the titration with $Co(ClO_4)_2$ from 0-2 equivalents.*

On continuous addition of $Zn(ClO_4)_2$ to a solution of **6d** (Fig. 6.27) the peak decreases but in comparison to monomers **6a** and **6b** it was less. This may be due to the formation of weaker

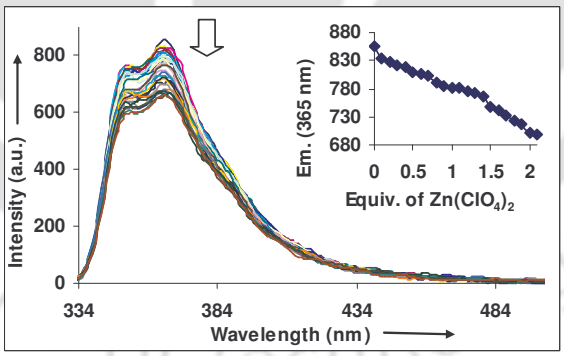

Figure 6.27: *Emission spectra of* ***6c*** *(8.8 x 10^{-7} M in dry $CHCl_3$: CH_3CN = 4 : 1) during the titration with $Zn(ClO_4)_2$ from 0-2 equivalents*

organometallic bond between the C-H part of the benzene ring of the monomer and metal. However quenching of **6d** by metal salts was few orders higher in comparison to monomer

6c. Figure 6.27 inset shows the changes in the titration profile of the band at 365 nm corresponding to the **6d** : $Zn(ClO_4)_2$ metallo-supramolecular complex.

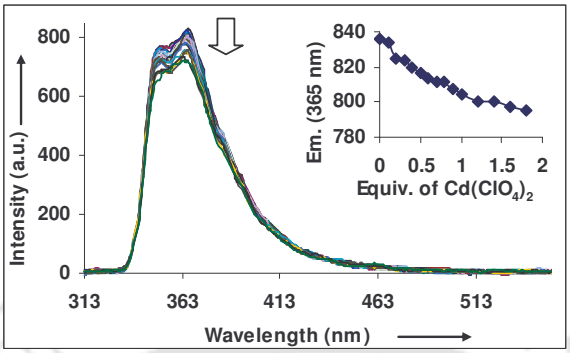

Figure 6.28: *Emission spectra of* ***6c*** *(8.6 x* 10^{-7} *M in dry* $CHCl_3$ *:* CH_3CN *= 4 : 1) during the titration with* $Cd(ClO_4)_2$ *from 0-2 equivalents.*

Similar fluorescence titration of monomer **6d** was carried out with other metal ions e.g. Cd^{2+} and Co^{2+}. In both the cases the amount of quenching was less as observed with the Zn^{2+} metal ion. In all the titrations quenching was less in comparison to the monomers **6a** and **6b.** Fig. 6.28-29 inset shows the changes in the titration profile of the band at 365 nm corresponding to the **6d** : $Cd(ClO_4)_2$ and **6d** : $Co(ClO_4)_2$ metallo-supramolecular complexes.

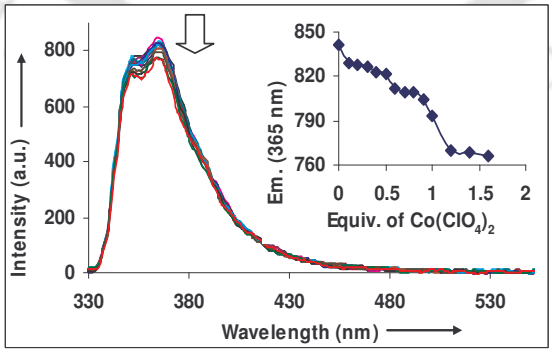

Figure 6.29: *Emission spectra of* ***6d*** *(8.66 x* 10^{-7} *M in dry* $CHCl_3$ *:* CH_3CN *= 4 : 1) during the titration with* $Co(ClO_4)_2$ *from 0-2 equivalents*

6.2.4 Possibility of Foldamer formation

Formation of foldamer, a folding polymer, can be monitored by UV/Visible and fluorescence titration. As all these monomers contain pentaethylene glycol as a spacer having six oxygen atoms they can bind selectively to smaller cations like potassium, ammonium, etc.. Although these monomers can form metallo-supramolecular polymers on the addition of transition metal ions, the monomers may be directed to fold in the presence of K^+ ions to particular arrangement such as helical structure that lead to foldamers finally.

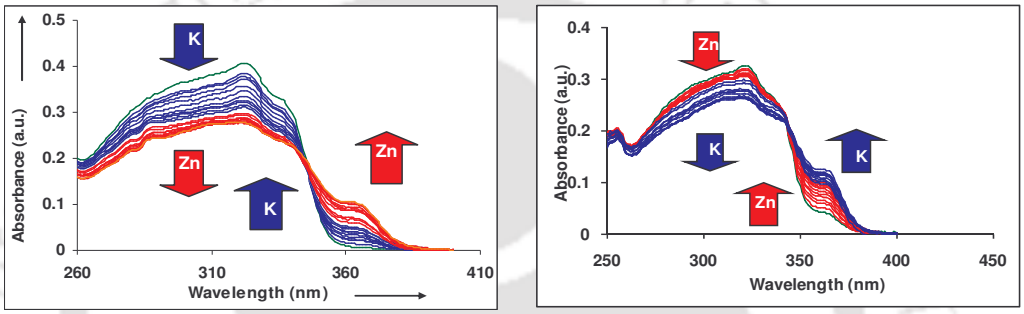

Figure 6.30: *UV/Visible spectra of* ***6a*** *(5.6 x 10^{-6} M in dry $CHCl_3$: CH_3CN = 4 : 1) during the titration with (a) first K^+ then Zn^{2+} and (b) first Zn^{2+} then K^+ $Co(ClO_4)_2$ from 0-2 equivalents*

Figure 6.30a shows the changes in UV/visible spectra on performing titration of monomer **6a** first with KSCN and secondly with $Zn(ClO_4)_2$. It was observed that on increasing the concentration of the K^+ ion, progressive decrease of intensity in the initial absorption band having λ_{max} at 323 nm resulted and the peak was red shifted with a clear formation of isosbestic point at 348 nm. Decrease of intensity as well as shift in the peak position with a clear isosbestic point explained the formation of complex between the pentaethylene glycol part of monomer **6a** and K^+ ion. After addition of 1 equivalent K^+ ion, Zn^{2+} ion (up to 1 equivalent) was added to the same solution. It was observed that the peak intensity of the monomer **6a** decreased and red shifted with a clear formation of isosbestic point at 340 nm on adding Zn^{2+} ion. This decrease in intensity of 323 nm peak

of **6a** on the addition of Zn^{2+} ion confirmed the formation of complex between Zn^{2+} and benzthaizol part of the monomer.

Similar titration was repeated by first adding 1 equivalent of Zn^{2+} ion to the monomer **6a** followed by the addition of K^+ ion to the same solution. Figure 6.30b showed the changes of UV/Visible spectra on the addition of Zn^{2+} ion followed by that of K^+ ion. On the addition of Zn^{2+} ion the peak intensity of the monomer **6a** decreased with a formation of clear isosbestic point at 337 nm, which confirmed the complex formation between **6a** and Zn^{2+} ion. After addition of 1 equivalent Zn^{2+} ion, K^+ ion (up to 1 equivalent) was added to the same solution. It was observed that the peak intensity of monomer **6a** further decreased on the addition of K^+ ion and was red shifted to 360 nm with a clear formation of new isosbestic point at 346 nm. Decrease of peak intensity and shifting of peak also support the complex formation between K^+ and penta ethylene glycol part of the monomer **6a.**

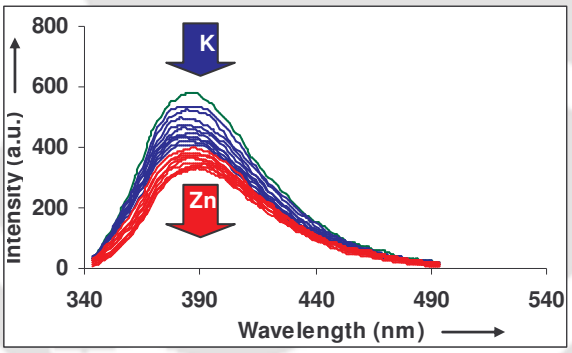

Figure 6.31: *Emission spectra of* ***6a*** *(6.2 x* 10^{-7} *M in dry* $CHCl_3$ *:* CH_3CN *= 4 : 1) during the titration with first* K^+ *then* Zn^{2+} *from 0-2 equivalents.*

The metallo-supramolecular complex formation of **6a** with 1 equivalent Zn^{2+} ion and K^+ ion was also monitored by fluorescence titration experiments. Figure 6.31 represents the fluorescence quenching of **6a** on the addition of both these metal ions. It was observed that on addition of K^+ ion (1 equivalent) to the monomer **6a** in acetonitrile and chloroform solvent mixture, about 30% of the emission peak was quenched. To the same solution,

Zn^{2+} ion was added which resulted in further quenching of the emission peak by about approximately 20%. Initial quenching observed for the addition of K^+ ion established the complex formation between the pentaethylene glycol part of the monomer **6a** and K^+, to give a folded structure that resulted in the quenching of fluorescence peak. Further quenching that was observed by the addition of Zn^{2+} ion was due to the formation of metallo-supramolecular complexes between the Zn-metal and **6a** containing K^+ ion. From the UV/Vis and fluorescence studies it was concluded that the monomers of the type **6a** can form metallo-supramolecular complexes and the spacer part (pentaethylene glycol in this case) can be efficiently utilized to form helical / folded structures by incorporating additional guest molecules. Importantly the nature of the spacer in the monomer **6a** can also be utilized for the recognition and identification of K^+ ion in the presence of salts such as Na^+ and Li^+.

6.2.5 Measurement of Viscosity

Having demonstrated the formation of metallo-supramolecular complexes from a combination of UV/Vis, photoluminescence, and FT-IR studies, this complex formation was further studied by viscosity measurement in solution state as done in the previous chapter. The intrinsic viscosity, [η], of a sample is related to the molecular weight M of the polymer through the Mark-Houwink-Sakurada equation: $[\eta] = KM^a$, where K and a are experimentally determined polymer and environmentally specific constants. Viscosity studies were carried out using a Cannon-Ubbelohde microdilution viscometer, and the relative viscosities of the complexes were measured at different concentrations. Figure 6.32 shows the Huggins plot (reduced viscosity vs concentration) for Zn^{2+} complexes of the monomers **6a**, **6b**, **6c** and **6d**. Keeping the total solute concentration constant, the data show a steady increase of the reduced viscosity on dilution.

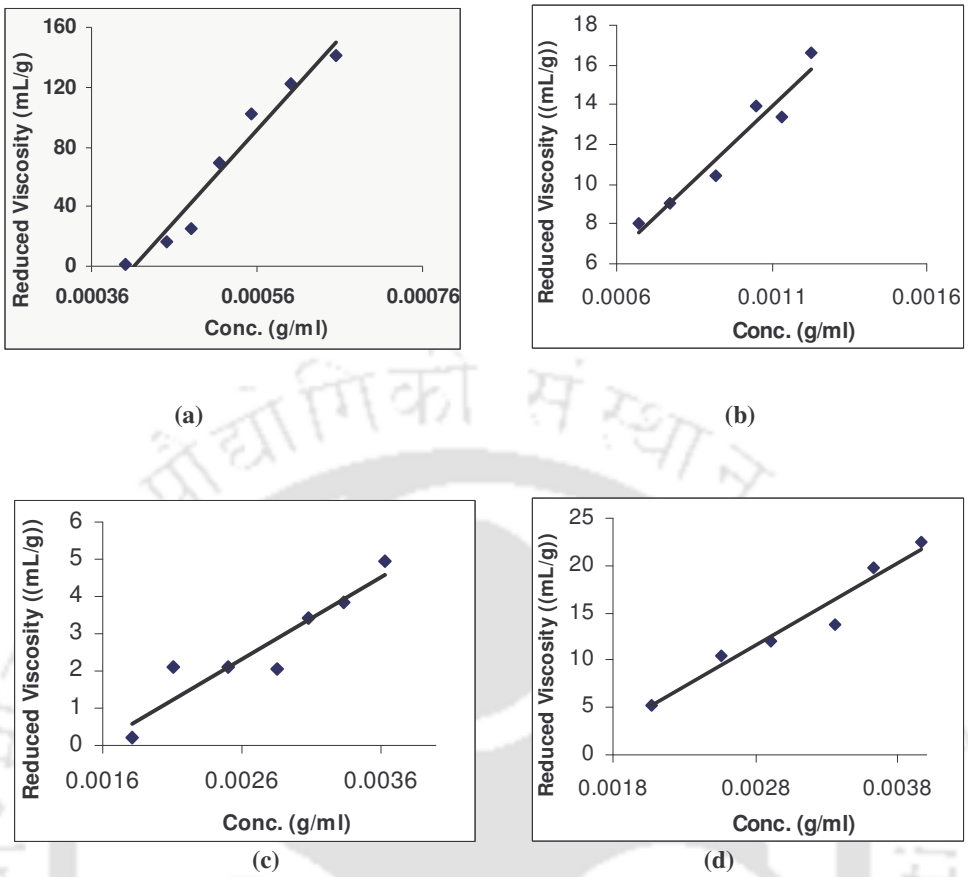

Figure 6.32: *Plot of reduced viscosity vs concentration for the Zn^{2+} complexes of ditopic monomers (a)* ***6a,*** *(b)* ***6b,*** *(c)* ***6c*** *and (d)* ***6d.***

6.2.6 Study of thermal behaviour

The thermal properties of the metallo-supramolecular complexes and the parent monomers **6a**, **6b**, **6c** and **6d** were investigated by means of thermogravimetric analysis (TGA). A series of experiments were carried out in order to understand the thermal properties of these metallo-supramolecular complexes. The thermograms were recorded in atmospheric conditions. The working temperature range of the instrument is from ambient to 1300°C.

TGA traces of monomer (neat) **6a** (Figure 6.33) acquired under nitrogen atmosphere shows the onset of significant weight loss (2%) at 156°C, corresponding to the loss of the water molecules present in the monomer. The Zn^{2+} and Cd^{2+} metallo-supramolecular complexes of **6a** show almost similar thermal degradation behaviour. The stability to

higher temperature, but the 4% weight loss occurs at somewhat lower temperatures. We ascribe this situation to the thermal degradation of the perchlorate counter ions.

TGA traces of monomer neat **6b** (Figure 6.34) acquired under nitrogen atmosphere shows the onset of significant weight loss (2%) at 102°C, corresponding to the loss of the water molecule present in the monomer. The metallo-supramolecular complexes of **6b** with Cd^{2+} show a rather similar thermal degradation behaviour which is stable to higher temperature, but the 4% weight loss occurs at temperature 205 °C. We ascribe this situation to the thermal degradation of the perchlorate counter ions.

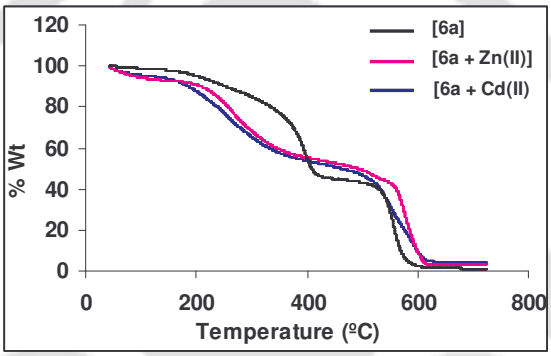

Figure 6.33: *Thermogravimetric analysis (TGA) traces of monomer **6a** and its supramolecular complexes with Zn^{2+} and Cd^{2+}*

.

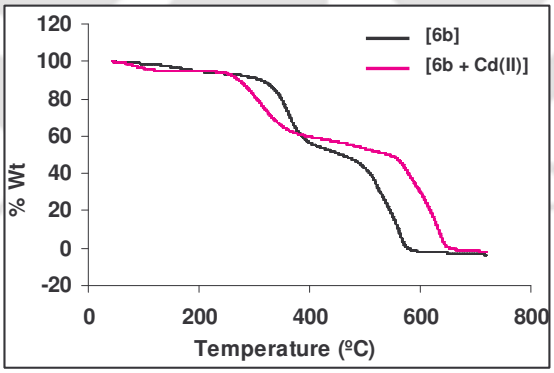

Figure 6.34: *Thermogravimetric analysis (TGA) traces of monomer **6b** and its supramolecular complex with Cd^{2+}.*

TGA traces of monomer neat **6c** (Figure 6.35) acquired under normal atmosphere and shows the onset of significant weight loss (2%) at 320°C, corresponding to the loss of the

water molecule present in the monomer. The metallo-supramolecular complexes of **6c** with Cd^{2+} and Zn^{2+} show a rather similar thermal behaviour which is not stable to higher temperature, but the 4% weight loss occurs at lower temperature which may be due to the thermal degradation of the perchlorate counter ions. The lower thermal stability of the complexes also supports the weaker bond formation between the monomer and the metal ions.

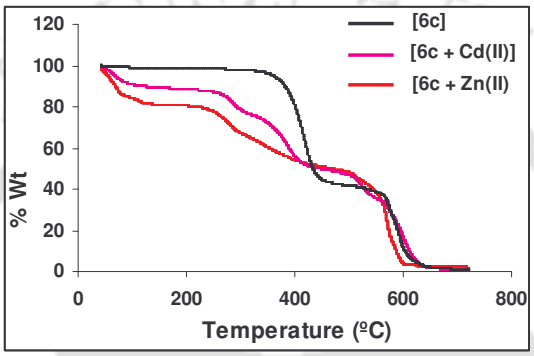

Figure 6.35: *Thermogravimetric analysis (TGA) traces of monomer* ***6c*** *and its supramolecular complexes with* Zn^{2+} *and* Cd^{2+}.

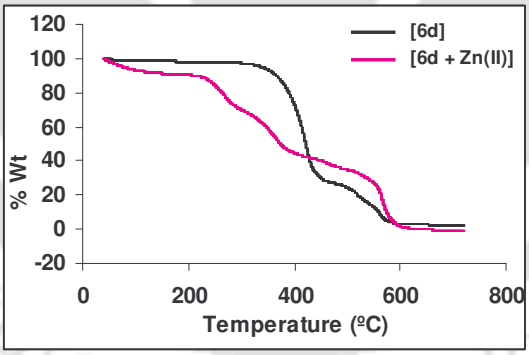

Figure 6.36: *Thermogravimetric analysis (TGA) traces of monomer* ***6d*** *and its supramolecular complexes with* Zn^{2+} *and* Cd^{2+}.

A TGA trace of monomer (neat) **6d** (Figure 6.36) acquired under normal atmosphere and shows the onset of significant weight loss (2%) at 253°C, corresponding to the loss of the water molecule present in the monomer. The metallo-supramolecular complex of **6d** with Zn^{2+} shows a rather similar thermal behaviour but it is unstable to higher temperature.

Initial 8% weight loss occurs at temperature 113°C. We ascribe this situation to the thermal degradation of the perchlorate counter ions. Thermal degradtion at lower temperature shows the weaker complex formation between the monomer and metal ion.

6.2.7 FT-IR Spectroscopy

The FT-IR spectra of all the complexes were recorded in KBr pellets. In case of complexes of **6a**, **6b**, **6c** and **6d** with different metal ions the characteristic perchlorate vibrations appear at ~1089 cm^{-1} which are absent in case of the monomers. Again, the C=N vibration peak which appear at ~1593 cm^{-1} slightly shifted after addition of the metal ions (Fig. 6.37)

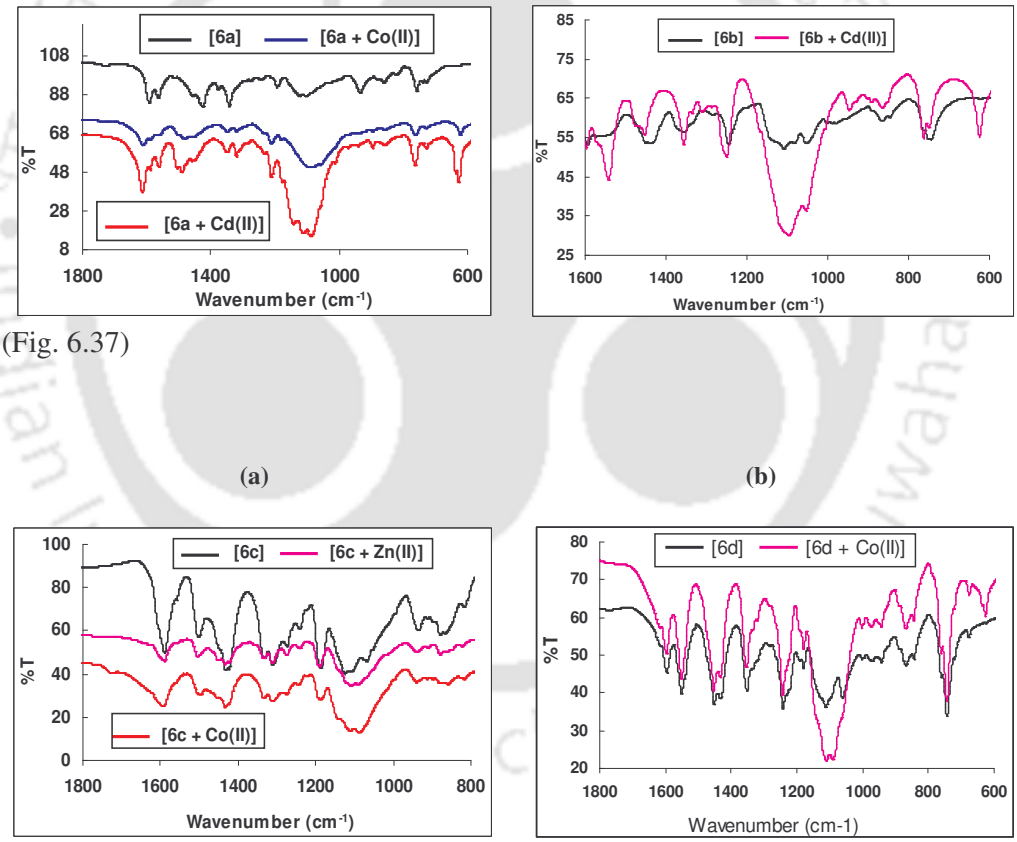

Figure 6.37: *FT-IR spectra for metal complexes of (a) monomer **6a**, (b) monomer **6b**, (c) monomer **6c** and (d) monomer **6d** in KBr pellets.*

6.3 Conclusion

We have synthesized four ditopic ligands having pentaethylene glycol chain as a spacer from simple tridentate ligands. The various ligands used for the synthesis are 2,6-bis-benzothiazol-2-yl-pyridin-4-ol, 2,6-bis-benzoxazol-2-yl-pyridin-4-ol, 3,5-bis-benzothiazol-2-yl-phenol and 3,5-bis-benzoxazol-2-yl-phenol. All these ligands were synthesized in one step from commercially available compounds. The products were well characterized by ^{1}H NMR, ^{13}C NMR, FT-IR and mass spectroscopy. The metallo-supramolecular complex formation of these monomers has been studied with different metal ions e.g. Zn^{2+}, Co^{2+}, Cd^{2+} etc. using UV/Vis, fluorescence and FT-IR spectroscopy. Additionally, since these ligands possess pentaethylene glycol as spacer unit, they can be used to recognize K^{+} ion. On binding this K^{+} ion the ligand is expected to fold which further forms a helical foldamer on adding Zn^{2+} ions to the solution. UV/Vis spectra showed that on continuous addition of the different metal ions the absorption maximum decreases and the peak gradually red shifted with a clear formation of isosbestic point in all the monomers. Again from the fluorescence titration it was clear that on the addition of the metal ions to **6a** and **6b** the emission peak was quenched due to the formation of the metallo-supramolecular complex and the peak was red shifted, while addition of the metal ions to **6c** and **6d** showed less quenching due to the formation of weaker metal-carbon bond by the C-H part of benzene ring of the monomer with metal atoms. Among the monomers **6c** and **6d**, the monomer **6c** shows more shift in UV/Vis titration as well as in fluorescence titration also, which may be because of the better binding nature of the oxazol part in comparison to thiazol part. Thermal studies showed that some of these complexes were stable at elevated temperature. The wide range of possible core as well as spacer part that can be studied, in accordance with the available metal ions, which not only exhibit different binding kinetics and thermodynamics but also can impart functionality, e.g., catalysis, luminescence, etc., opens the door to the creation of easy to process

organic/inorganic hybrid materials in which their functionality and mechanical properties can easily be tailored. Again, UV/Visible and fluorescence titration of monomer **6a** with K^+ and Zn^+ ion together, concluded that the monomers of the type **6a** can form metallo-supramolecular complexes and the spacer part (pentaethylene glycol part in this case) can be efficiently utilized to form helical / folded structures by incorporating additional guest molecules. Importantly the nature of the spacer in our monomer **6a** can also be utilized for the recognition and identification of K^+ ion in the presence of salts such as Na^+ and Li^+.

6.4 Experimental section

6.4.1 General

All reagents were used as received without further purification unless mentioned. These materials were of reagent grade or better. Acetonitrile was distilled from calcium hydride. UV/visible spectra were recorded on a Perkin Elmer Lambda-25 spectrophotometer. Fluorescence spectra were recorded on a Varian Cary Eclipse Fluorescence spectrophotometer. ^{1}H-NMR spectra were obtained with a 400 MHz Varian FT spectrometer. Chemical shifts (ppm) were referenced to the residual solvent peaks. Thermogravimetric analyses (TGA) were carried out on a Shimadzu DT-30 thermal analyzer.

6.4.2 Preparation of different ligands and monomers

Preparation of 2,6-bis-benzothiazol-2-yl-pyridin-4-ol ligand (OHBTP)

The 2,6-bis-benzothiazol-2-yl-pyridin-4-ol ligand has been prepared by the known literature method.[4]

Chelidamic acid (1.8 g, 8.94 mmol) and 2-aminothiophenol (2.74 g, 21.8 mmol) were dispersed in 20 ml orthophosphoric acid. The mixture was stirred and refluxed at 220°C for 14 hrs. After cooling to about 100°C, the hot mixture was poured to ice cold water and

stirred for half an hour. The precipitate formed was filtered and poured to hot 10 % Na_2CO_3 solution and stirred. The product was filtered and acidified to P^H 4. The precipitate was again filtered, washed with water and recrystalised from methanol to yield 3 grams of greenish powder compounds. (> 92% yield)

Preparation of 2,6-bis-benzoxazol-2-yl-pyridin-4-ol ligand (OHBOP)

Chelidamic acid (1 g, 4.97 mmol) and 2-aminophenol (1.2 g, 10.9 mmol) were dispersed in 10 ml polyphosphoric acid. The mixture was stirred and refluxed at 220°C for 5 hrs. After cooling to about 100°C, the hot mixture was poured to ice cold water and stirred for half an hour. The precipitate formed was filtered and poured to hot 10 % Na_2CO_3 solution and stirred. The product was filtered and acidified to P^H 4. The precipitate was again filtered, washed with water and recrystalised from methanol to yield 1.1 grams of white powder type compounds. (> 75% yield)

Preparation of 3,5-bis-benzothiazol-2-yl-phenol ligand (OHBTPH)

5-Hydroxyisophthalic acid (3 g, 16.4 mmol) and 2-aminothiophenol (4.68 g, 37.3 mmol) were dispersed in 25 ml orthophosphoric acid. The mixture was stirred and refluxed at 220°C for 16 hrs. After cooling to about 100°C, the hot mixture was poured to ice cold water and stirred for half an hour. The precipitate formed was filtered and poured to hot 10 % Na_2CO_3 solution and stirred. The product was filtered and acidified to P^H 4. The precipitate was again filtered, washed with water and recrystalised from methanol to yield 5.4 grams of greenish powder compounds. (> 91% yield)

Preparation of 3,5-bis-benzoxazol-2-yl-phenol ligand (OHBOPH)

5-Hydroxyisophthalic acid (2 g, 10.9 mmol) and 2-aminophenol (2.6 g, 23.8 mmol) were dispersed in 15 ml polyphosphoric acid. The mixture was stirred and refluxed at 220°C for 4 hrs. After cooling to about 100°C, the hot mixture was poured to ice cold water and stirred for half an hour. The precipitate formed was filtered and poured to hot 10 %

Na_2CO_3 solution and stirred. The product was filtered and acidified to P^H 4. The precipitate was again filtered, washed with water and recrystalised from methanol to yield 1.1 grams of white powder compounds. (> 61% yield)

Preparation of bis-p-Tosyl-penta(ethyleneglycol) from pentaethyleneglycol

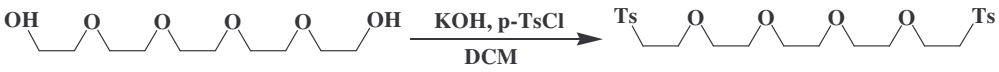

Pentaethylene glycol (1.13 g, 4.7 mmol) was dissolved in DCM and in ice cold condition p-TsCl (3.0 g, 15.7 mmol) was added and stirred for 20 minutes. Then in ice cold condition powdered KOH (3.0 g) was added and stirred for 12 hrs. To this ice cold water and DCM was added. The organics were collected and again the water part was extracted with DCM. The organics were evaporated and the residue dried under vacuum. The material was purified via column chromatography (100:0 Hexane:Ethylacetate ⟶ 50:50 Hexane:Ethylacetate) to give 2.4 grams of the product. (93% yield)

^{1}H NMR (400 MHz, $CDCl_3$): δ 7.77 (d, 4H), 7.32 (d, 4H), 4.12 (t, 4H), 3.66 (t, 4H), 3.55-3.57 (m, 12H), 2.41 (s, 6H).

^{13}C NMR (100 MHz, CDCl3): δ 144.7, 132.7, 129.7, 127.8, 70.6, 70.5, 70.3, 69.1, 68.4, 21.5.

Preparation of bisiodo(ethylene glycol)

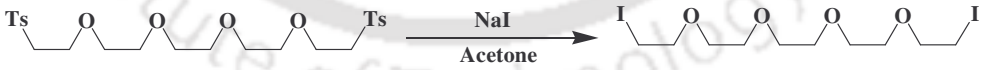

Bis-p-Tosyl-penta(ethylene glycol) (1.00 g, 1.8 mmol) was dissolved in acetone and slowly NaI was added to the solution and stirred for 48 hrs. Water was added after removal of the solvent and the product was extracted using chloroform. The solvent was evaporated to give the product to yield 0.8 g of product as a liquid. (96% yield)

^{1}H NMR (400 MHz, $CDCl_3$): δ 3.73 (t, 4H), 3.24 (t, 4H), 3.64-3.65 (m, 12H)

^{13}C NMR (100 MHz, $CDCl_3$): δ 70.6, 70.5, 70.3, 69.1, 68.4.

Preparation of monomer 6a

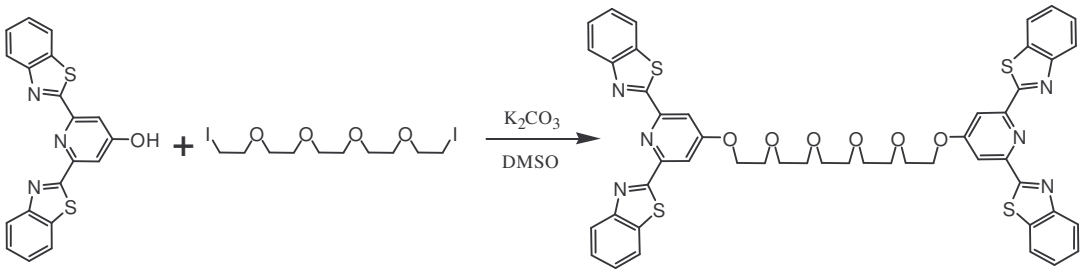

Fig. 6.38: *Preparation of monomer **6a***

HOBTP (2.0 g, 5.5 mmol) and bisiodopenta(ethylene glycol) (0.58 g, 1.26 mmol) were dissolved into a solution of K_2CO_3 (4.1 g) in 10 mL of DMSO and stirred at 90°C for 24 hrs. After removing heat, the mixture was poured into 200 mL of half-saturated NH_4Cl and washed with 100 ml of chloroform. The organics were collected and extracted again from a mixture of water and chloroform. The organics were evaporated and the residue dried under vacuum. The material was purified via column chromatography (100:0 $CHCl_3$:MeOH ⟶ 97:3 $CHCl_3$:MeOH) to yield 0.8 grams of product as a solid. (68% yield)

^{1}H NMR (400 MHz, $CDCl_3$): δ 8.01 (d, 4H), 7.89 (d, 4H), 7.44 (t, 4H), 7.35 (t, 4H), 7.87 (s, 4H), 4.37 (t, 4H), 3.93 (t, 4H), 3.75 (t, 4H), 3.71-3.68 (m, 8H).

^{13}C NMR (100 MHz, $CDCl_3$): δ 168.7, 166.6, 154.3, 152.7, 136.6, 126.3, 125.8, 123.6, 122.1, 108.3, 71.2, 70.8, 69.2, 68.4.

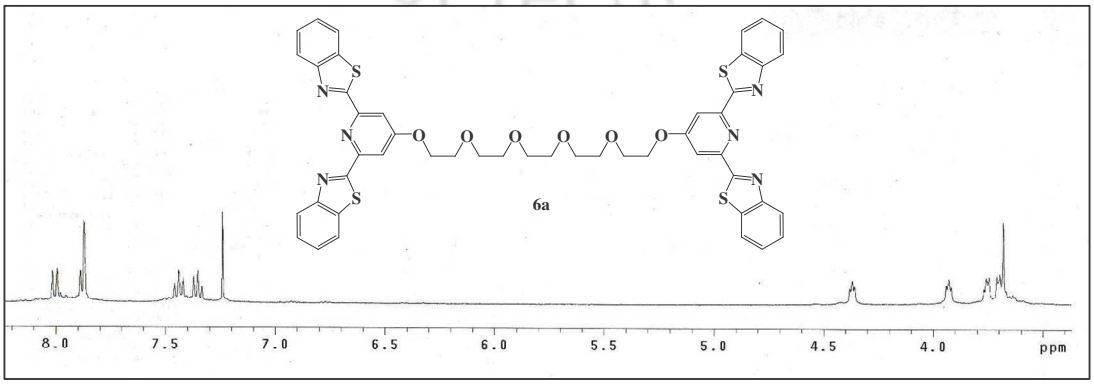

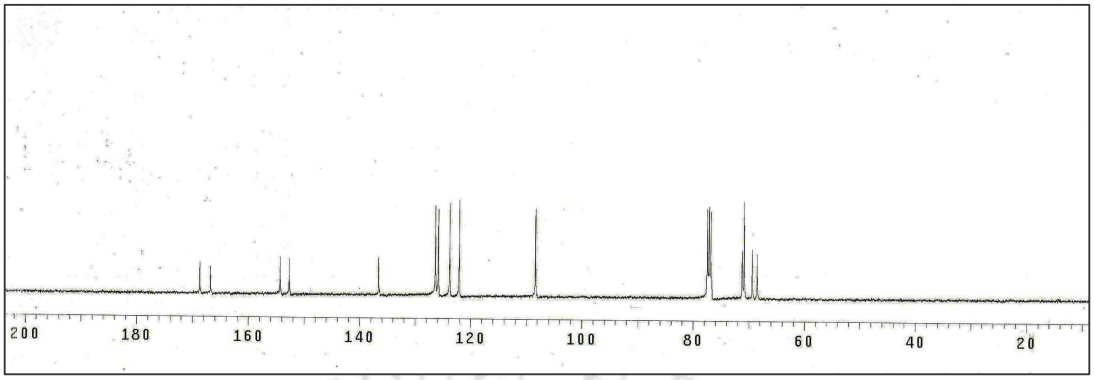

Figure 6.39: *^{1}H-NMR and ^{13}C-NMR spectra of monomer **6a** in $CDCl_3$ solvent.*

Preparation of monomer 6b

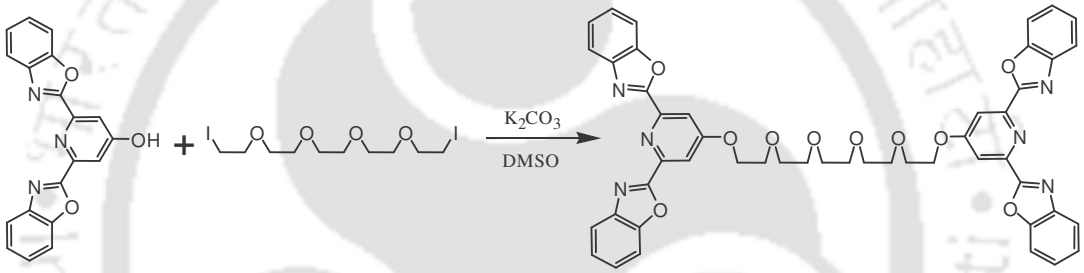

Fig. 6.40: *Preparation of monomer **6b***

HOBOP (2.0 g, 6.07 mmol) and bisiodopenta(ethylene glycol) (0.55 g, 1.2 mmol) were dissolved into a solution of K_2CO_3 (4.4 g) in 12 mL of DMSO and stirred at 90°C for 24 hrs. After removing heat, the mixture was poured into 200 mL of half-saturated NH_4Cl and washed with 100 ml of chloroform. The organics were collected and extracted again from a mixture of water and chloroform. The organics were evaporated and the residue dried under vacuum. The material was purified via column chromatography (100:0 $CHCl_3$:MeOH ⟶ 98:3 $CHCl_3$:MeOH) to yield 0.6 grams of product as a solid. (58% yield)

^{1}H NMR (400 MHz, $CDCl_3$): δ 7.97 (s, 4H), 7.79 (d, 4H), 7.65 (d, 4H), 7.37 (m, 8H), 4.36 (t, 4H), 3.90 (t, 4H), 3.72 (t, 4H), 3.70-3.64 (m, 8H).

^{13}C NMR (100 MHz, $CDCl_3$): δ 166.7, 160.9, 151.3, 148.2, 141.8, 126.4, 125.1, 120.8, 111.8, 111.6, 71.2, 70.5, 69.3, 68.6.

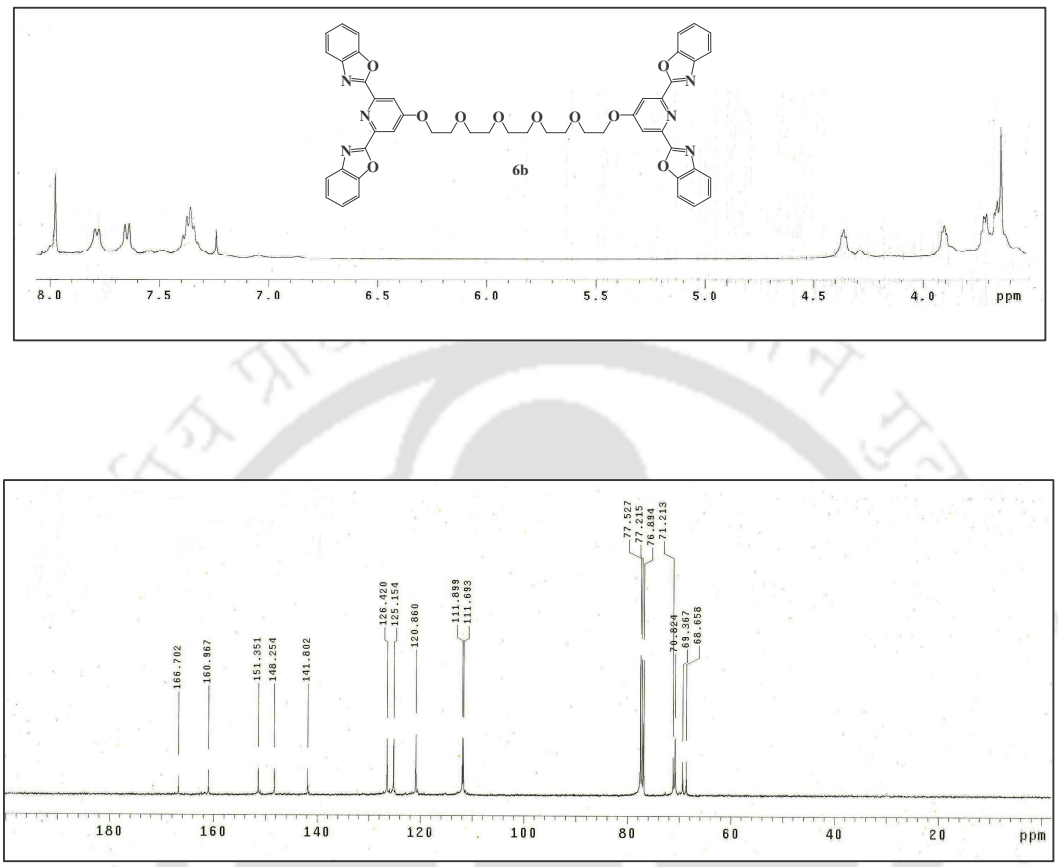

Figure 6.41: *^{1}H-NMR and ^{13}C-NMR spectra of monomer **6b** in $CDCl_3$ solvent.*

Preparation of monomer 6c

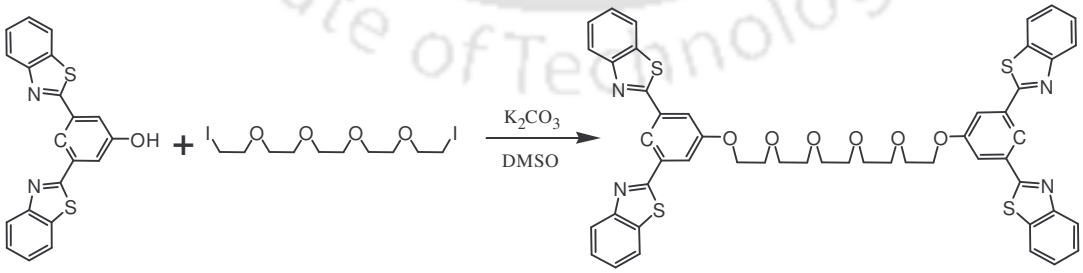

Fig. 6.42: *Preparation of monomer **6c***

HOBTPH (2.2 g, 6.12 mmol) and bisiodopenta(ethylene glycol) (0.70 g, 1.52 mmol) were dissolved into a solution of K_2CO_3 (4.8 g) in 10 mL of DMSO and stirred at 90°C for 24

hrs. After removing heat, the mixture was poured into 200 mL of half-saturated NH_4Cl and washed with 100 ml of chloroform. The organics were collected and extracted again from a mixture of water and chloroform. The organics were evaporated and the residue dried under vacuum. The material was purified via column chromatography (100:0 $CHCl_3$:MeOH ⟶ 95:3 $CHCl_3$:MeOH) to yield 1.0 grams of product as a solid. (70% yield)

^{1}H NMR (400 MHz, $CDCl_3$): δ 8.26 (s, 2H), 8.05 (d, 4H), 7.85 (d, 4H), 7.71 (s, 4H), 7.45 (t, 4H), 7.36 (t, 4H), 4.28 (t, 4H), 3.90 (t, 4H), 3.75 (t, 4H), 3.71-3.67 (m, 8H).

^{13}C NMR (100 MHz, $CDCl_3$): δ 166.9, 159.7, 154.1, 135.6, 135.3, 126.5, 125.5, 123.5, 121.8, 119.4, 115.8, 71.4, 71.2, 70.2, 68.2.

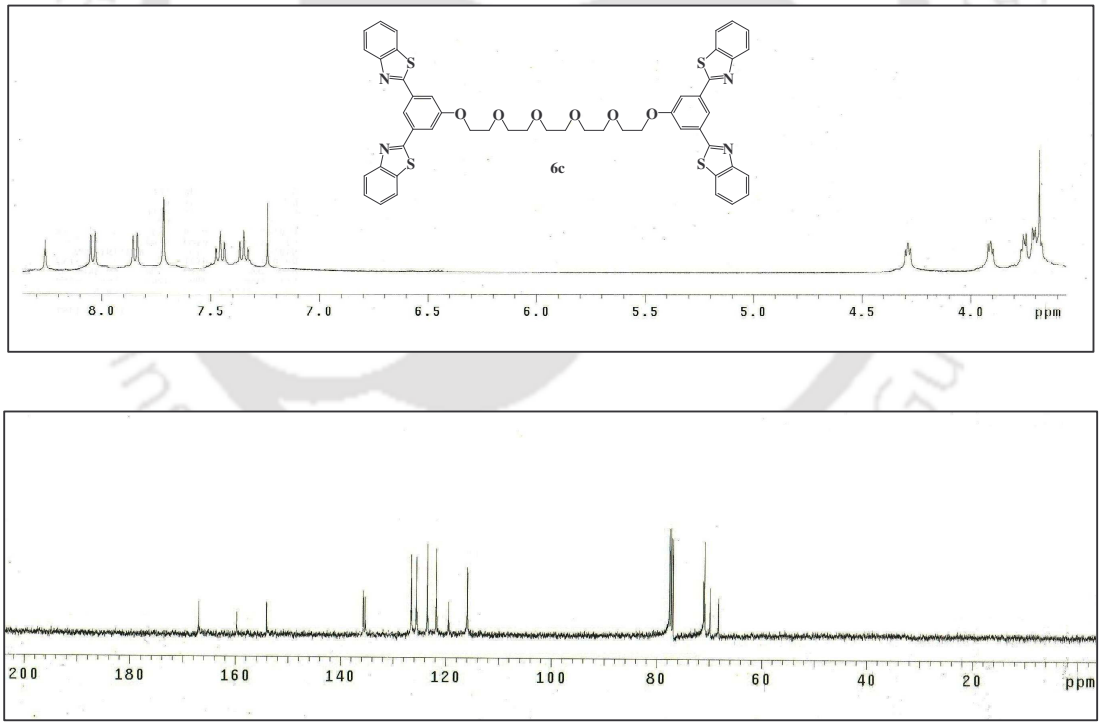

Figure 6.43: *^{1}H-NMR and ^{13}C-NMR spectra of monomer **6c** in $CDCl_3$ solvent.*

Preparation of monomer 6d

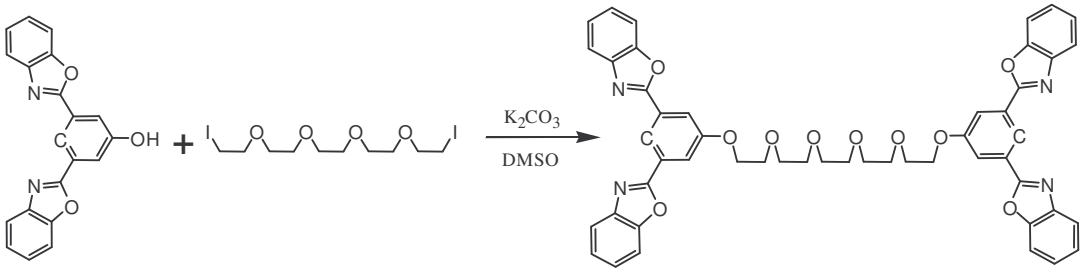

Fig. 6.44: *Preparation of monomer* ***6d***

HOBOPH (3.2 g, 9.77 mmol) and bisiodopenta(ethylene glycol) (1.12 g, 2.44 mmol) were dissolved into a solution of K_2CO_3 (6.8 g) in 18 mL of DMSO and stirred at 90°C for 24 hrs. After removing heat, the mixture was poured into 300 mL of half-saturated NH_4Cl and washed with 100 ml of chloroform. The organics were collected and extracted again from a mixture of water and chloroform. The organics were evaporated and the residue dried under vacuum. The material was purified via column chromatography (100:0 $CHCl_3$:MeOH ⟶ 92:3 $CHCl_3$:MeOH) to yield 1.1 grams of product as a solid. (52% yield)

^{1}H NMR (400 MHz, $CDCl_3$): δ 8.62 (s, 2H), 7.88 (d, 4H), 7.73 (d, 4H), 7.54 (d, 4H), 7.32-7.30 (m, 8H), 4.30 (t, 4H), 3.93 (t, 4H), 3.76 (t, 4H), 3.72-3.67 (m, 8H).

^{13}C NMR (100 MHz, $CDCl_3$): δ 161.9, 159.5, 150.8, 141.9, 129.1, 125.5, 124.8, 120.2, 119.2, 116.3, 110.7, 71.0, 70.8, 69.6, 68.2.

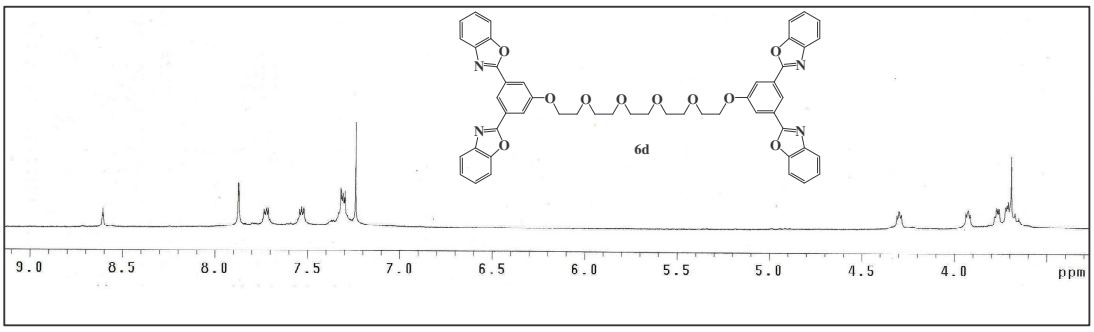

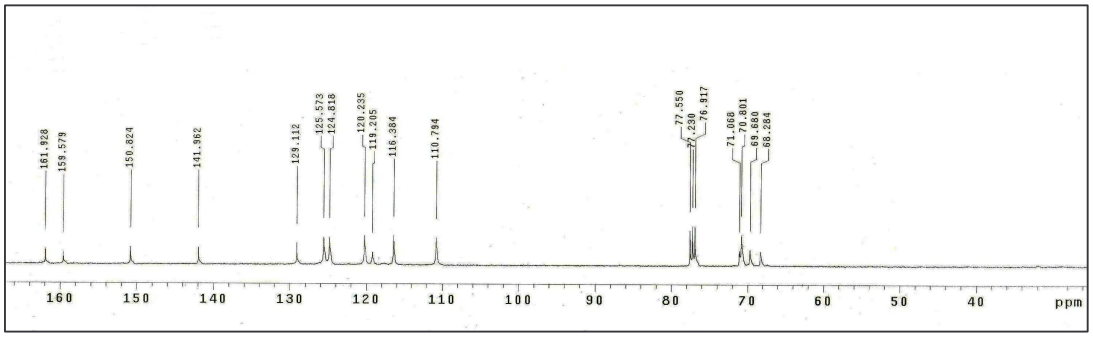

Figure 6.45: *^{1}H-NMR and ^{13}C-NMR spectra of monomer **6d** in $CDCl_3$ solvent.*

6.4.3 Mass Spectroscopy

The electrospray mass spectra for all the complexes were recorded in CH_3CN with (0.1%) formic acid. The (M + Na) molecular ion peaks for the ditopic ligands **6a**, **6b**, **6c** and **6d** appear at 947.02, 883.22, 945.03 and 881.24 respectively (Figure 6.46).

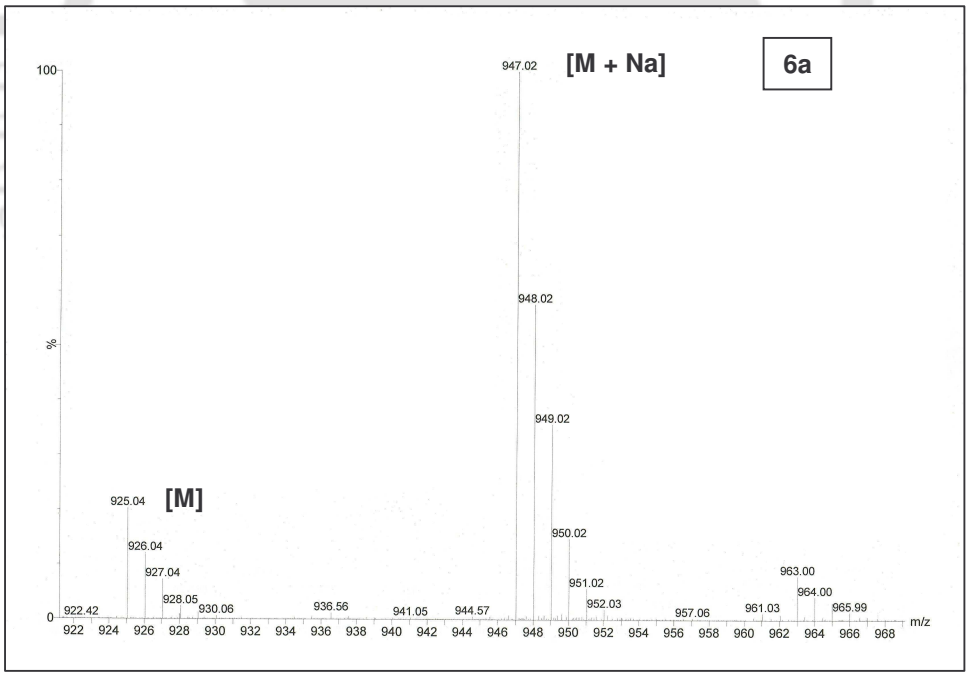

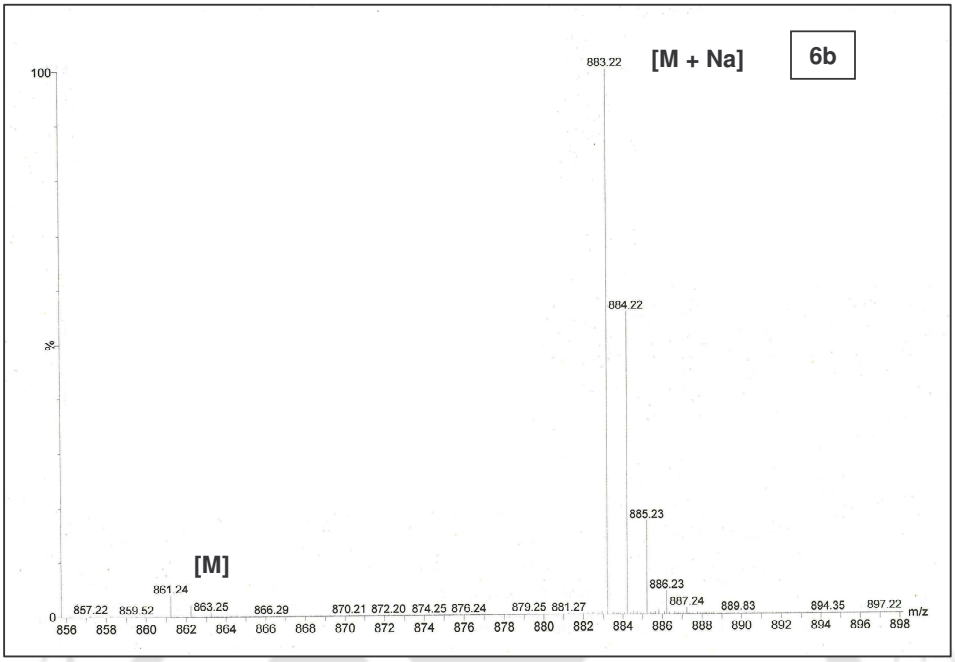

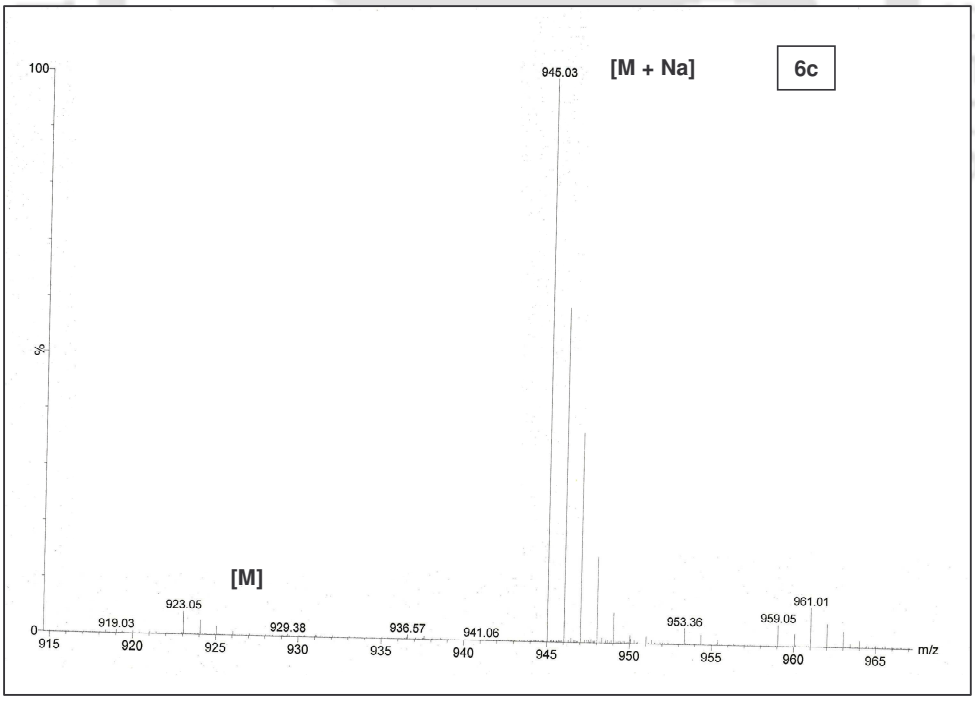

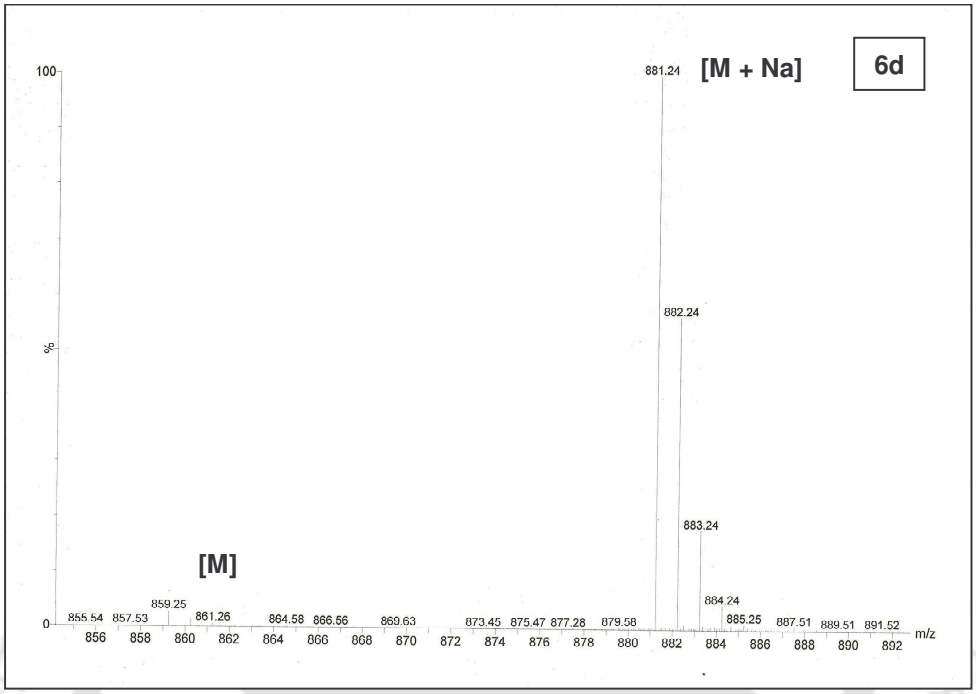

Figure 6.46: *ESI-Mass spectra for the monomers (a)* ***5a*** *and (b)* ***5b*** *in CH_3CN with (0.1%) formic acid.*

6.5 References

1. (a) Lohmeijer, B. G. G.; Schubert, U. S. *J. Polym. Sci., Part A: Polym. Chem.* **2003**, *41*, 1413. (b) Dobrawa, R.; Würthner, F. *J. Polym. Sci., Part A: Polym. Chem.* **2005**, *43*, 4981-4995. (c) Holliday, B. J.; Swager, T. M. *Chem. Commun.* **2005**, 23. (d) Friese, V. A.; Kurth, D. G. *Coord. Chem. Rev.* **2008**, *252*, 199.
2. (a) Zych, A.J.; Iverson, B.L. *J. Am. Chem. Soc.* **2000**, *122*, 8898. (b) Sadowsky, J.D.; Schmitt, M.A; Lee, H-S.; Umezawa, N. Wang, S. *J. Am. Chem. Soc.* **2005**, *127*, 11966. (c) Prince, R.B.; Barnes, S.A.; Moore, J.S. *J. Am. Chem. Soc*. **2000**, *122*, 2758. (d) Imamura, Y.; Watanabe, N.; Umezawa, N.; Iwatsubo, T.; Kato, N.; Tomita, T.; Higuchi, T. J. Am. Chem. Soc. **2009**, *131*, 7353.
3. (a) Iyer, P. K.; Beck, J. B.; Weder, C.; Rowan, S. J. *Chem. Commun.***2005**, 319. (b) Knapton, D.; Burnworth, M.; Rowan, S. J.; Weder, C. *Angew. Chem., Int. Ed.* **2006**, *45*, 5825. (c) Burnworth, M.; Rowan, S. J.; Weder, C. *Chem.sEur. J.* **2007**, *13*, 7828. (d) Knapton, D.; Rowan, S. J.; Weder, C. *Macromolecules* **2006**, *39*, 651. (e) Burnworth, M.; Knapton, D.; Rowan, S. J.; Weder, C. *J. Inorg. Organomet. Polym. Mater.* **2007**, *17*, 40, 91.
4. (a) Addison, A. W.; Burke, P. J. *J. Heterocycl. Chem*. **1981**, *18*, 803–805. (b) Addison, A. W.; Rao, T. N.; Wahlgren, C G. *J. Heterocycl. Chem.* **1983**, *20*, 1481–1484.

List of publications and patents:

1. 2,6-bis(2-benzimidazolyl)pyridine receptor for urea recognition. *Tetrahedron Lett.* **2006**, *47*, 8115-8117, B. Chetia, P. K. Iyer.

2. Utilization of 2,6-bis(2-benzimidazolyl)pyridine to detect toxic benzene metabolites. *Tetrahedron Lett.* **2007**, *48*, 47-50. B. Chetia, P. K. Iyer.

3. Novel low temperature chemical synthesis and characterization of zinc oxide nanostructures. *J. Nanosci. Nanotech*. **2008**, *4*, 4290-4294. P. K. Giri, S. Bhattacharyya, B. Chetia, B. K. Panigrahi, K.G. M. Nair, P. K. Iyer.

4. Proton induced redox tuning of Ruthenium monoterpyridine complex with 2,6-bis(benzimidazol-2-yl)-pyridine ancillary ligand: Synthesis, characterization and crystal structure. *Polyhedron* **2008**, *8*, 1983. Amardeep, B. Chetia, S. Mobin, P. K. Iyer, B. Mondal.

5. 2,6-Bis(2-benzimidazolyl)pyridine as a chemosensor for fluoride ions. *Tetrahedron Lett.* **2008**, *49*, 94-97. B. Chetia, P. K. Iyer.

6. Imidazole derivatives as the organic precursor of ZnO nano particle.*Tetrahedron Letters*, **2010**, *20*, 2751-2753. A. K. Padhy, B. Chetia, S. Mishra, A. Pati, P. K. Iyer.

7. Synthesis and optical properties of benzimidazol based metallo supramolecular complexes (Communicated) B. Chetia, P. J. Goutam, P. K. Iyer.

8. Benzthiazol and benzoxazol based metallo supramolecular complexes (Communicated) B. Chetia, P. J. Goutam, P. K. Iyer.

9. Effect of ligand structure on its optical properties and potential application in anion sensing. (Communicated) B. Chetia, P. K. Iyer.

10. Self-assembling metallosupramolecular foldamers. (Under revision) B. Chetia, P. J. Goutam, F. Chipem, S. Behera, P. K. Iyer.

Patent:

11. Method to synthesize nano sized zinc oxide. Indian Pat. Appl. Number IN 2006KO00563. P. K. Iyer, P.K Giri, S. Bhattacharyya, B. Chetia.